Understanding the role of Kirrels in circuit formation in the mouse olfactory system

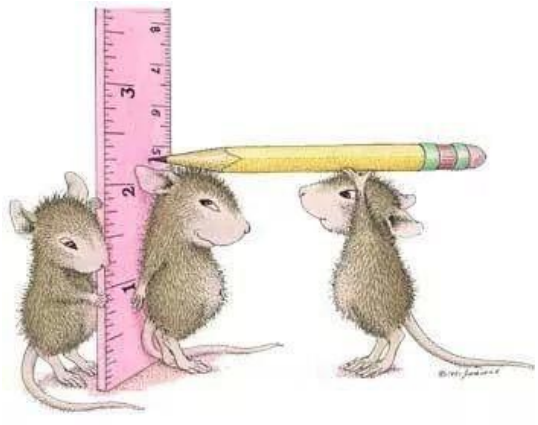

House Mouse Designs

-Neelima Vaddadi

Integrated Program in Neuroscience

Montreal Neurological Institute

McGill University

Montreal, Quebec, Canada

August 2022

A thesis dissertation submitted to the Department of Graduate and Postdoctoral Studies of McGill University in partial fulfillment of the requirements of the degree of Doctor of Philosophy in Neurological Sciences

Table of Contents:

Abstract

The human nervous system is made up of billions of neurons that form precise connections allowing the smooth functioning of individuals in their day-to-day life. Even if a small proportion of these neurons miswire, it can have a major impact on how the brain develops, possibly resulting in neurodevelopmental disorders, such as autism. It is therefore important to establish how a healthy brain wires itself in order to gain insight into what goes wrong in disease. In order to further our understanding of how neural circuits in a healthy brain are formed, we use the mouse olfactory system as a model. The mouse olfactory system serves as an effective model to understand neural circuit formation because it is organized to form a stereotypic map allowing us to easily access and visualize individual components of the circuit. We investigate the role of Kirrels in neuronal circuit formation in the mouse olfactory system since they have been shown to have a conserved role in neural circuit formation across species, such as in flies and worms, and mutations in Kirrel3 have been associated with intellectual disability in humans.

We first investigate the role of Kirrels in olfactory sensory neuron axon and vomeronasal neuron axon sorting in the main and accessory olfactory systems respectively. We show using *in vivo* approaches that Kirrels are required for axon sorting in a region-specific manner in the main olfactory system and that their homophilic cell adhesion property plays an important role for its function in axonal sorting. Furthermore, we identify a novel function of Kirrel3 in modulating dendritic development in the nervous system. We show that Kirrel3 is required in regulating dendritic complexity in mitral cells of the olfactory system. In contrast to its function in axonal coalescence, Kirrel3 effects on dendritic complexity is independent of its cell adhesion properties.

All in all, this thesis provides new insights into how Kirrel family proteins contribute to the wiring of neurons in the nervous system taking us a step closer to understanding how circuits miswiring may be implicated in neurodevelopmental disorders.

Résumé

Le système nerveux chez l'humain est composé de milliards de neurones qui forment des connexions précises permettant le bon fonctionnement des individus dans leur vie quotidienne. Même une petite proportion de mauvaises connections entre certains de ces neurones peut avoir un impact majeur sur le développement du cerveau et entraîner des troubles neurologiques, comme par exemple les troubles du spectre de l'autisme. Il est donc important de déterminer comment un cerveau sain forme ses connections afin de mieux comprendre ce qui ne va pas dans les cas de maladie. Afin de mieux comprendre comment se forment les circuits neuronaux dans un cerveau sain, nous utilisons le système olfactif de la souris comme modèle. Chez la souris, le système olfactif est un bon modèle pour étudier la formation des circuits neuronaux car l'organisation de ses connections forment un schéma stéréotypé qui nous permet d'identifier facilement les composants individuels du circuit et de les visualiser. Nous étudions le rôle des protéines Kirrels dans la formation des circuits neuronaux dans le système olfactif de la souris, car il a été démontré que ces molécules jouent un rôle dans la formation des circuits neuronaux chez d'autres espèces, comme chez les mouches et les nématodes, et que des mutations dans le gène Kirrel3 ont été associées à certaines déficiences intellectuelles chez l'humain.

Nous avons d'abord étudier le rôle des Kirrels dans le tri des axones des neurones sensoriels olfactifs du système olfactif principal et des neurones voméronasaux du système olfactif accessoire. Nous démontrons en utilisant des approches *in vivo,* que les Kirrels sont nécessaires pour le tri des axones dans une région spécifique du bulbe olfactif et que leurs propriétés d'adhésion homophiliques jouent un rôle important pour leur fonction dans le tri des axones. De plus, nous avons identifié une nouvelle fonction de Kirrel3 dans la modulation du développement dendritique dans le système nerveux. Nous montrons que Kirrel3 est nécessaire à la régulation de la complexité dendritique dans les cellules mitrales du système olfactif. Contrairement à sa fonction dans la coalescence axonale, les effets de Kirrel3 sur la complexité dendritique sont indépendants de ses propriétés d'adhésion homophiliques.

Dans l'ensemble, cette thèse fournit de nouvelles informations sur la façon dont les protéines de la famille Kirrel contribuent au câblage des neurones dans le système nerveux, ce qui nous rapproche d'une meilleure

compréhension de la façon dont les erreurs de connections durant la formation des circuits neuronaux peuvent être impliquées dans les troubles neurologiques du développement.

List of Figures

Chapter 1

Chapter 2

Chapter 3

Chapter 4

Chapter 5

List of Abbreviations

μm^2	Micrometer square
3D	3 dimensional
ABP	AMPA receptor binding protein
AC3	Adenylyl cyclase
ACE	Acetylcholine esterase
ACSF	Artificial cerebrospinal fluid
AMPA	α-amino-3-hydroxy-5-methyl-4-isoxazole propionic acid
AOB	Accessory olfactory bulb
AOS	Accessory olfactory system
ASD	Autism spectrum disorder
ATP	Adenosine Triphosphate
BDNF	Brain derived neurotrophic factor
BMP	Bone morphogenetic protein
BMPR	Bone morphogenetic protein receptor
BS Lectin	Bandeiraeae simplicifolia Lectin
C.elegans	Caenorhabditis elegans
CA	Cornu ammonis
Ca^{2+}	Calcium
CAM	Cell adhesion molecule
cAMP	Cyclic adenosine monophosphate
CASK	Calcium/calmodulin dependent serine protein kinase
CD226	Cluster of differentiation 226
cDNA	Complementary deoxyribonucleic acid
CNGA2	Cyclic nucleotide gated channel

CNS	Central nervous system
Cntn	Contactin
CREB	Cyclic AMP response element binding protein
CRISPR Cas9	Clustered regularly interspaced short palindromic repeats and CRISPR-associated protein 9
cRNA	Complementary Ribonucleic acid
CSF	Cerebrospinal fluid
DCC	Deleted in colorectal carcinoma
DiI	1,1′-dioctadecyl-3,3,3′,3′-tetramethylindocarbocyanine
DIP-DPR	Dpr interacting protein-Defective proboscis extension response
DIV	Days *in vitro*
DNA	Deoxyribonucleic acid
Dox-tet	Doxycycline-tetracycline
DREADDS	Designer receptors exclusively activated by designer drugs
DSCAM	Down syndrome cell adhesion molecule
E	Embryonic day
E/I	Excitation/Inhibition
ECM	Extracellular matrix
EDTA	Ethylenediaminetetraacetic Acid
EGF	Epidermal growth factor
Eph	Ephrin
EPL	External plexiform layer
FACS	Fluorescence activated cell sorting
F-actin	Filamentous actin
FGFR	Fibroblast growth factor receptor
FLRT	Fibronectin Leucine repeat rich transmembrane

GABA	Gamma-aminobutyric acid
GFP	Green fluorescent protein
Glom	Glomerular
GPI	Glycosylphosphatidylinositol
GRIP	Glutamate receptor interacting protein
gRNA	Guide ribonucleic acid
Gαolf	Gαolfactory
H	Hour
HC	Horizontal cell
HEK293	Human embryonic kidney 293
HEPES	4-(2-hydroxyethyl)-1-piperazineethanesulfonic acid
HSC/HSP	Heat shock cognate/heat shock protein
HSN	Hermaphrodite specific motor neuron
ICAP1	Integrin cytoplasmic associated protein 1
IGF	Insulin growth factor
IgLON	Immunoglobulin LSAMP OBCAM Neurotrimin
IgSF	Immunoglobulin super family
ILK	Integrin like kinases
IRES	Internal ribosome entry site
IRM	Irre recognition module
Jag-1	Jagged-1
K2	Kirrel2
K3	Kirrel3
KD	Knockdown
Kir2.1	Inwardly rectifying potassium (K^+) 2.1 channel

KO	Knockout
KV	Kilo Volt
LAMP	Lysosomal-associated membrane protein
LAR	Leucocyte antigen related
LIMK	LIM Kinase
LNS	Laminin nectin sex hormone
LOT	Lateral olfactory tract
LRR	Leucine repeat rich
LRRTM	Leucine repeat rich transmembrane
LSAMP	Limbic system associated membrane protein
LTP	Long term potentiation
Maml1	Mastermind like 1
MAPK	Mitogen activated protein kinase
Max	Maximum
MeA	Medial Amygdala
mEPSC	Mini excitatory postsynaptic current
MHC	Major histocompatibility complex
mM	Millimolar
MMP	Matrix metalloproteinase
MOB	Main olfactory bulb
MOS	Main olfactory system
N-cadherin	Neural cadherin
NCAM	Neural cell adhesion molecule
Necl	Nectin-like
NEGR1	Neuronal growth regulator1

NGL	Netrin G Ligand
NICD	Notch intracellular domain
NMDA	N-methyl-D-aspartate
Nrp	Neuropilin
NT4	Neurotrimin4
OB	Olfactory bulb
OBCAM	Opioid binding cell adhesion molecule
OE	Olfactory epithelium
Olfr	Olfactory receptor
OMP	Olfactory marker protein
OR	Olfactory receptor
OSN	Olfactory sensory neuron
P	Postnatal day
Pax6	Paired box protein 6
PBS	Phosphate buffer saline
Pcdh	Protocadherin
PDZ	postsynaptic density protein (PSD95), Drosophila disc large tumor suppressor (Dlg1), and zonula occludens-1 protein (zo-1)
pH	Potential of Hydrogen
PKA	Protein Kinase A
PSA	Polysialylation
PSD95	Postsynaptic density protein
PTP	Protein tyrosine phosphatase
PV	Posterio-ventral
PVDF	Polyvinylidene fluoride

Q128A	Glutamine128Alanine
RET	Rearranged during transfection
RFP	Red fluorescent protein
RIPA	Radio-Immunoprecipitation Assay
RNAi	Ribonucleic acid interference
Robo	Roundabout
RT	Room temperature
SALM	Synaptic cell adhesion like molecule
SC-CA1	Schaffer collateral- cornu ammonis 1
SDS-PAGE	Sodium dodecyl sulfate–polyacrylamide gel electrophoresis
Sema	Semaphorin
SNP	Single nucleotide polymorphism
SYG	Synaptogenesis protein
SynCAM	Synaptic cell adhesion molecule
Tag1	Transiently expressed Axonal Glycoprotein 1
Tbr1	T-box brain protein 1
Tbr2	T-box brain protein 2
Tbx21	T-box transcription factor 21
tdTomato	Tandem dimer Tomato
TrKB	Tropomyosin receptor kinase B
Fc	Fragment crystallizable
Trp2	Transient receptor potential 2 (ion channel)
VGLUT2	Vesicular glutamate transporter 2
VNO	Vomeronasal organ
VR	Vomeronasal receptor

VSN	Vomeronasal sensory neuron
WT	Wild type
X-gal	5-Bromo-4-Chloro-3-Indolyl β-D-Galactopyranoside
β gal	β-galactosidase

Acknowledgements

It takes a village to make a PhD….in my case it most certainly did! I would like to extend my heartfelt gratitude to **my supervisor Dr. Jean Francois Cloutier** for being one of the most supportive supervisors anyone could have! He has been there throughout this journey extending words of praise and appreciation during the high points and offering encouragement, assistance, and support during the low points of my PhD. I am indebted to **all the members of Cloutier lab** viz. Emilie Dumontier (for asking tough questions and providing useful insights during Labmeeting and managing all our mouse colonies), Reesha Rajah (for being so resourceful and for helping with editing a lot of my presentations and also teaching me western blots and *insitus*), Sabrina Quilez (for being the best littermate ever , helping me practice for my presentations, listening to me vent and teaching me primary neuron culture!), Sydney Fearnley (for showing me how to clone and make probes and listening to me vent), Katrine Zander Iversen (for introducing me to musicals and teaching me a lot of basic techniques in the lab such as dissections, perfusions, IHC, cryosectioning and also helping me with using CRISPR cas9 genome editing technology), Barbara Morquette (for being so supportive and training me on how to DiI label brains, vibratome sectioning, IMARIS analysis and using the confocal microscope) Candice Wiedman (for introducing me to 'The Great British Bake Off', the fun badminton sessions and being such an approachable labmate), Chris Baim (for suggesting that I practice mouse OB dissections on mice that need to be euthanized, for the fun jam sessions and being a great dungeon master at DnD (and Alex Mclean for co-hosting DnD)), Allen Scholl (for being a great littermate, and showing me how to take sagittal AOB sections and hosting fun boardgame sessions and trivia nights), Allen Li (for providing me with technical assistance such as downloading statistical software on my laptop), Aarushi Chaudhary (for showing me how to do fluorescent *insitus* and for offering me chocolates whenever I was feeling low) , and Fannia Xu and Anastasia Zhong-Vorkapic (For helping me practice for my defense and keeping me up to date with the latest gen Z trends and terminologies). Shoutout to the undergrads in our lab; Stella (for keeping me motivated to exercise daily), Anna, Michelle (for asking a lot of questions and inviting me to give a departmental methods talk), Mohini, Sally, Yan-Ru and Frederique. I am grateful to **Xinzhu Tan** for teaching me viral injections in P0 pups and **Benjamin Kacerovsky** for teaching me *in utero* electroporations. Special shoutout to some of **my furry friends** for keeping me calm and grounded and providing me with pet therapy. These furry friends include JF's cats Hamlet and Houdini and my friend Malosree's cat Trilokonath aka Tiramisu.

I would like to extend my heartfelt gratitude to **my committee members** Dr. Alyson Fournier and Dr. Don Van Meyel for supporting me throughout my PhD with useful feedback and comments and providing me with timely advice and encouragement. I would like to thank **my IPN mentor** Dr. Thomas Stroh and **all the professors who have been a part of our departmental talk series called 'research discussion'** for providing me with useful comments and advice on how to become an effective public speaker and presenter. Special thanks to Dr. Alyson Fournier, Dr. Austen Milnerwood, Dr. Edward Ruthazer, Dr. Gary Armstrong, Stefano Stefani, Dr. Tim Kennedy, Dr. Wayne Sossin, and Dr. Yang Zhou for being active members of this discussion series and providing me with useful feedback and comments on my project. I would also like to thank **all the professors at the IPN who taught the different PhD courses** I've taken so far. In addition, I would like to thank **ex- IPN director Dr. Reza Farivar** for providing me with assistance when I needed it. I am extremely thankful to **our collaborators** Dr. Engin Ozkan and his lab members specially Joseph Pak for explaining

to me some of the structural data in our publication (Wang, Vaddadi and Pak et al 2021, Cell Reports). **Special thanks to Mitra Cowan** for being so supportive during times of distress and providing all the technical help with generating our CRISPR knockin mouse and for conducting the microinjections. I am grateful to some of **the previous lab members** viz Janet Prince, Alexandra Brignall and Alina Phen for contributing valuable data that formed the basis of Chapter 2 and 3.

I am indebted to **all my friends from the IPN** for being my support system at different stages of my PhD. Some of these people include **Malosree Maitra** (and Debajyoti Saha)**, Saishree Badrinarayan (these two have been my rocks through thick and thin. They've been my academic, emotional and social support all throughout my PhD)**, Zahraa Chorghay (for chai and valuable feedback on my presentations), Pratap Singh Markam (for keeping me well fed with yummy food), Oscar Bedford (and Lisa Miron)(for jam sessions, food and boardgames), Irem Ulku (for the yummy food), Ben Gold (for jam sessions and helping me in times of distress), Simon Hua (for being a supportive peer and keeping me company for some of my more tedious experiments), Dhruv Mehrotra (for the fun walks and chats and giving me feedback on my presentations), Shashank Srikarta (for fun chats and fun times), Rahul Kumar (for hearing me vent), Sushmetha Mohan (for long heart to heart conversations), Max Wolpert (for being my study buddy during PN1 and also my thesis writing buddy), Maran Ma (for long insightful chats), Keren Ginzberg (and Yo Hann) (for boardgames and fun chats), Daniel Almeida (for providing me support when I was struggling with poor mental health), Jennifer Novek (for being my PN2 study buddy), Sriram Jaybal (for helping me find my bearings here in Montreal as my IPN buddy) and Kasia Szyszkowicz (and Moe Malik) (for the fun times). A lot of these people have been my social support in the form of long heart to heart conversations, Jam sessions, movie nights, boardgames, potlucks, fun GSAN events and have provided me with academic support as well by giving feedback on my presentations and assignments throughout my PhD. I would also like to make a special mention of **fellow grad students and colleagues I have interacted with over the years through GSAN, PGSS or BrainReach or just from working on the same floor and institute** (I might have missed some names but I thank everyone I've crossed paths with) viz Alberto Osa Garcia, Alexander Bailey, Alice Bruneau, Ana Koshy, Ana Robert, Behrang Shariff ,Belal Howidi, Camille Juzwick, Claire Honda, Claudia Belliveau, Dakota Treleaven, Daniel Andrews, Daryan Chitsaz, Dianne Nakamura, Edwin Wong, Elena Kutsarova, Elizabeth Hua,Etienne Maes, Farin Bourojeni, Fernando Gonzales, Gerardo Ramos, Hannah Swick, Harriet Yan, Hyo Lee, Isabelle Arsenau, Isabelle Rambaldi, Jasmine Lee, Jeanne Madranges, Jemal Yesuf, Jimin Lew, John Aspler, Jonathan Coté, J-P, Kaija Sander, Kaitlyn Easson, Kali Heale, Kim Gruver, Lawrie Shabazian, Malak Abuzgaya, Manesh Girn, Marcel Farres, Mardja Bueno, Maria Zamfir, Marie-Pier, Mario Comaduran, Marion Van Horn, Marissa Cresati, Melissa McSweeney, Melissa Pestemalciyan, Mina Andalou, Morgan KF, Nicole Sanchez, Noor Al sharif, Rafa Perez,Ranjini Garani, Renee Yu, Rita Lo, Robin Sawaya, Ronan Da Silva, Roni Setton, Rowan Pentz, Ryan Mcphedrain, Sabine Ranio, Shanshan Shi, Shubhobrata Das, Sia Kermani, Sienna Drake, Sophie Aurelie, Sreeparna Pradhan, Sujeevini Sujanthan, Sumana Basu, Tara Del, Tasnia Rahman Tony Lin, Tristan Simas, Trycia Kouchache, Vincent Francis and Ziyaan Harji. All these people have been a part of a supportive graduate student community at the IPN that I have had the chance to be a part of for the past 6 years and have made my journey here at McGill an amazing one. I would like to thank **our ex-IPN administrators** Dhabisha, Katherine and Vivian for all that they have done to keep our PhDs smooth and running. I would like to extend my gratitude to **some of my friends from my masters** Danielle Michaud, Natalie Shek, Pradeep De, Monaly Mistry, Sandra Mould, Damar PS and Patricia Goentoro and **some of my friends from my**

undergrad viz Joshua Miranda and Rohan Ichhaporia for providing me with valuable feedback on my thesis seminar presentation and social and emotional support whenever I needed it specially in my final year. I would like to thank **my friends from IISER Pune and ACTREC** viz Sishil Sushanth, Ayantika Sengupta, Roopali Pradhan, Maithilee Khot, Devika Ranade, Apoorva Kulkarni, Trupti, Shalaka Patil and Archit Bagul for offering their support at different points in my PhD. My sincere thanks to **all my friends at Presbyterian College Residence for providing me with social, academic, and spiritual support** (I might have forgotten some names, but I thank everyone). Some of these people include Roland de Vries, Mario, Chitra Ramsurn, Annie Baldessari, Prudence Neba (for our prayers together and for being such a hard-working dean of rez), Fresia Saborio (for prayers and hugs), Michelle Jeong (for all our food dates and long chats), Alexa Nordine (for listening to me present my work), Grace Chen (long chats in the washroom and Zumba sessions), Ankit Gongal, Angello Alcazar, Loveni Hanumanthudu (for Jam sessions), Nashwa Rezwan, Rosaleen Le(for introducing me to the latest rom coms), Anna Sauder (for surfing with me and all the fun times), Elkanah Shekari (for being such an amazing dean of Rez),Alex Marlowe (for the squishy hugs), Maureen (for Zumba sessions), Oliver, Margarita Muinelo, Adrien Mercat, Fatma Said (for sharing her wisdom with me), Satyakam Baruah (for fun conversations in the kitchen), Jeremiah Scalia (for listening to me talk about my work), Silvana, Angella Gallo, Jae, Vincent Li, Grace Wijaya, Kaitlynn, Luisa Hernandez (for helping me in times of distress) and Zafeerah. I would also like to thank **my best friend from high school** Bercila Sathya for being there for me when things got rough in the last few months of my PhD.

I would like to extend my heartfelt gratitude to **Dr. Julie Desmarais, Dr. Alex Ferland, Julie Bédard and Dr. Eric Morris** for providing me with all the necessary tools and support to navigate through grad school. I would also like to thank **Orenda Boucher, Alex Sarakbi and Melanie Demers** for sharing their stories with me and inspiring me to push forward.

My sincere thanks to **all my family members** specially my uncle Dr. Sivarao Digavalli for inspiring me to pursue Neuroscience and advising me to apply to McGill University for a PhD, my aunt Dr. Kamala Digavalli and my grandma Vijayalakshmi Digavalli and my late grandpa Venkataratnam Digavalli for showering me with love always. Last but not the least, I would like to extend my heartfelt gratitude to **my boyfriend Blaize Giangiulio and my parents Syamala Vaddadi (mom) and Uday Vaddadi (dad)** for being my rocks and cheerleaders throughout this journey!! I would like to thank these three people for being my strongest support system during the pandemic and for staying by my side through rough times towards the end of my PhD and seeing me through my journey. I love you guys!!

Contributions

Chapter 1: General Introduction

Writing: N.V. (N.V. prepared Figures 1, 2 and 8)

Editing: J.F.C

Figures 3 and 5 were reproduced with permission from the book Principles of animal communication, 2nd edition.

Figure 4 was reproduced from Nagayama et al. 2014, with permission from the journal Frontiers in Neural Circuits

Figure 6 was reproduced from Cho et al. 2009, with permission from Springer Nature

Figure 7 was reproduced from Brignall et al. 2015, with permission from Springer Nature

Chapter 2: Kirrel2 is differentially required in populations of olfactory sensory neurons for the targeting of axons in the olfactory bulb

This chapter was published in *Development* in 2019. (Vaddadi*, Iversen*, Rajah* et al. 2019) * first co-authors. This paper has only been reproduced in the thesis of Neelima Vaddadi.

Conceptualization: N.V., K.I., R.R., and J.-F.C.

Experimentation: N.V., K.I., R.R., A.P., A.B, and E.D.

Formal analysis: N.V., K.I., R.R., A.P., and A.B.

Writing and editing: N.V., K.I., R.R., A.P., A.B, E.D., and J.-F.C.

Supervision: J.-F.C.

Chapter 3: Understanding the role of homophilic cell adhesion property of Kirrel3 in axonal coalescence in the mouse accessory olfactory system

The data from this chapter was published in *Cell Reports* 2021 (Wang*, Vaddadi*, Pak* et al. 2021) * first co-authors

For this thesis, the manuscript was modified as to include only the data generated to assess the effect of blocking Kirrel3 homophilic interactions *in vivo*. The crystal structure analyses performed by our collaborators are not included but are referenced throughout the chapter as Wang et al., 2021.

Conceptualization of study: N.V, and J.F.C.

Design, development, and characterization of mutant mouse: N.V, and J.F.C.

Experimentation: N.V., S.Q., and E.D.

Formal analysis: N.V.

Writing and editing: N.V. and J.-F.C

Supervision: J.-F.C.

Chapter 4: Understanding the role of Kirrel3 in the regulation of mitral cell dendritic complexity in the mouse main olfactory system

Conceptualization of study: N.V., B.M., and J.-F.C.

Experimentation: N.V., B.M., R.R, E.D.

Formal analysis: N.V., B.M.

Writing and editing: N.V. and J.-F.C

Supervision: J.-F.C.

Chapter 5: Discussion and Conclusion

Writing and Figure preparation: N.V.

Editing: J.F.C

Chapter1: Introduction

1.1. Understanding neural circuits in the developing brain

From a simple knee jerk response to complex cognitive processes, neural circuits in the brain have diverse functional roles. Right from the formation of the neural tube to development of different mature cortical layers in the brain, the brain undergoes a number of different biological processes necessary for forming various functional circuits [1]. These biological processes include different steps such as neuronal outgrowth, growth cone mobility, axonal fasciculation and defasciculation, contact with dendrites, strengthening of synapses between axons and dendrites and pruning of excess dendrites in the brain. The formation of precise neural connections in the brain enables us to execute complex cognitive tasks required for our optimal functioning in our day-to-day life. Inability to form these precise connections as well as malfunctioning of these connections in the brain have been linked to debilitating developmental disorders such as autism spectrum disorders and intellectual disability[10,112]. It is therefore of utmost importance to understand the mechanisms by which neurons make synaptic contacts in the developing brain.

The mouse model proves to be an effective mammalian model system. Within the mouse model, sensory systems such as the visual and olfactory systems form a stereotypic map enabling us to understand how neural circuits are formed. The visual system in particular involves connections between the retinal ganglion cells extending their axons ipsilaterally and contralaterally from the retina to the lateral geniculate nucleus (LGN) where they synapse onto neurons of the LGN [2]. Neurons in the LGN extend their axons ipsilaterally to the visual cortex thereby forming a stereotypic map [2]. Thus, this stereotypic map allows us to break down individual components of the visual circuit and understand how neurons make connections in the brain. In addition to that, this system is easily accessible and easy to manipulate, making it an effective system to examine at neural circuit formation in the brain.

The mouse model can be subjected to numerous genetic manipulations to understand formation and function of neural circuits in the brain. Some genetic approaches that have proven to be useful in understanding mouse

neural circuits include CRISPR cas9 gene editing and homologous recombination in embryonic stem cells to generate knock in and knockout mice, cell type specific manipulation of genes such as the Lox-Cre system whereby genes are knocked out in a cell type specific manner and the inducible dox-tet on system whereby genes can be turned on or off in an inducible manner [3]. Other approaches include optogenetics involving the expression of light sensitive ion channels, pumps or enzymes in specific cell types and understanding their neural connectivity in the brain and behavioral responses upon exposure to light, cell based genomic approaches such as single cell sequencing and fluorescence activated cell sorting FACS and use of DREADDs (designer receptors exclusively activated by designer drugs) [3].

1.2. Cell Adhesion Molecules in Circuit Formation in the Brain

The formation of precise neural circuits in the brain enables us to perform various tasks in our day-to-day life. From an embryo to adulthood, various molecules in addition to neuronal activity, participate in forming and shaping neural circuits in the brain. In addition to spontaneous and induced neuronal activity, neuronal connectivity relies on various molecular guidance cues. Some of them are long range guidance cues such as trophic factors and secreted guidance molecules, and some of them include short range contact dependent cues such as cell adhesion molecules (CAM)[4]. In this chapter, we will be focusing on the role of CAMs in neural circuit formation.

CAMs can be broadly categorized into six categories based on their structures: 1) Integrins, 2) Neuroligins-Neurexins, 3) Cadherins, 4) Leucine repeat rich molecules, 5) Eph ligands, and 6) Immunoglobulin Superfamily molecules [4, 5, 6, 7, 8, 9]. These CAMs modulate a variety of processes during neural circuit formation and function, including axon-axon interactions such as the fasciculation and defasciculation of axons, dendrite-axon interactions, synapse formation and maintenance/destabilization as well as dendrite-dendrite interactions [4]. CAMs can play an important role in circuit formation through contact mediated repulsion or contact mediated attraction. As a result, mutations in several genes encoding CAMs have been identified in human patients with neurological disorders, such as Gilles de la Tourette syndrome, cortical dysplasia-focal epilepsy syndrome, autism spectrum disorders and intellectual disability [10] . In this chapter, a brief overview has been provided of

some of the roles the above-mentioned families of CAMs play in neural circuit formation in the brain, with a special emphasis on immunoglobulin superfamily proteins.

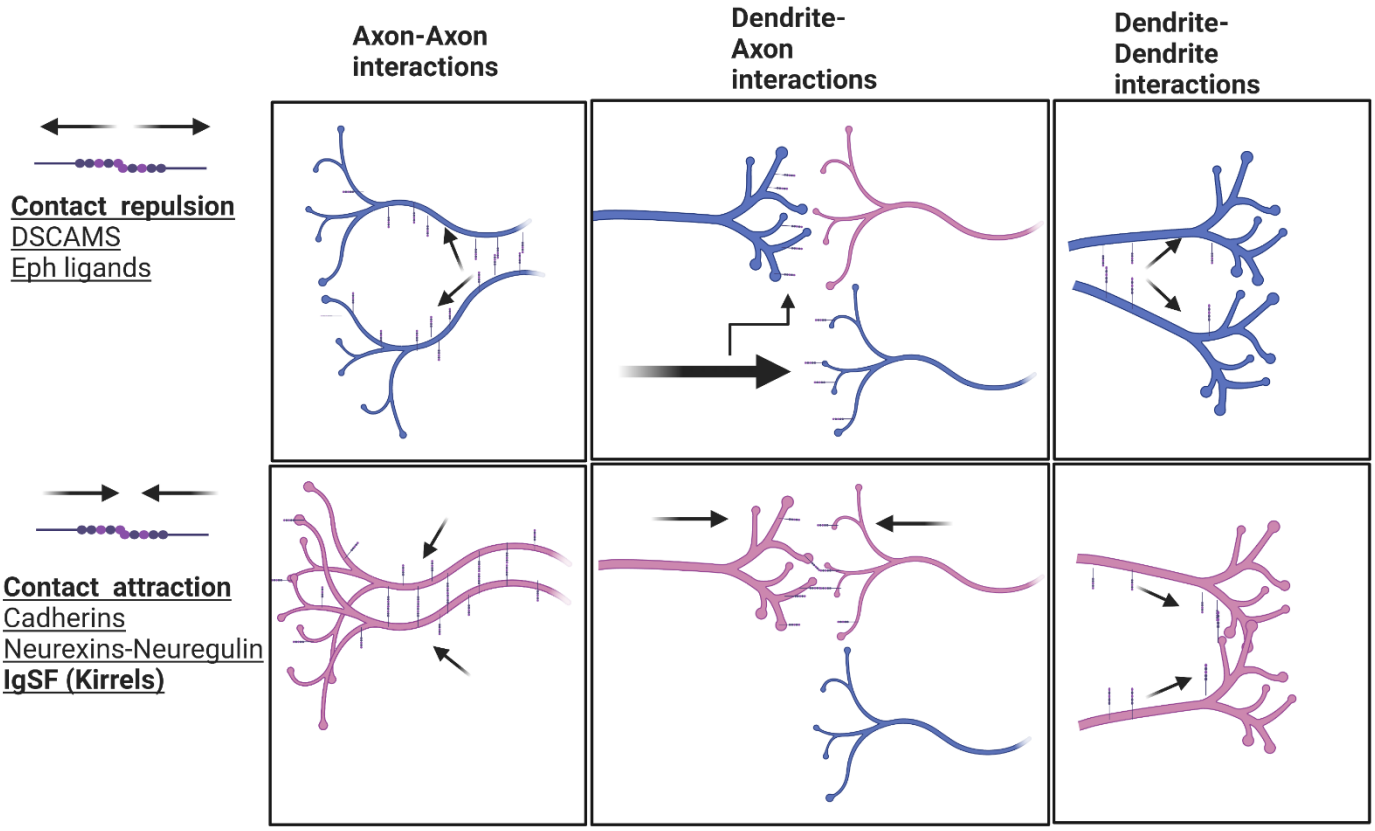

Figure 1. Role of CAMs in neural circuit formation. CAMs can promote both contact mediated attraction or repulsion depending on the identity of the molecules involved. For example, certain members of specific families of CAMs such as DSCAMs, Ephrins and Semaphorins promote repulsion. In contrast, Cadherins, Neurexins and IgSF CAMs such as Kirrels promote interactions between neuronal processes.

Integrins: Integrins are comprised of a heterodimeric complex of different types of α and β subunits [7]. There are 18 different α subunits and 8 different β subunits and in total 24 different αβ heterodimer combinations [7]. Integrins signal in two primary ways: 1) Inside out signaling – the binding of an intracellular protein such as talin activates the extracellular domains of the α and β subunits thereby triggering an interaction with the extracellular matrix (ECM) and 2) Outside in signaling – the binding of an ECM protein to integrins activates intracellular binding to downstream integrin activators such as kindlins, talins or ILKs (Integrin like Kinases) or Integrin inactivators such as Filamin, ICAP1 (integrin cytoplasmic associated protein1) resulting in a downstream signaling cascade [11,12,7]. As a component of tetrapartite synapses involving pre- and post-synaptic

neurons, glial cells, and extracellular matrix, integrins are excellent sensors of dynamic changes occurring in the microenvironment of a synapse [7].

Functionally, integrins have been shown to play a role in cell migration, axonal growth, synapse formation and maturation, homeostatic synaptic scaling, and long-term potentiation (LTP) [13,14, 15, 16, 17, 18, 7]. The subunit composition of integrins underlies their ability to influence different processes in the developing brain. For example, integrins containing the β1 subunit can modulate cell migration, dendritic arborization, NMDA receptor mediated synapse formation, and LTP in the CA1 region of the hippocampus while β3 subunit-containing integrins have been implicated in synapse maturation and homeostatic synaptic scaling [13, 19, 20]. Defects in these processes in mice bearing genetic deletions of the β1 subunit or β3 subunit are associated with behavioral alterations reminiscent of neurological disorders, such as ASD and schizophrenia [7]. β1 subunit-deficient mice appear to be protected against the early effects of drug consumption [21]. In contrast, β3 subunit-deficient mice display ASD-like behaviors, altered anxiety responses, and cocaine craving [22, 23]. In addition, deleting β1 integrin subunit has been associated with impairment in working memory whereas deleting β3 integrin subunit in mice has been linked with dysregulation of emotional behavior [24, 22, 23].

Neurexins and Neuroligins: Neurexins are single pass transmembrane proteins [25]. There are two types of neurexins – α and β and within each type, there are three subtypes (1,2 and 3) [26]. αNeurexins have 6 LNS globulin domains (Laminin, nectin sex hormone binding domain) and 3 EGF (epidermal growth factor) repeats, a transmembrane region, and an intracellular PDZ binding motif [26]. β Neurexins have 1 LNS domain and 1 PDZ binding intracellular domain [26]. Neurexins form calcium-dependent heterophilic interactions with single pass transmembrane proteins called neuroligins [26]. Neuroligins have an AChE (acetylcholine esterase) in the extracellular region and a PDZ binding intracellular motif [26]. Together Neurexin-Neuroligin interactions are bidirectionally involved in the formation and maturation of synapses in the brain.

The inductive role of Neurexins-Neuroligin interactions in synapse formation was demonstrated through experiments in which hemi synapses are formed when either neurexin or neuroligin is artificially expressed in non-neuronal cells and co-cultured with hippocampal neurons[27–29]. When neurexins are expressed in non-

neuronal cells, postsynaptic specializations are observed in neurons and when neuroligins are expressed in non-neuronal cells, pre-synaptic specializations are observed in neurons indicating that both neurexins and neuroligins play an inductive role in synaptogenesis [27–29]. Neurexins can promote presynaptic assembly by interacting with CASK, Mint and 4.1 actin binding protein thereby allowing assembly of synaptic vesicles [4,26]. Neuroligins are involved in post-synaptic assembly by interacting with PSD95 thereby facilitating NMDA and AMPA receptor recruitment to the cell surface [4,26,30].

Mice with a triple knockout of all three types of α Neurexin die shortly after birth due to respiratory failure because of a reduction in type 2 synapses i.e., symmetric inhibitory synapses in the brainstem [10,31]. On the other hand, β Neurexin triple knockout mice show a reduction in excitatory neurotransmitter release in hippocampal neurons [10,32]. Neuroligin1 has been shown to be localized at excitatory synapses and its ablation results in a deficit in NMDA mediated synaptic transmission [30,33,34]. Neuroligin2 has been shown to be localized at inhibitory synapses and a KO result in a deficit in GABA mediated synaptic transmission [33–35]. Neuroligin3 has been shown to be localized at both inhibitory and excitatory synapses [26,33]. RNAi knockdown of neuroligins3 result in a decrease in excitatory and inhibitory synapse numbers in hippocampal neuronal cultures [26,33,36]. These synapses have been shown to be functional as neurons in culture have shown changes in mEPSCs upon manipulation of neurexin or neuroligin levels in culture in several studies [26,33,34]. Manipulation of neurexin or neuroligin levels has also been linked to changes in Excitation to Inhibition ratio (E/I) [37]. E/I ratio changes are a classic hallmark of ASDs and thus mutations in Neurexins and Neuroligins have been linked to autism spectrum disorders [38–41]. Thus, both Neuroligins and Neurexins play crucial roles for synapse formation and function in the nervous system.

Cadherins: Cadherins can be classified into several sub-families which include fat cadherins, protocadherins, seven-pass transmembrane cadherins and classical cadherins [42]. In this review we focus on classical cadherins. Classical cadherins have 5 extracellular domains that bind to calcium, a single transmembrane domain, and an intracellular tail region with PDZ binding domain [43]. Out of the classical cadherins that exist, N-cadherin is the most studied and understood in neural circuits. The extracellular domain of cadherins obtain a rod-like rigidity

upon binding to calcium thereby stabilizing the cadherin-cadherin interaction [6]. The levels of calcium in the synaptic cleft therefore greatly influence the stability of cadherin-cadherin adhesion [6]. Intracellularly, cadherin binds to different families of catenin proteins. There are four main types of β and α catenins that bind to the more distal intracellular tail of cadherin, and p-120 and δ catenins that bind to the proximal end of the intracellular tail of N-cadherin. α catenins are known to associate with β catenin and F actin and thereby serve as a bridge between cadherins and polymerization of F-actin [42]. Phosphorylation of β catenin is linked to its detachment from N-cadherin thereby weakening cadherin-cadherin adhesion [42]. P120 catenin is involved in the process of indirectly activating a phosphatase that dephosphorylates β catenin thereby stabilizing β catenin- N-cadherin contact and thereby stabilizing N-cadherin adhesion [42]. Cadherins are typically localized to excitatory synapses, although cadherin 11 and cadherin 13 are known to promote inhibitory synapse formation [42,44].

Presynaptically, cadherins are important in the localization of synaptic vesicles and exocytosis of synaptic vesicles into the synaptic cleft, while cadherins are important for regulating dendritic spine morphology in the post-synaptic neuron, thereby regulating mEPSCs [6,42,43]. Cadherins are also involved in the recruitment of NMDA and AMPA receptors by physically associating with these receptors and other receptor binding proteins such as ABP (AMPAR binding Protein) and GRIP (Glutamate Receptor Interacting Protein), and by preventing the lateral diffusion of these receptors [42,45]. Cadherins thus play an important role in LTP induction and maintenance [6,46,47]. Disruption of N-cadherins using antibodies has been shown to disrupt LTP in cultured hippocampal neurons [6,46,47].

Leucine Repeat Rich Molecules: Leucine repeat rich (LRR) proteins have been shown to be effective organizers of excitatory and inhibitory synapses in neural circuit development [48]. LRR proteins are transmembrane proteins with an extracellular horseshoe solenoid structure whose concave side constitutes continuous β sheets and form excellent protein binding motifs [5]. The LRR family of proteins contain five main members which include: 1) The Netrin G Ligands (NGLs), 2) Leucine repeat rich transmembrane neuronal proteins (LRRTMs), 3) The Slitrks 4) Synaptic cell adhesion like molecules (SALMs) and 5) The Fibronectin Leucine repeat rich Transmembrane proteins (FLRTs) [5,48]. All the above mentioned LRR family proteins

except FLRTs induce presynaptic differentiation in axons of neurons when expressed in non-neuronal cells co-cultured with neurons [48,49].

The NGLs include NGL1, NGL2 and NGL3 that bind to Netrin G1, Netrin G2 and LAR respectively [48,50]. Netrin G ligand is different from the secreted Netrin family members in that they are GPI anchored proteins, they do not have any invertebrate homologs, and they do not bind to DCC and Unc5 [50]. NGLs have been implicated in excitatory synapse formation and regulation of dendritic spine morphology in hippocampal neurons in culture [50,51]. They mediate their synaptogenic effects by allowing clustering of AMPA and NMDA receptors via their PDZ domain [51]. NGL-Netrin G expression is also important in the retinal circuitry whereby NGL2 is expressed in Horizontal cells and Netrin G2 is expressed in photoreceptor rod cells [52]. Knockdown of Netrin G2 causes Horizontal cell axons to overshoot the photoreceptor rod cells and form inaccurate synapses [52]. NGL3-LAR interactions are also important in presynaptic specification as LAR interacts with lipirinα which is involved in clustering of synaptic vesicles [50].

The LRRTMs constitute 4 members and are known to interact with neurexins in trans [53,54]. LRRTM1-3 interact with neurexins lacking splice site 4 however, LRRTM4 interacts with neurexins with or without splice site 4 [55,56]. LRRTM4 is also known to interact with heparan sulfate glypicans in trans along with co-receptor Protein tyrosine Phosphatase (PTP) σ to induce presynaptic differentiation in neurons co-cultured with non-neuronal cells expressing LRRTM4 [56]. Overexpression of LRRTM2 or 4 increases the density of excitatory but not inhibitory synapses in culture and LRRTM1 knockout results in more dispersed synaptic vesicles, immature dendritic spines, and a decrease in excitatory synaptic density [5,53,54,57–59].

Slitrks include members 1 to 6 and they bind to PTP δ and PTPσ from LAR Receptor Protein tyrosine phosphatase (RPTP) family [60–62]. Slitrk1,2,4,5 and 6 are involved in the formation of excitatory synapses whereas Slitrk 3 is actively involved in the formation of inhibitory synapses [61,63]. The effect of Slitrks on excitatory synapses requires interactions with PTPσ whereas their effect on inhibitory synapses involves an interaction with PTPδ [61,63]. Slitrk3 knockdown has been linked to decreased inhibitory synapse density in the

hippocampus [5,48,61,63]. Slitrks may also regulate dendritic arbour complexity as loss of Slitrk 5 has been linked to a reduction in dendritic arbor complexity of striatal neurons and reduction in NMDA and AMPA levels [5,48,64].

The SALM family includes 5 members (1-5) [5]. While some family members such as SALM 4 and 5 can undergo homophilic adhesion, SALM 3 and 5 interact with LAR RPTPs [65–67]. SALM 5 knockdown is linked to a decrease in mEPSC frequency in CA1 neurons while SALM 3 knockout is linked to a decrease in mEPSC frequency indicating that a reduction in the level of these molecules results in reduced excitatory synaptic density [5,48,66,67]. On the other hand, Knockout of SALM4 is linked to increase in mEPSC frequency and PSD density in CA1 neurons and an increase in excitatory synapse numbers [5,48,65]. This is because SALM4 inhibits SALM3 synaptogenic activity in cis [65].

FLRTs 1-3 are known to interact with Latrophilins 1-3 respectively[49,68]. Latrophilins also bind to teneurins [5,48]. While FLRTs do not induce pre-synaptic specification in culture, teneurins do, indicating different modes of action of different molecules with similar interactors [49,69]. FLRT 2 and 3 bind to Unc5 in the cortex and control neuronal migration and FLRT3 regulates glutamatergic synapse formation in cultured neurons and in vivo via interactions in trans with latrophilins but not via teneurins [48,70]. FLRTs do not have a PDZ binding domain but mediate their effects by binding to other receptors in cis such as Fibroblast Growth Factor Receptor, Protocadherins, cadherins and Robo1 [48].

Thus, LRR proteins are involved in various neuronal functions such as neurite outgrowth, neuronal migration, synapse formation and maturation and growth cone regulation [5,48].

Ephrins: Ephrin ligands interact with their receptors EphR [4]. Ephrin-EphR interaction results in bidirectional signalling [4]. Evidence suggests that depending on whether the signalling is forward or reverse, Ephrin-EphR interaction can result in repulsion or attraction between individual components of neural circuits [4,71,72]. Ephrins are known to be presynaptic ligands for EphR [4]. EphRs have been shown to modify postsynaptic organization through recruitment of NMDA and AMPAR receptors [4,73–76]. Signalling downstream of EphR involves EphR kinase dependent phosphorylation of Rho-GEF followed by Rac/PAK activation leading to actin rearrangement [4,75]. Studies suggest that signalling downstream of EphRs specially EphB results in shortening of dendrite

filopodia [4]. Knockout of EphB1, Eph B2 and Eph B3 results in viable mice [4,76]. However, these mice have 40% fewer synapses in the cortex [76]. Expressing EphB2 in individual neurons in cultured brain slices rescues defects observed in EphB2 -/- mice indicating a cell autonomous role of ephB2 in synaptogenesis and formation of excitatory postsynaptic specialization [76]. Eph-Ephrin interactions have been shown to be repulsive in nature in the mouse visual and olfactory system [71]. In the mouse accessory olfactory system however EphrinA5-Eph A6 reverse signalling through interaction between ephrin A5 on VSN axons and EphA6 on mitral cells in the accessory olfactory bulb serves as an attractive cue for VSN axons targeting the anterior AOB [77]. On the other hand, Eph-Ephrin expression levels have been shown to be regulated by neuronal activity in the mouse main olfactory system [78]. Ephrin ^{low}/Eph ^{high} – Ephrin ^{high}/Eph^{low} axon-axon interactions allow for the repulsion of non-like axons directing them to their appropriate targets [79]. Expression level of Ephrins and EphRs in OSNs has been shown to be regulated by OR derived cAMP [78].

IgSF cell adhesion proteins: Immunoglobulin superfamily IgSF cell adhesion molecules are cell adhesion molecules that contain extracellular immunoglobulin domains [80]. These can be GPI anchored proteins such as IgLONs, Contactins and NCAM 120 or transmembrane proteins such as some isoforms of NCAM (NCAM 180 and NCAM 140), SynCAM, Nectin, DSCAM and Kirrel family of proteins [81–87].

The IgLON family includes IgLON 1 or opioid binding cell adhesion molecule (OBCAM), IgLON 2 or Neurotrimin, IgLON3 or LAMP or LSAMP, IgLON4 or Kilon or neuronal growth regulator (NEGR1) and IgLON5 [81,88–92]. IgLONs exhibit homophilic and heterophilic adhesion properties and have been implicated in neurite outgrowth, axonal fasciculation and synaptogenesis [81]. Combinatorial expression of Drosophila equivalent of IgLONs i.e. DIP-DPRs have been implicated in sorting and targeting of olfactory receptor neuron axons [81,93]. IgLON4 or Kilon is a crucial modulator for synapse number in the hippocampus [88].

Contactins are another example of GPI anchored IgSF CAMs. Contactin 1 (Cntn1) has been shown to play an important role in myelination and oligodendrocyte maturation while contactin 6 and 4 (Cntn6 and Cntn4) have been identified as candidate risk genes for schizophrenia [82]. Cntn4 is a well-known axon guidance molecule important in odor map formation in the olfactory bulb [10]. Knockout of Cntn4 results in the misprojection of

olfactory sensory neurons to glomeruli [10]. Cntn6 plays an important role in dendritic arborization in deep layer cortical neurons and branching of axons in the corticospinal tract [82]. Knockout of Cntn4 results in impaired Long-Term Potentiation in the CA1 region of the hippocampus and abnormal dendritic arborization and spines in CA1 neurons [82]. Whether the abnormal spine morphology in the CA1 was a cause or consequence of impaired LTP is unknown. Furthermore, an increase in contextual fear conditioning was observed in Cntn4 knockout mice indicating a connection between altered CA1 circuitry and impaired associative learning [82].

Neural cell adhesion molecule NCAM has three isoforms NCAM 180,140 and 120 [94]. NCAM 120 is GPI anchored while NCAM 180 and 140 are transmembrane IgSF proteins [94]. NCAM has been shown to play a very important role in learning and memory [94]. Mice deficient in NCAM have been shown to have a dysregulated CREB pathway [95]. Polysialylation of NCAM has been strongly implicated in neural plasticity and abolition of polysialylation impairs learning in mice [83,94]. The addition of a PSA group to NCAM is thought to provide a strong negative charge on NCAM preventing NCAM-NCAM interaction, thereby acting as a spacer in labile synapses [94]. Extracellularly NCAMs can interact with tyrosine kinase receptors, Fibroblast growth factor receptors and Glutamatergic receptors. Intracellularly, NCAM associates with spectrin, Fyn and MAPK [94,96]. Thus, PSA-NCAM is associated with plastic changes in a synapse, whereas NCAM-NCAM interactions are associated with stability and consolidation of memory [94]. Absence of PSA group on NCAM has been linked with impairment in learning and memory and premature differentiation of newly born neurons [94,96]. Typically, an increase in PSA-NCAM is observed after spatial and non spatial learning tasks followed by a decrease [83,94–96]. Ablation of polysialylation impairs learning in mice [94].

SynCAMs are another class of transmembrane IgSF molecules with a cytoplasmic tail with a PDZ binding motif [84]. SynCAM protein levels are lower at birth in mice and rats and are found to increase over the first three postnatal weeks which is a major period for synaptogenesis [84]. The cytoplasmic tail of SynCAM is known to bind to CASK and neuroligin 1 thereby highlighting the molecules role in synaptogenesis [84,97]. SynCAM is expressed in pre and postsynaptic compartments and overexpression of SynCAM in cultures not only increases synapse numbers but also increases mini frequency two to threefold [84]. Overexpression of full length SynCAM

increased spontaneous synaptic activity and presynaptic induction by SynCAM in heterologous cultures [84]. No difference in functionality of synapses was observed between regular synapses and heterologous synapses [84].

Nectins and Nectin-like molecules (Necls) are transmembrane cell adhesion molecules belonging to the IgSF family [98]. Nectins comprise of three Immunoglobulin domains, a transmembrane domain and a cytoplasmic tail that binds to the adaptor protein afadin, which is involved in F-actin polymerization [99]. There are 4 members in the nectin family nectin 1,2,3 and 4 [99]. Necls on the other hand are similar to nectins extracellularly but the cytoplasmic domain does not bind afadin [99]. Nectins exhibit homophilic and heterophilic interactions with other nectins and necls [98,99]. The heterophilic interactions have been shown to be stronger than homophilic interactions [99]. Nectin interactions are calcium independent [99].

Down Syndrome Cell Adhesion Molecule DSCAM is another transmembrane IgSF CAM important in neural circuit formation[86]. Dscam 1 in flies has been shown to be very important for dendrite self avoidance [86]. A mix of different isoforms of Dscam1 are expressed on dendrites from a particular neuron that are different from that of the adjacent neurons [86]. Thus, dendrites from adjacent neurons intersect but dendrites from the same neuron do not thereby maximizing the arborization and coverage area [86]. Similarly, neurons in certain brain regions can be organized as columns whereby neurons in one column or area do not intersect with neurons from another column [86]. This is called tiling. Dscam2 in flies has been shown to play an important role in tiling [86]. Homophilic interactions followed by repulsion between neurons in the adjacent columns rather than in the same column is crucial for tiling [86]. Loss of cytoplasmic domain of Dscam 1 or 2 has been linked to loss of self avoidance or tiling respectively indicating that the cytoplasmic domain of Dscam is important for contact mediated repulsion in dendrite self avoidance and tiling [86,100]. In vertebrates DSCAM has been shown to play an important role in tiling between amacrine cells in the visual system [86,101].

The Kirrel family of proteins: The Kirrel family of proteins are transmembrane proteins with 5 extracellular immunoglobulin domains with a signal peptide region, a transmembrane domain and an intracellular domain with a PDZ binding motif [102]. In vertebrates, the family consists of 3 members Kirrels 1,2 and 3 (also known as Nephs) [102]. Kirrel family of proteins were first described to play a role in the formation and maintenance of

the slit diaphragm and filtration barrier in the kidneys [103]. In addition to the kidney, Kirrels are widely expressed in other tissues, including brain, muscle and adipose tissue [104].

The homolog of Kirrel in C.elegans SYG-1 has been shown to play a role in synapse formation, synapse specificity and synaptic pruning [105,106]. Homologs of Kirrels in Drosophila (IRM proteins) have been shown to play a role in intercellular adhesion, cell-cell recognition and cell signalling events important for morphogenesis [107–109]. These proteins have also been shown to play an important role in axon path finding, target selection and cell sorting [72,107,110]. Homologs of Kirrels in Drosophila have been shown to play an important role in sense organ pattern formation and axon targeting of visual columnar neurons [107–109]. Meanwhile Kirrel homolog SYG-1 in glial cells in C.elegans interacts with the cleaved extracellular fragment of Robo released from neurons allowing the migration of glial cells [111]. Interaction between Kirrel homolog SYG-1 and Nephrin homolog SYG-2 in c.elegans is important for guiding HSN (Hermaphrodite specific motor Neurons) to their target vulval epithelial guidepost cells indicating that heterophilic interaction between Kirrels and Nephrins are important in axon targeting [106].

In the mouse, Kirrel3 has been implicated in synapse formation in the hippocampus [102]. Ablation of Kirrel3 leads to loss of feed forward inhibition from GABAergic neurons in the Dentate Gyrus to the CA1 pyramidal neurons resulting in increased excitability of CA1 neurons [102]. Results from this study indicate that Kirrel3 plays an important role in the target specific synapse development in the hippocampus [102,112]. Kirrels have been shown to possess a homophilic cell adhesion property in vitro [112,113]. However, whether this property is required for target specific synapse formation in vivo has not yet been demonstrated. This study proposes a role for Kirrel3 homophilic cell adhesion property in target specific synapse formation in the hippocampus [102]. A recent study examining the impact of missense variants in Kirrel3 (implicated in autism and intellectual disability) on synaptogenesis reveals that 5 out of 6 missense variants when expressed in hippocampal neurons cultured in vitro displayed weakened synaptogenesis [112]. Interestingly, only two of these missense variants lacked homophilic cell adhesion in trans between Kirrel3 molecules, the other three missense variants were observed

in the intracellular domain [112]. This suggests that the homophilic cell adhesion property of Kirrel3 is necessary but not sufficient for its synaptogenic function [112].

Kirrel2 and Kirrel3 have been shown to be expressed in the olfactory system during embryonic and early postnatal stages [114,115]. Kirrel2 and Kirrel3 are expressed in different amounts and combinations along the surface of sensory neuron axons whereby some axons express high Kirrel3 and low Kirrel2, some axons express low Kirrel3 and high Kirrel2, some axons express high Kirrel3 and no Kirrel2 while some express high Kirrel2 and no Kirrel3[87,114,115]. It has been proposed that these sensory neuron axons with similar expression profile of Kirrel2 and Kirrel3 group together and sort into specific glomeruli in the CNS where they synapse onto mitral cells [87,113,114]. Our lab has shown that in the accessory olfactory system Kirrel2 and Kirrel3 are essential for coalescence and sorting of vomeronasal sensory neurons into glomeruli [114,115]. It has been proposed that Kirrels serve as molecular Velcro allowing the coalescence of like neurons via their homophilic cell adhesion property [113–115]. However, the role of this homophilic cell adhesion property in vivo has not yet been demonstrated.

Evidence from behavioural studies suggests that the neuroanatomical defects observed in *Kirrel3-/-* mice are associated with reduced novelty seeking behaviour and reduced socialization which are common behavioural alterations observed in patients with autism spectrum disorder [9,116]. In addition to that, mutations in *KIRREL3* have been reported in human patients with learning disabilities and autism spectrum disorders suggesting a potential role for Kirrel3 in neurodevelopment thus making this gene an interesting gene candidate [117,118].

Concluding Remarks: Thus, in this section, we looked into the role of various cell adhesion molecules in neural circuit formation. Manipulation of these cell adhesion molecules in mice either by knocking out these CAM genes or by introducing mutations in these genes results in various neurodevelopmental defects [7,10,42,48]. A lot of these cell adhesion molecules are also risk candidate genes for neurodevelopmental conditions in humans further emphasizing their important role in circuit formation [10].

A majority of the above-mentioned cell adhesion molecules play a very important role in synaptogenesis by strengthening interactions between dendrites and axons and through the recruitment of synaptogenic proteins such as NMDA and AMPA receptors and PSD95 at the postsynaptic synapse and through the recruitment of synaptic vesicles at the presynaptic site. Some of these molecules are involved in contact mediated repulsion (example: Eph Ligands [71] and DSCAMs [86]) while some of these CAMs are involved in contact mediated attraction (examples IgSF: Kirrels [113] and Neurexins-Neuregulins [26]). The specific roles of these different families of CAMs are highlighted in summary Figure 2 below.

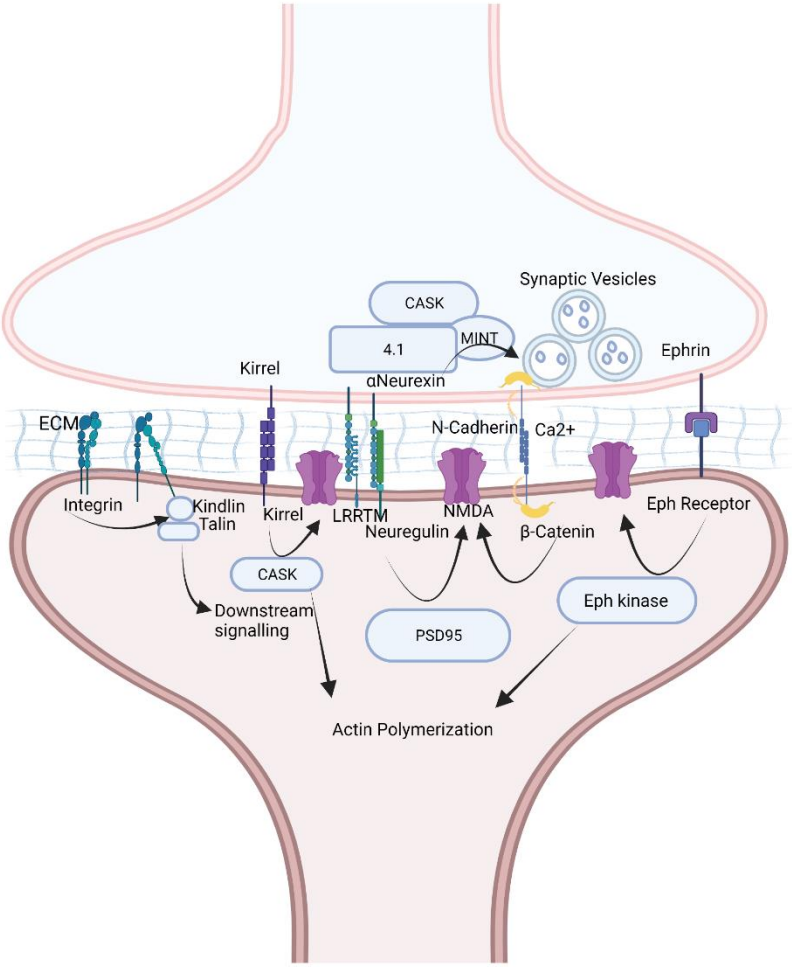

Figure 2. Summary of role of CAMs at synapses. In this figure, the role played by various CAMs at synapses during circuit formation is represented. Integrins bind to the ECM and change conformation to interact with integrin activators such as kindlins and talin further resulting in a downstream signaling cascade. Kirrels have a PDZ domain that might play a role in recruitment of NMDA receptors to the cell surface. The intracellular domain of Kirrels also interacts with CASK resulting in actin polymerization downstream. Neurexins and Neuregulins interact resulting in the recruitment of NMDA receptors to the cell surface by neuregulin on the postsynaptic side and clustering of synaptic vesicles Neurexin and CASK-Mint-4.1 complexes on the presynaptic side. Similar processes occur when LRRTMs interact with Neurexins. Cadherins bind to β catenin, which in the presence of calcium stabilizes cadherin-cadherin interaction. Binding of β catenin to cadherin results in the recruitment of NMDA receptor to the cell surface. Binding of EphR to Ephrin results

in postsynaptic recruitment of NMDA receptors to the cell surface and also results in F-actin polymerization via Eph Kinases**.**

1.3 The Mouse Olfactory Systems

The olfactory system, is crucial for the survival of living organisms such as bacteria and some mammals that rely on the detection of odorants and chemosignals to find their food and reproduce such as rodents, dogs and wild animals [119]. In this chapter, we will be focusing on the mouse olfactory system. The mouse olfactory system can be subdivided into the main and accessory olfactory systems. The circuits of both of these systems are organized in such a way so as to form stereotypical neural maps of activation in the brain. In addition to that, the mouse olfactory system is easily accessible for manipulation and is involved in the control of various innate social and sexual behaviors. Thus, the impact of manipulating the olfactory system on behavior can be easily identified making the mouse olfactory system an important model system for neurodevelopmental research.

The main olfactory system is an excellent sensor of the environment in mice used to detect food, predators, prey, and mark territory while the accessory olfactory system has specially developed for the task of finding a receptive mate [119]. In addition to that, the accessory olfactory system plays an important role in modulating social behaviors such as aggression, suckling and territoriality [119]. Thus, both systems are complementary in their function and are very similar in their broad organization.

1.3.1 Organization of the main olfactory system

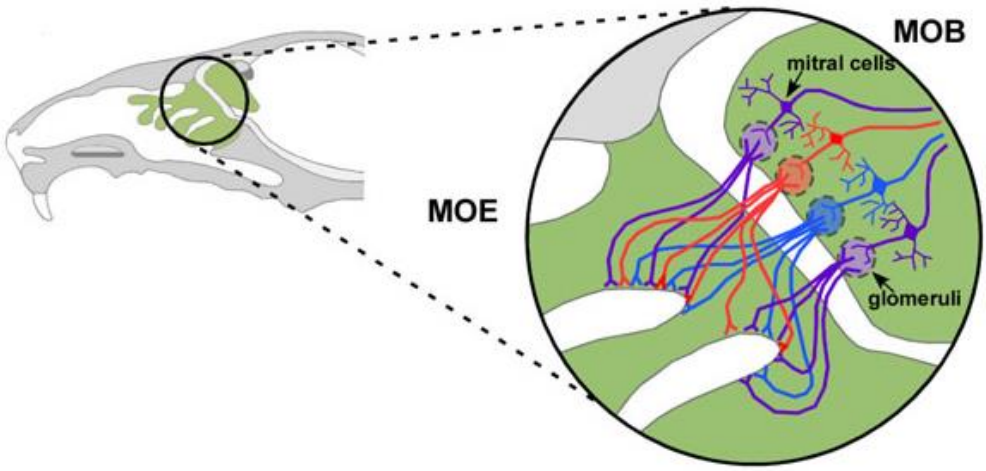

Figure 3. Overview of the mouse main olfactory system. Olfactory sensory neurons (OSNs) project their axons from the olfactory epithelium (MOE) to the main olfactory bulb (MOB). Each OSN expresses an olfactory receptor (OR). All OSNs expressing the same OR coalesce into common target neuropil structures, called glomeruli, and synapse onto the dendrites of 2nd order projection neurons termed mitral cells. (Reproduced with permission from Principles of animal communication 2nd Edition [120])

The main olfactory system is comprised of olfactory sensory neurons (OSNs) whose cell bodies reside in the olfactory epithelium which is formed by a series of cartilaginous outcroppings called turbinates in the upper nasal cavity of mice [78]. The OSN is a bipolar neuron which has a single dendrite extending up to the olfactory epithelium [78]. It ends in a knob-like swelling from which 20-30 cilia emerge in the olfactory epithelium [119]. The cilia are covered in a layer of mucous secreted by Bowman's glands that sit on top of a connective tissue called lamina propria [119]. In addition to the OSNs, there are supporting cells called sustentacular cells in the olfactory epithelium that provide nourishment to the OSNs [78,119]. Basal cells, located closer to the basement membrane, are stem cells that give rise to OSNs in the continually regenerating olfactory epithelium[121]. The olfactory sensory neuron axons project from the olfactory epithelium to a region of the mouse brain called the main olfactory bulb (MOB) [121](as shown in Figure 3). In the mouse, each OSN expresses a single olfactory receptor (OR) out of a repertoire of over 1000 ORs [121]. A single OSN expresses a single OR [122]. ORs bind to volatile odorant molecules [122]. All OSNs expressing the same OR regardless of the position of its cell body in the OE coalesce into two spatially conserved homogenously innervated neuropil structures called glomeruli in the OB [122]. These axons then synapse onto the dendrites of second order projection neurons called mitral cells

that project their axons to higher centers in the brain such as the piriform cortex, the amygdala, the olfactory cortex, the olfactory tubercle, the anterior olfactory nucleus, and the entorhinal cortex [123].

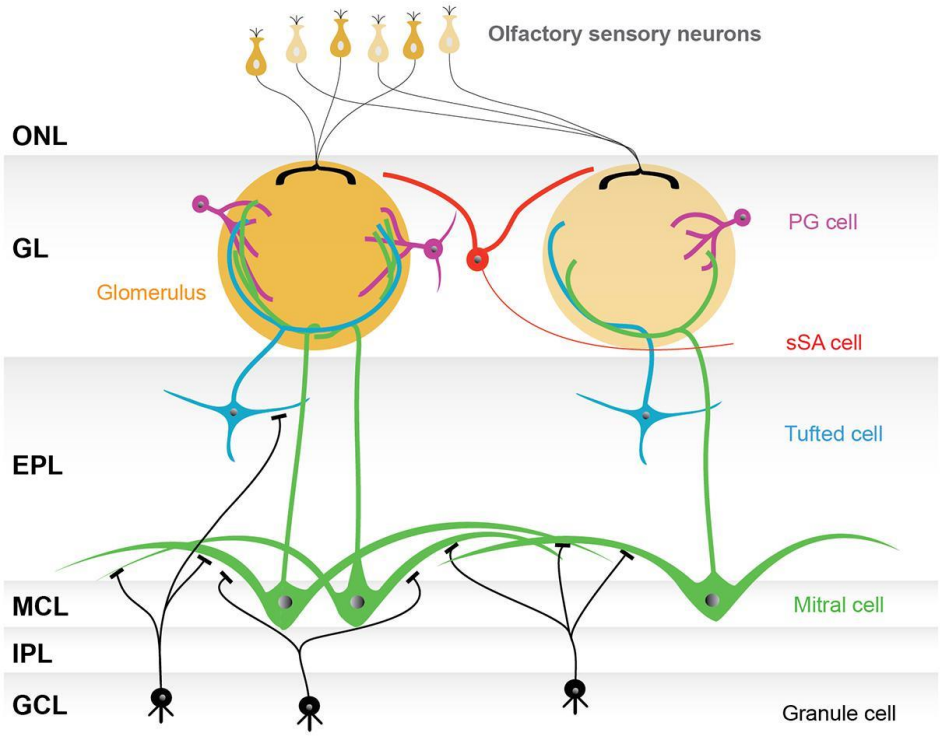

Figure 4. Organization of cells of the olfactory bulb. The olfactory bulb is organized into 5 different layers of cells viz Glomerular layer, External Plexiform Layer, Mitral cell layer, Internal Plexiform Layer and Granule Cell Layer. Mitral cell bodies reside in the mitral cell layer and project their dendrites into glomeruli in the glomerular layer. (Reproduced with permission from Nagayama et al., 2014 [124]).

The adult mouse olfactory bulb can be divided into 5 layers, from exterior to interior, that include the glomerular layer, external plexiform layer, mitral cell layer, internal plexiform layer and granule cell layer (See figure 4) [124]. As the name suggests, the mitral cell bodies reside in the mitral cell layer and project their dendrites to the glomerular layer where they receive inputs from the OSN axons [124].

Mitral cells arise from precursor cells born in the ventricular zone of the brain between E11.5 to E13 [125]. These mitral cell precursors then migrate from the ventricular zone to the intermediate zone of the OB [125]. From the intermediate zone, they then project their axons to the olfactory cortex via the lateral olfactory tract. Following this event, the mitral cells reorient themselves from a tangential position to a radial position and around E15-E16, they project their dendrites towards the glomerular layer of the OB, where they form synapses with OSN axons [125]. The dendrites can be classified as primary dendrites which are primary extensions from the mitral

cell body in the mitral cell layer to the glomerular layer (as indicated in Figure 4) and secondary dendrites which include extensions coming out of the primary dendrite instead of the mitral cell body [126]. The mitral cell primary dendrites meet OSN axons in the glomerular layer to form a protoglomerulus [125]. During the initial phases of development, immature mitral cell extends multiple primary and secondary dendrites into the glomerular layer [126]. However, over the course of development, as mitral cells mature, some of these extensions are pruned off such that a single mature mitral cell innervates a single glomerulus [126]. From P0 to P4 more than 50% of the mitral cells innervate more than one glomerulus [126]. However, from P6 to adulthood, a reduction in that proportion is observed. In adults, about 85% of the mitral cells are mature, i.e., a single mitral cell innervates a single glomerulus [126,127].

Some examples of other cell types in the OB include periglomerular cells, tufted cells and granule cells [124]. Periglomerular cells are inhibitory interneurons whose cell bodies are located in the interglomerular space in the glomerular layer [124]. The cell bodies of these cells are found lining glomeruli in the glomerular layer and are the most abundant type of neuron in the glomerular layer [128]. Each periglomerular cell extends its dendrites into a single glomerulus and it receives inputs from and sends outputs to other periglomerular cells, mitral cells, tufted cells and OSNs [124]. A periglomerular cell usually has an axon that extends as far as 5-6 glomeruli and terminates in the interglomerular space [129]. However, some axonless periglomerular cells also exist [124]. Tufted cells on the other hand, have their cell bodies located in the external plexiform layer (EPL) and they extend their dendrites into the glomerular layer and their axons into the anterior part of the olfactory cortex [124]. Tufted cells differ from mitral cells morphologically in the location of their cell bodies (mitral cell soma in the MCL whereas tufted cell soma in the EPL) and functionally in the manner in which they process odor evoked stimuli [124]. Tufted cells display a higher sensitivity to odor evoked stimuli than mitral cells [124]. Granule cells are axonless inhibitory neurons that extend dendrites onto mitral cells and tufted cells forming reciprocal dendrodendritic synapses with these cells [124]. Granule cells have their soma present in the granule cell layer (GCL) from where they form dendrodendritic synapses with mitral cells and tufted cells [124].

1.3.2 Organization of the accessory olfactory system

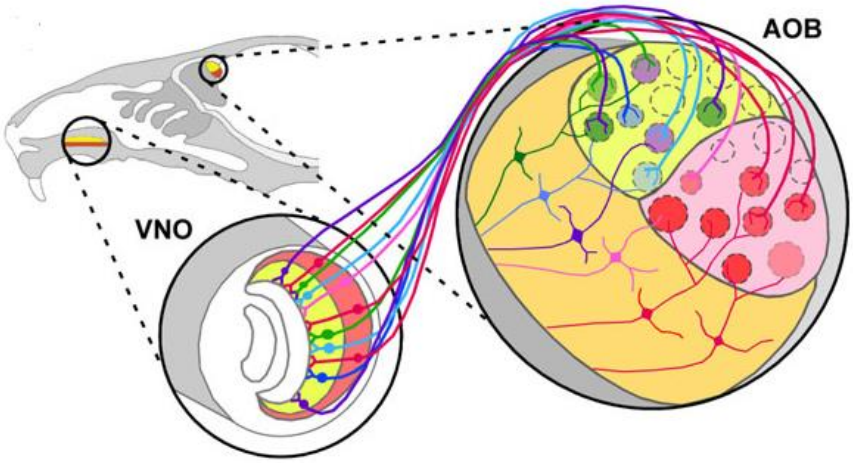

Figure 5. Overview of the mouse accessory olfactory system. Vomeronasal sensory neurons (VSNs) project their axons from the vomeronasal organ (VNO) to the accessory olfactory bulb (AOB). Each VSN expresses a vomeronasal receptor (VR). All VSNs expressing the same VR coalesce into spatially conserved homogenous glomeruli and synapse onto dendrites of 2nd order projection neurons called mitral cells in glomeruli. (Reproduced with permission from Principles of animal communication 2nd Edition[120])

The accessory olfactory system is very similar in its broad organization to the main olfactory system. It consists of Vomeronasal sensory neurons (VSNs) whose cell bodies reside in the Vomeronasal organ (VNO) located at the base of the nasal septum [130]. VSNs are present in the basal and apical VNO [130]. VSN cell bodies present in the apical VNO express members of the V1R family of vomeronasal receptors that signal through a G protein that contains the Gαi subunit and project their axons to the anterior part of the accessory olfactory bulb (AOB) or in the posterior dorsal part of the OB [130–132]. VSN cell bodies present in the basal VNO express the V2R family of VRs and signal through the Gαo subunit [130–132]. These VSNs project their axons to the posterior part of the AOB [130]. In addition to that, a sub-population of VSNs express a family of non-classical class 1 major histocompatibility Mhc genes also known as H2-Mv genes, which have been shown to regulate cell surface expression of VRs [130,133–135]. V2R/H2-Mv positive axons target the posterior most part of the AOB thus forming a tripartite organization in the AOB- V1Rs, V2Rs and V2R/H2-Mv [130,133–135]. Unlike the main olfactory system, a mature mitral cell in the accessory olfactory system can innervate more than one glomerulus [120,136]. Some mitral cells innervate glomeruli receiving VSN axons expressing the same VR type and are therefore called

homotypic mitral cells and some mitral cells innervate glomeruli receiving VSN axons expressing different VR type and are therefore called heterotypic mitral cells [120,136–138]. The presence of homotypic and heterotypic mitral cells and the fact that a mature mitral cell in the accessory olfactory system innervates more than one glomerulus in the mature mouse brain makes understanding mitral cell development of mitral cells in the accessory olfactory system more challenging than that in the main olfactory system.

1.3.3. Establishment of neural circuitry in the olfactory systems

During development of the main olfactory system, olfactory sensory neurons project their axons into glomeruli of the olfactory bulb in a stereotypic fashion to form glomerular olfactory maps [78]. The coarse projection of OSN axons in the three-dimensional structure that is the OB is regulated by axon guidance cues that direct the growth of OSN axons [78]. The projection of OSN axon along the dorso-ventral axis of the OB correlates with the location of OSN cell bodies along this axis in the olfactory epithelium [78,139–141]. For example, OSN cell bodies in the dorsomedial region of the OE project their axons to the dorsal part of the MOB whereas OSN cell bodies in the ventrolateral region of the OE project to the most ventral region of the MOB [78].

The selective distribution of axons guidance receptors also modulate the anterior-posterior and medial-lateral targeting of OSN axons in the OB [78,121].

On the other hand, the coalescence of OSN axons along the anterior-posterior (A-P) axis to form glomeruli, does not depend on the position of OSN cell bodies in the OE but still require expression of axon guidance receptors in OSNs [78,121]. The expression of these guidance receptors is regulated by OR-dependent second messenger cAMP levels in the projecting OSN axons [78,121].

In the OSN, olfactory receptors are G protein coupled receptors (GPCRs) that are activated by the binding of odorant to the OR [122]. Once the OR is activated, it activates adenylate cyclase 3, which then converts ATP to cAMP [122]. The cAMP then activates PKA and CREB that regulate transcription of various axon guidance molecules that influence the guidance of these axons [122]. The cAMP also further activates CNGA2 channels i.e., cyclic nucleotide gated channels that allow the influx of calcium and that further activates the opening of

chloride channels which allows the efflux of chloride ions from OSNs to the extracellular space thereby depolarizing the OSN [72,122]. The influx of calcium ions into the OSN cell, can regulate expression of of various cell adhesion molecules that are important in the sorting of OSN axons into glomeruli once they reach their broad target [72].

Similarly, to the MOS, VSN axons respond to axon guidance cues to reach broad regions of the AOB (anterior and posterior) where they coalesce into glomeruli. However, in contract to OSN axons expressing the same OR that coalesce into one or two glomeruli of the OB, VSN axons expressing the same VR coalesce into 10 to 30 spatially conserved glomeruli [130]. Furthermore, the contribution of neuronal activity to this process is not as well characterized in this system as compared to the MOS.

1.4) Guidance molecules in the olfactory system

1.4.1.) Main Olfactory System: Molecules involved in OSN targeting and sorting

Various axon guidance molecules are involved in the coarse targeting and fine tuning of OSN axons in the main olfactory system. Coarse targeting of OSNs includes appropriate targeting of OSN axons from the olfactory epithelium (OE) to the olfactory bulb (OB) along the dorso-ventral, antero-posterior and medio-lateral axes. Fine tuning of OSNs involves the coalescence of OSN axons expressing the same Olfactory receptor (OR) into two bilaterally symmetrical homogenously innervated target glomeruli in the OB [142,143].

Position of the OSN cell bodies in the OE and neuronal activity contribute to the coarse targeting of the OSN axons to the OB [78]. The position of OSN cell bodies in the OE is represented in the targeting of axons along the dorso-ventral axis of the OB; For example, OSNs whose cell bodies reside in the dorso-medial OE target their axons to the dorsal OB whereas, OSN cell bodies in the ventro-lateral OE target their axons to the ventral part of the OB [139–141].The targeting of OSN axons along the D-V axis is modulated by two sets of axon guidance receptors that are differentially expressed along the DV axis of the OSNs in OE. The Slit receptor, Robo-2 is highly expressed in OSNs in the dorsomedial OE and its expression is low in OSNs in the ventrolateral OE [144]. The repulsive guidance cue Slit-1 is expressed at higher levels in the ventral OB and at lower levels in the

dorsal OB [144]. Thus, high levels of Slit-1 in the ventral OB repel Robo-2 expressing axons to the dorsal part of the OB [144]. A conditional knockout of Robo-2 in OSNs results in the mistargeting of dorsal targeting OSNs to the ventral OB [144]. Similarly, knockout of Slit-1 also results in the mistargeting of dorsal OSN axons to the ventral OB [144]. On the other hand, ventral projecting OSN axons do not mistarget to the dorsal OB in Robo-2 and Slit-1 knockout suggesting that other cues maintain these axons in the ventral region of the OB [144,145]. The lower levels of Robo-2 expression in ventrally-targeting axons also contribute to their accurate positioning along the D-V axis [146]. Indeed, loss of Robo2 in OSNs results in a reduction in the number of ventral glomerulus formed by OSNs expressing the OR MOR28 [146]. Similarly, knockout of Slit1 results in the formation of more ventral glomeruli innervated by P2 OR expressing axons [146].

In the same manner in which Robo-2 -Slit-1 repulsive interactions guide OSNs in the dorsomedial OE to project their axons to the dorsal OB, the repulsive interaction between the Neuropillin-2 (Nrp-2) and its ligand, the secreted Semaphorin guides OSN axons in the ventrolateral OE to project their axons to the ventral OB [78,147]. Sema 3F is secreted by early arriving dorsal zone OSN axons and deposited in the anterodorsal OB [78,147]. This newly deposited molecule serves as a repulsive cue to repel late arriving Ventral zone OSN axons that are positive for Nrp2 receptor [78,147]. In addition, Sema 3F is also important in the retraction of OSNs that overshoot the glomerular layer earlier on in development [148]. In Sema 3F-/- mice , ectopically projecting OSN axons are observed that overshoot the glomerular layer and fail to get pruned off over the course of development [148].

Neuropillin-1-Semaphorin 3A signalling has been shown to be important for medio-lateral segregation of OSN axons in the OB [78,149–151]. The expression of secreted semaphoring in the OB is complementary to the expression of Nrp-1 on the targeting axons. Nrp-1 positive axons are repelled to lateral targets in the anterior OB and medial targets in the posterior OB [78,149–151]. In Sema 3A mutant mice, defective medio-lateral segregation of Npn1 positive axons is observed thereby indicating that Sema 3A- Npn-1 interaction is very important for the coarse targeting of OSN axons along the medio-lateral axis of the OB [149–151]. In addition to Sema 3A and Npn-1, Insulin Growth Factor -IGF1 and IGF2 have also been implicated in the medio-lateral targeting of OSNs in

the OB [152]. More specifically, IGFs seem to be required in guiding OSNs to their appropriate targets in the lateral region of the OB [152].

Neuronal activity in presynaptic OSNs but not postsynaptic mitral cells plays a role in guiding OSNs along the anterior posterior axis of the OB [72,78]. Although some studies suggest that guidance of OSN axons along the anterior posterior axis depends primarily on the type of OR expressed but not neuronal activity of cAMP levels or GPCR signalling, some studies indicate that GPCR signalling coupled with changes in cAMP levels as a result of adenyl cyclase 3 activity is a crucial determinant for the level of guidance molecules such as Neuropillin1, Plexin A, and Ephrin, that have been shown to be important for the targeting of OSN axons along the anterior-posterior axis of the OB [72,126,153–155].

Npn1 has been shown to be expressed highly in OSN axons targeting the posterior OB while levels of Npn1 are low in OSN axons targeting the anterior OB [78,154–156]. Similarly, OSN axons targeting the anterior OB express higher levels of Sema 3A, while OSN axons reaching the posterior OB have low levels of Sema 3A expression along the axons [78,154–156]. Thus, Sema 3A-Npn-1 repulsion is proposed to promote the pre-target sorting of OSN populations of axons allowing them to reach their appropriate targets along the anterior posterior axis [157]. The levels of cAMP in OSNs has been associated with the levels of Npn1 expressed [157]. Higher level of cAMP in OSNs is associated with higher level of Npn1 expression on their axons, while lower level of cAMP is associated with lower level of Npn1 expression [157]. Thus, it has been proposed that ablating Npn1 should result in anteriorization of posterior glomeruli, while overexpressing Npn1 would result in posteriorization of anterior glomeruli [79,156]. Although ablation of Np1 in OSN axons can lead to anteriorization of glomerular targeting, the defects observed are not as pronounced, suggesting that additional mechanisms modulate A-P targeting [158].

Ephrin A3 and Ephrin A5 ligand interaction with EphA receptors in the OB have been implicated in the anterior-posterior patterning of the OB [8]. EphA receptors are tyrosine kinases and Ephrins are GPI linked proteins [8]. EphA receptors are expressed by mitral cells and tufted cells in the OB and EphrinA3 and EphrinA5 are expressed along OSN axons [8]. Deletion of Ephrin As results in a posterior and dorsal shift in glomerulus

formed by OSN axons expressing the OR P2 while overexpression of ephrin As results in an anterior and ventral shift of the P2 glomerulus thereby indicating that ephrins instruct the formation of an accurate olfactory map along the A-P axis [8].

Once OSN axons reach the broad region of the OB to which they target the differential expression of cell adhesion molecules on theses axons has been proposed to modulate their precise coalescence into glomeruli. The differential expression of at least some of these families of CAMs is regulated by OSN neuronal activity [72]. When an odorant binds to the odorant receptor it activates GPCR Gαolf, which results in the activation of adenyl cyclase 3 leading to increased production of cAMP [72,120,122,153]. Increase in cAMP levels result in the opening of CNGA2 channel i.e., cyclic AMP nucleotide gated channel, which allows the entry of Ca2+ ions inside the OSNs [122,153]. Increase in calcium results in activation of PKA and CREB, which modulates expression of CAMs [72,122]. Thus, OR activity in OSNs controls the expression level of various cell adhesion molecules along the surface of OSN axons [72]. Some examples of cell adhesion molecules whose expression levels are correlated with OR expression include the Kirrel family of proteins, namely Kirrel2 and Kirrel3, Big2/contactin 4, Ephrin A5, and EphA5 receptor [72,159]. It has been shown that Kirrel2 and Kirrel3 are expressed in complementary levels in different OSN populations expressing different ORs in the main olfactory system [72,87]. Thus, it is has been hypothesized that the differential expression of Kirrels along the surface of OSN axons contributes to a molecular identity code along with other cell adhesion molecules such as Big-2 and Ephrins [72,159]. Knocking out BIG-2 results in formation of multiple glomeruli at ectopic locations [159]. Evidence suggests that Big-2 has a heterophilic binding partner that is yet to be identified [159]. Similarly, overexpression of Kirrel2 and Kirrel3 result in duplication of a glomerulus innervated by axons expressing the OR MOR28 in the OB, thereby suggesting that Kirrels also play an important role in axon sorting via cell adhesion [72]. Meanwhile, EphA5 and ephrinA5 show complementary expression levels on OSN axons [72]. It has been thus proposed that axons expressing high EphA5/low ephrinA5 interact with axons expressing high ephrinA5/low EphA5, which results in axon repulsion allowing the sorting of axons into appropriate glomerular targets [72]. Hence, the combined effect of selective adhesion and repulsion of populations of OSN axons dictates their accurate coalescence into glomeruli.

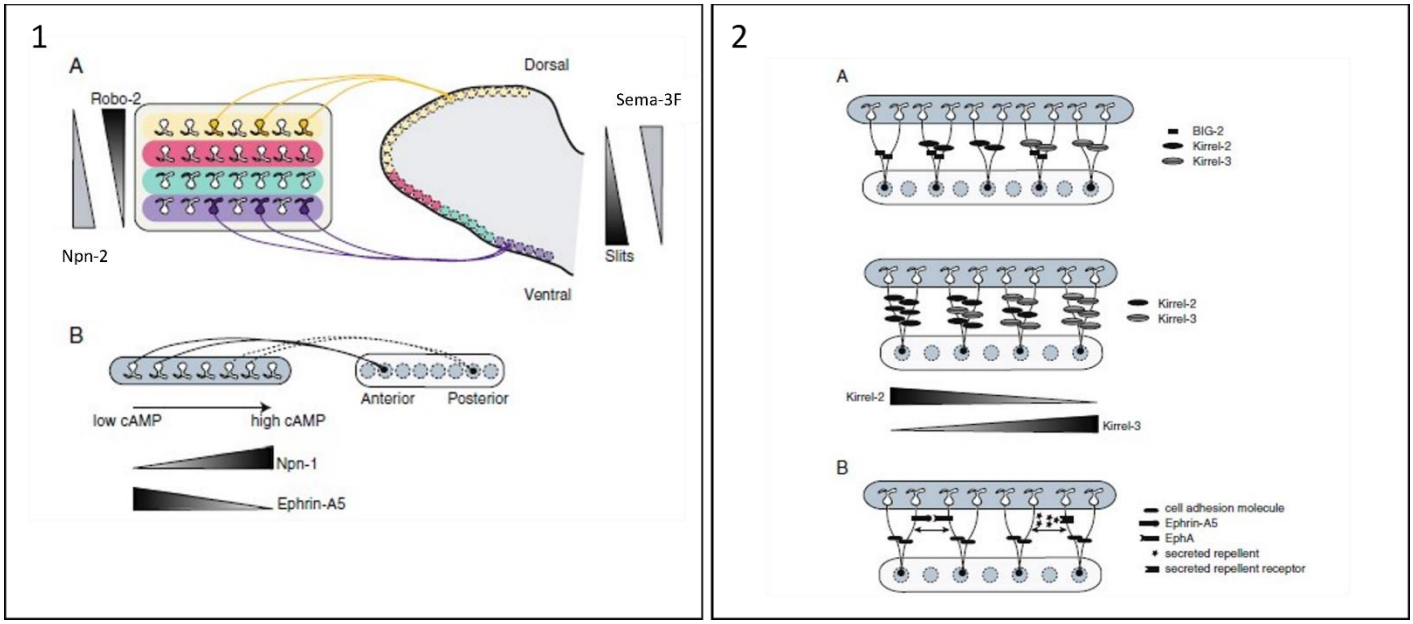

Figure 6. Summary of guidance molecules involved in the targeting and sorting of OSN axons. 6.1 A combination of secreted repulsive molecules, Slits and Sema3F, regulate the dorso-ventral targeting of OSN axons by activating their receptors, Robo2 and Npn2, respectively. The levels of expression of Npn1 and EphrinA5 on OSN axons contribute to their targeting along the anterio-posterior axis. 6.2 Once OSN axons reach their broad targets, they sort with the help of contact dependent attractive cues such as BIG-2 and Kirrel2 and Kirrel3 and repulsive cues such as Ephrin A5 and EphA receptor. (Figure is modified and reproduced from Cho et al., 2009[78])

1.4.2.) Accessory Olfactory System: Molecules involved in VSN targeting and sorting

As observed in the MOS, specific families of axon guidance cues modulate the targeting of VSN axons to broad regions of the AOB which is followed by coalescence into target glomeruli.

Neuropillin-2 (Nrp-2) and Semaphorin 3F (Sema 3F) have been shown to play an important role in maintaining the fasciculation of VSN axons as they project to the AOB and in modulating their segregation once they reach this structure[130,148]. Expression of Nrp-2 on VSN axons is necessary to maintain their fasciculation in response to Sema 3F secreted by cells on the medial side of the main olfactory bulb [130,148]. In vitro studies have shown that VSNs emerging from the VNO are repelled by a source of Sema 3F or a medial MOB explant in a Nrp-2 -dependent manner [130,148]. Furthermore, Loss of Nrp-2 or Sema 3F results in severe defasciculation of VSN axons traversing across the MOB and results in ectopic innervation of MOB glomeruli by VSN axons [130,148].

Once VSN axons reach the AOB, various ligand-receptor pairs such as EphrinA5- Eph A6, Nrp2 and Robo-2-Slit1 and Slit 2 have been shown to dictate in the zonal segregation of apical and basal VSNs into the anterior and posterior AOB respectively [77,130,160].

EphrinA5 is expressed highly along the axons of apical VSNs that project to the anterior AOB [77]. EphA6 is expressed in the anterior region of the AOB and proposed to promote attraction of Ephrin A5 positive axons through reverse EphrinA5 signalling [77]. Ephrin A5 deficient mice show mistargeting of apical VSN axons to the posterior AOB [77]. Since ephrin A5 is a GPI anchored protein, various proteins such as the tyrosine kinase RET or neurotrophin receptors, such as p75 and TrkB, could serve as ephrin A co-receptors as seen in other systems [77]. Thus, EphrinA5- EphA6 signalling serves as an attractive cue for apical VSNs guiding them to the anterior AOB [77].

Neuropillin-2 is another molecule highly expressed in apical VSN axons targeting the anterior AOB. Nrp-2 $^{-/-}$ mice show misrouting of apical VSNs to posterior AOB [161]. Interestingly, Nrp-2 repulsive ligand Sema 3F does not show any specific gradient of expression in the AOB mitral cells or VNO [161]. Sema 3F $^{-/-}$ mice show minor defects unlike the more pronounced defects in Nrp-2$^{-/-}$ mice in the targeting of apical VSNs to anterior AOB[161]. This suggests that additional Nrp2 ligands likely contribute in conjunction with Sema 3F to prevent Npn-2 positive axons from entering the posterior region of the AOB[161].

The segregation of basal VSN axons to the posterior AOB is dependent on repulsive forces mediated by Slit-Robo2 interactions[160]. Robo-2 is highly expressed and confined to basal VSNs[160]. Members of the secreted Slit family of cues are expressed in the AOB, with Slit1 being highly expressed in the anterior region of the AOB, while Slit2 is expressed more uniformly across the AOB[160]. Conditional knockout of Robo2 in VSNs leads to mistargeting of axons to the anterior region of the AOB[160]. Loss of Slit1 and Slit2 expression similarly results in mistargeting of the VSN axons, indicating that these two ligands promote Robo-2 dependent repulsion of basal VSN axons to the posterior AOB[160].

In addition to axonal fasciculation and zonal segregation of VSN axons, fine tuning of VSN axons such that they coalesce into glomeruli is also extremely important for the formation of accurate neural maps in the AOB.

Knocking out V1Rs or V2Rs results in mistargeting of VSN axons resulting in aberrant glomeruli formation [130,162,163]. However, appropriate zonal segregation of axons in these knockouts is achieved [130,162,163]. This tells us that VRs potentially serve as an important instructive cue for the coalescence of VSN axons into glomeruli [130,162,163]. Just as in the main olfactory system, neuronal activity of VSNs might serve as an important regulator for the expression level of various cell adhesion molecules that might guide the appropriate coalescence of VSN axons into glomeruli [130]. Trp2 ion channel activity is an important regulator of the expression level of the members of the Kirrel homophilic cell adhesion family [115,130]. Differential expression of Kirrel 2 and Kirrel 3 along VSN axons has been proposed to serve as a molecular identity code that regulate axonal adhesion, allowing the coalescence of VSN axons that are similar in their expression profile of Kirrel 2 and Kirrel 3 [114,115]. Loss of Kirrel3 and Kirrel2 in mice results in aberrant glomerular formation i.e., fewer and larger glomeruli in the posterior AOB demonstrating their requirement in this process [114,115]. Thus, the appropriate expression patterns of Kirrel2 and Kirrel3, likely in combination with other cell adhesion molecules, is essential for the coalescence of like axons into glomeruli [72,114,115].

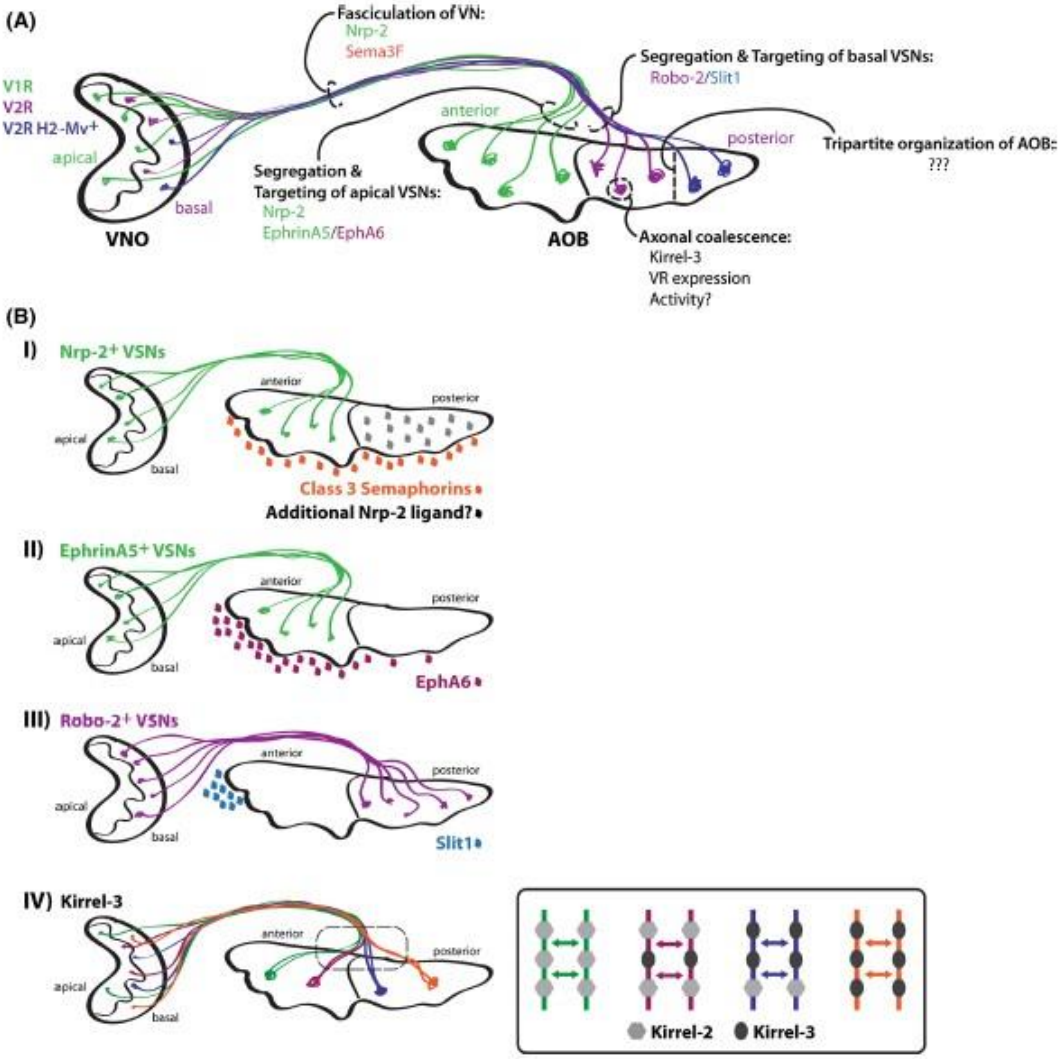

Figure 7. Summary of guidance molecules involved in targeting and sorting of VSN axons. In this figure we observe that Nrp-2 is involved in the targeting of VSNs to the anterior AOB (B I). The attractive interaction between Ephrin A5 and EphA6 allows apical VSNs to reach the anterior AOB (B II). Similarly, the repulsive interaction between Robo-2 and Slit1 allows basal VSNs to reach the posterior AOB (B III). Once these axons reach their broad targets, attractive contact mediated interactions between homophilic cell adhesion molecules Kirrel2 and Kirrel3 allows these VSN axons to sort into their appropriate glomerular targets (B IV). (Reproduced from Brignall et al., 2015 [130])

1.4.3.) Molecules involved in mitral cell development

The relay of olfactory information from OSNs to higher brain structure relies on synapses formed in glomeruli between OSN axons and mitral cell dendrites [125]. The development of these mitral cells involves neurogenesis, migration, differentiation, morphogenesis, and maturation through pruning of dendritic arbors [125]. Mitral cells are born in the ventricular zone (VZ) and migrate to the intermediate zone (IZ) [125]. Birth and differentiation of mitral cells are controlled by transcription factors Sall1 and Pax6 [164, 165]. Once in the intermediate zone, mitral

cell bodies reorient themselves radial to the OB surface [166, 125].Cell adhesion molecule Tag1 has been shown to be important for the migration of mitral cells [166]. In addition, the repulsive interaction between Sema3F in dorsal targeting OSNs and Neuropillin-2 on a subset of mitral cells allows the targeting of subsets of mitral cell bodies to the posterior-ventral region of the mitral cell layer in the main olfactory bulb [123]. Similarly, the presence of Sema 3F around the anterior Medial Amygdala (MeA) guides the targeting of posterior-ventral mitral cell axons to the anterior MeA [123]. Following migration to the appropriate region in the mitral cell layer, mitral cell bodies undergo changes in their orientation and their dendrites, a change in their complexity [125]. TARSH, BMPR2, TrkB, Notch, and Nectin are important molecules that have been shown to regulate mitral cell dendritic complexity [167, 127, 168, 169, 98].

Mechanisms regulating mitral cell dendritic complexity

Role of Neuronal activity in the regulation of mitral cell dendritic complexity

Mitral cell dendritic development can be primarily divided into two main phases, Phase 1: Regulation of branching of mitral cell dendrites and Phase 2: Pruning the supernumerary primary apical dendrites [170]. Neuronal activity has been implicated in modulating the development of mitral cell dendrites and proposed to modulate dendritic pruning. It has been shown that diminishing spontaneous and odorant evoked activity in OSNs through naris closure and CNGA2 channel knockout in OSNs result in changes in the olfactory bulb size and appears to cause delayed pruning of mitral cells [126, 169, 170]. However, this impact on mitral cell pruning might be secondary effects to an overall reduction in olfactory bulb size, since these mouse pups do not suckle very well in comparison with their wild type counter parts [126]. When these pups are hand reared, along with their wild type counter parts, the mice and their OB are more or less comparable in size and the delay in pruning is mild [170]. In addition to this, diminished spontaneous activity in OSNs by overexpression of inward rectifying potassium channel Kir2.1, does not have any impact on mitral cell dendritic complexity, thereby indicating that both spontaneous and odorant evoked activity in OSNs does not affect mitral cell dendritic complexity [171]. Furthermore, silencing spontaneous activity in mitral cells by overexpression of Kir2.1 channel in mitral cells perturbs dendritic pruning in these cells in a cell autonomous fashion [170]. Similarly blocking NMDA

neurotransmission in the olfactory bulb results in perturbed dendritic pruning of mitral cells [170]. Thus, neuronal activity in OSNs has limited impact on mitral cell dendrite development, mitral cell activity is critical for accurate pruning of their dendrites.

Molecules involved in phase 1 of mitral cell dendritic complexity regulation

Notch: It has been shown that an important player of Notch signalling, Maml1 a protein that binds to DNA along with the Notch Intracellular domain NICD1, is crucial for regulating dendritic morphology and complexity of mitral cells [169]. It was shown that knocking out Maml1 resulted in reduced Notch signalling and in an increase in dendritic complexity in mitral cells [169]. Furthermore, in order to have an impact on dendritic complexity, notch signalling needs to be disrupted at a critical time point in development i.e. E18.5, suggesting it affects early branching of developing dendrites [169]. Conditional misexpression of dominant negative Maml1 gene in mitral cells before or after E18.5 had no impact on mitral cell dendritic complexity [169]. This shows that during development there is a notch signalling dependent phase and an independent phase when it comes to the regulation of mitral cell dendritic morphology. Conditional misexpression of dominant negative Maml1 increases mitral cell dendritic stabilization as in the Maml1 knockouts [169]. On the other hand, constitutively active Notch when expressed embryonically in mitral cells results in a severe reduction in mitral cell dendritic complexity [169]. Interestingly, it was shown that inhibition of a Notch ligand Jag-1 in mitral cells does not have any effect on mitral cell dendritic stabilization but the inhibition of the ligand in OSNs increases mitral cell dendritic stabilization, suggesting that OSNs release ligands for Notch signalling in mitral cells [169]. An increase in mitral cell dendritic complexity has been associated with defective homing behaviour in these mice, as these mice are unable to recognize home scents [169].

TrkB: Activation of TrkB receptors by BDNF and Neurotrophin 4 has been shown to stimulate formation of apical dendrites and branching in cortical pyramidal neurons [168]. TrkB is a good candidate protein for the regulation of mitral cell morphology as it is expressed on dendrites of Mitral cells and Tufted cells [168]. Activation of TrkB receptors using Neurotrophin 4 or BDNF *in vitro* in cell cultures increases survival of mitral cells [168]. The number of primary neurites and branching was also significantly increased upon TrkB receptor

activation with BDNF and NT4 application [168]. While the exact mechanism through which BDNF impacts mitral cell development in vivo is unknown, it is likely through its secretion from OSN axons or mitral cells. It is possible that spontaneous activity in mitral cells brings about a surge in intracellular calcium levels which causes the release of BDNF thereby acting on TrkB [168].

Nectin: Mitral cells extend lateral dendrites in addition to primary apical dendrite that form dendrodendritic synapses with other mitral cell lateral dendrites, mitral cell primary apical dendrites, and also granule cell dendrites in the deep sub-lamina of the EPL [98]. The formation of dendrodendritic synapses between mitral cells and mitral cells and granule cells is important for the lateral inhibition of nearby mitral cells not receiving a signal from glomeruli [85]. Cell adhesion molecule Nectin has been shown to stabilize these dendrodendritic synapses [98, 85]. Loss of Nectin-1 also results in reduced branch points for mitral cell lateral dendrites *in vivo* and an overall decrease in mitral cell dendritic branching *in vitro* [85].

Molecules involved in phase 2 of mitral cell dendritic complexity regulation

TARSH: TARSH is a secreted protein, transiently expressed in mitral cells and tufted cells during the dendritic refinement period [167]. Treatment of dissociated mitral cells in culture with purified TARSH protein reduces dendritic complexity [167]. Furthermore, when mitral cells were co-cultured with astrocytes transfected with TARSH, a significant reduction in dendritic complexity of the mitral cells was observed at 11 DIV [167]. To examine the effect of TARSH secretion on dendritic complexity in mitral cells, TARSH was overexpressed in cultured mitral cells and co-cultured with untransfected mitral cells [167]. It was observed that both the transfected and untransfected mitral cells showed a significant reduction in the dendritic complexity suggesting that TARSH might function as an extracellular factor that reduces mitral cell dendritic complexity [167]. This study therefore showed that TARSH is a secreted protein expressed at the base of apical dendrites in mitral cells and that it may function as an autocrine factor modulating mitral cell dendritic complexity during the dendritic refinement period [167]. Whether TARSH is necessary for dendritic pruning of mitral cells *in vivo* is yet to be answered. Furthermore, the signalling pathways through which TARSH mediates its effects remains unknown.

BMPR2: A recent study revealed a novel role for BMPR2 receptor in mitral cell dendrite stabilization and destabilization in the mouse olfactory bulb [127]. Analyses of BMPR2 knockout mice revealed no significant difference in mitral cell branching at P1 but a significantly higher proportion of mitral cells innervated more than one glomerulus in BMPR2 knockouts as compared to controls at P6 [127]. This effect could be rescued by expression of BMPR2 in mitral cells [127]. These observations suggested that BMP2R is necessary for mitral cell dendritic pruning, possibly by promoting their destabilization [127]. BMPR2 signalling was shown to inhibit LIMK activity, which likely induces actin depolymerization and destabilizes dendritic shafts [127]. This study also showed that when bound to a ligand such as BMPs, the inhibition on LIMK is released, thereby stabilizing dendrites [127]**.** However, this study does not show how this dual function of the BMPR2 receptor is used to bring about a very precisely timed pruning of mitral cell dendrites [127].

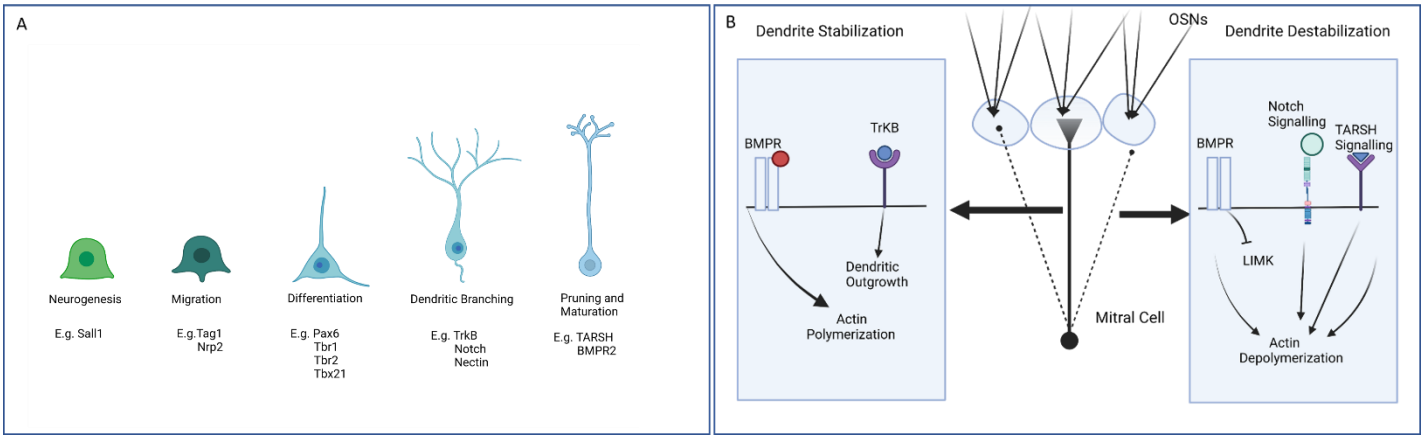

Figure 8. Summary of molecules regulating mitral cell development. Figure 8 A shows the different steps of maturation of mitral cells and molecules known to be involved in their regulation. While Sall1 is important for neurogenesis of mitral cells, Tag1 and Nrp2 are implicated in their migration, and Pax6, Tbr1, Tbr2 and Tbx21 are important for their differentiation. TrkB, Notch and Nectin are involved in mitral cell dendritic branching while TARSH and BPMR2 are involved in dendritic pruning and maturation. Figure 8 B shows a summary of the molecules involved in mitral cell dendritic stabilization and destabilization. BMPR and TrkB when bound to their respective ligands are involved in dendritic stabilization through actin polymerization and dendritic outgrowth, respectively. In contrast, unbound BMPR, activated Notch receptor, and TARSH, are involved in dendritic destabilization presumably through actin depolymerization.

Preface to Chapters 2 to 4:

In my thesis research I aimed to address three specific questions about the function of Kirrel family CAMs in circuit formation during neurodevelopment using the mouse olfactory system:

1) In Chapter 2, I determined whether Kirrel2 is required for the formation of the main olfactory bulb glomerular map, more specifically for axonal coalescence of OSN axons into glomeruli (Vaddadi*, Iversen*, Rajah* et al., 2019) (*co-first authors).

2) In Chapter 3, I assessed whether Kirrel3 cell adhesion properties are necessary for its function in mediating axonal coalescence of vomeronasal sensory neuron axons into glomeruli of the AOB, which tested the proposed model that Kirrel-mediated axonal adhesion contributes to glomerular map formation (Wang*, Vaddadi*, Pak* et al. 2021) (*co-first authors).

3) In Chapter 4, I examined whether, in addition to controlling sensory neuron axonal coalescence, Kirrel3 influences the development and maturation of dendrites of mitral cells in the OB during glomerular map maturation.

Rationale for Chapter 2

As discussed in the Introduction, given our knowledge of how the olfactory system in mice forms a stereotypic map in the brain, it makes it an excellent model system to understand neural circuit formation and the role of cell adhesion molecules in this process. Given what is known in literature about Kirrel family of proteins in the context of axon targeting across different species[102, 105-109,112] and their linkage to neurodevelopmental disorders[9,116], we chose to study the role of Kirrels in neural circuit formation using the mouse olfactory system as a model.

In Chapter 2 we aim at understanding the role of Kirrels 2 and 3 in axon sorting in the main olfactory system. Kirrels 2 and 3 are known to be differentially expressed on different populations of olfactory sensory neurons in the main olfactory system. Interestingly, when Kirrel2 or Kirrel3 are over-expressed in a sub-population of OSNs in the main olfactory system expressing olfactory receptor MOR28, defects in how these axons sort are observed indicating that Kirrels might play a role in OSN axon sorting [72]. However, whether Kirrels are actually necessary in OSN axon sorting using a loss-of-function approach has not yet been demonstrated. In Chapter 2, we use a loss-of-function approach *in vivo* to understand whether Kirrels are necessary for axon sorting in the main olfactory system. We looked at 5 different sub-populations of OSNs targeting dorsal and ventral OB including the ventral targeting MOR28 expressing OSN axons and study the effect of ablating Kirrel 2 and 3 on the sorting of these axon populations.

Chapter 2: Kirrel2 is differentially required in populations of olfactory sensory neurons for the targeting of axons in the olfactory bulb

Neelima Vaddadi*, Katrine Iversen*, Reesha Raja*, Alina Phen, Alexandra Brignall, Emilie Dumontier and Jean-François Cloutier

ABSTRACT

The formation of olfactory maps in the olfactory bulb (OB) is crucial for the control of innate and learned mouse behaviors. Olfactory sensory neurons (OSNs) expressing a specific odorant receptor project axons into spatially conserved glomeruli within the OB and synapse onto mitral cell dendrites. Combinatorial expression of members of the Kirrel family of cell adhesion molecules has been proposed to regulate OSN axonal coalescence; however, loss-of-function experiments have yet to establish their requirement in this process. We examined projections of several OSN populations in mice that lacked either Kirrel2 alone, or both Kirrel2 and Kirrel3. Our results show that Kirrel2 and Kirrel3 are dispensable for the coalescence of MOR1-3-expressing OSN axons to the most dorsal region (DI) of the OB. In contrast, loss of Kirrel2 caused MOR174-9- and M72-expressing OSN axons, projecting to the DII region, to target ectopic glomeruli. Our loss-of-function approach demonstrates that Kirrel2 is required for axonal coalescence in subsets of OSNs that project axons to the DII region and reveals that Kirrel2/3- independent mechanisms also control OSN axonal coalescence in certain regions of the OB.

INTRODUCTION

The elaboration of precise neural maps in developing sensory systems allows organisms to obtain an accurate representation of signals that are detected in their environment. Sensory coding of olfactory cues in mice relies on the formation of stereotypic glomerular maps within the olfactory bulb (OB). Olfactory sensory neurons (OSNs) of the olfactory epithelium (OE) project their axons to the OB where they synapse with dendrites of second-order neurons in spatially conserved neuropil structures termed glomeruli. Each OSN expresses a single

functional olfactory receptor (OR), and OSN axons expressing the same OR coalesce together in one or two stereotypically conserved locations of the OB. This occurs through a two-step process that involves the coarse targeting of these axons within defined regions of the OB, and their subsequent coalescence into specific glomeruli [79].

Targeting of OSN axons to broad regions of the OB is mediated by axon guidance molecules and by their receptors that are expressed on the growing axons [158, 144,146,172, 154,8 ,153,157 , 173, 145 , 149, 174, 147, 156]. In contrast, coalescence of OSN axons expressing the same OR into a specific glomerulus has been suggested to rely on selective interactions of OSN axons with similar identities. Axonal identity may be established through the combinatorial expression of multiple families of cell-surface molecules that promote adhesion of similar axons or repulsion of dissimilar axons [175, 159, 176, 72]. In addition, expression of the OR itself may provide a unique axonal identity that contributes to the coalescence of like axons through an as yet unidentified mechanism [177, 178, 179 , 180].

The differential expression of Kirrel family members on OSN axons has been suggested to serve as an axonal identity code to regulate coalescence of OSNs into glomeruli [72]. Kirrel2 and Kirrel3 are expressed in a complementary and OR-correlated manner in OSN axons, whereby axons that express high levels of Kirrel2 express low levels of Kirrel3, and vice versa [72], and all axons of a single OR population will express the same levels of each Kirrel family member. Furthermore, their differential expression is regulated by OR-evoked activity [72]. The main evidence implicating Kirrels in olfactory map formation comes from the mosaic overexpression of Kirrel2 or Kirrel3 in OSNs that express MOR28 (also known as Olfr1507), a manipulation that leads to the duplication of MOR28 glomeruli in the OB [72]. Although these experiments suggest that the levels of expression of these proteins in OSNs can regulate axonal coalescence, the requirement of Kirrels in olfactory map formation needs to be addressed by analysis of genetic loss-of-function mutations.

Here, we use a genetic approach to ablate expression of Kirrel2 alone or in combination with Kirrel3 and

study the projections of multiple OSN populations to their glomerular targets in different regions of the OB. We provide evidence that the differential expression of Kirrels in OSNs does not represent a universal mechanism to promote the coalescence of OSN axons, but rather that their expression contributes to the coalescence of subsets of OSN axonal populations, likely in a region-specific manner.

RESULTS

Kirrel2 and Kirrel3 are differentially expressed in specific OSN populations

The differential expression of Kirrel family members between OSN populations has been proposed to contribute to a molecular code

whereby OSN axons of a given population would be similarly coded and can find each other to coalesce into the same glomeruli [72]. To assess whether Kirrel family members are necessary for OSN axonal coalescence, we examined the targeting of five populations of OSN axons that express either *tau-lacZ* or *tau-GFP* in mice carrying a targeted deletion of exons 3 and 4 in the *Kirrel2* gene. We have previously shown that Kirrel2 protein expression is ablated and that coalescence of vomeronasal sensory neuron axons is altered in these mice [114]. We selected these five populations of OSN axons as they target to well-defined regions of the OB (Fig. 1W). Axons of S50 (Olfr545)- and MOR1-3 (Olfr66)-expressing OSNs innervate glomeruli in the most dorsal region of the OB, termed DI. M72 (Olfr160)- and MOR174-9 (Olfr73)-expressing axons project to glomeruli located slightly more ventrally, in a region designated DII. In addition, we examined the targeting of ventrally projecting MOR28-expressing axons, as overexpression of Kirrel2 or Kirrel3 in a mosaic pattern among these axons leads to glomeruli duplication [72].

We first examined the levels of Kirrel2 and Kirrel3 expression on OSN axons expressing specific ORs, as both Kirrel members have been reported to be differentially expressed in populations of OSNs [72]. Although high levels of Kirrel2 were observed on S50- and MOR174-9-positive axons, medium and low Kirrel2 expression was observed on MOR1-3-, and M72- and MOR28-expressing axons, respectively (Fig. 1A-J,U). The pattern of Kirrel3 expression between these glomeruli was different to that of Kirrel2: MOR28 axons expressed high

levels of Kirrel3 whereas S50-, MOR1-3-, MOR174-9- and M72-positive axons expressed lower levels of Kirrel3 (Fig. 1K-T,V).

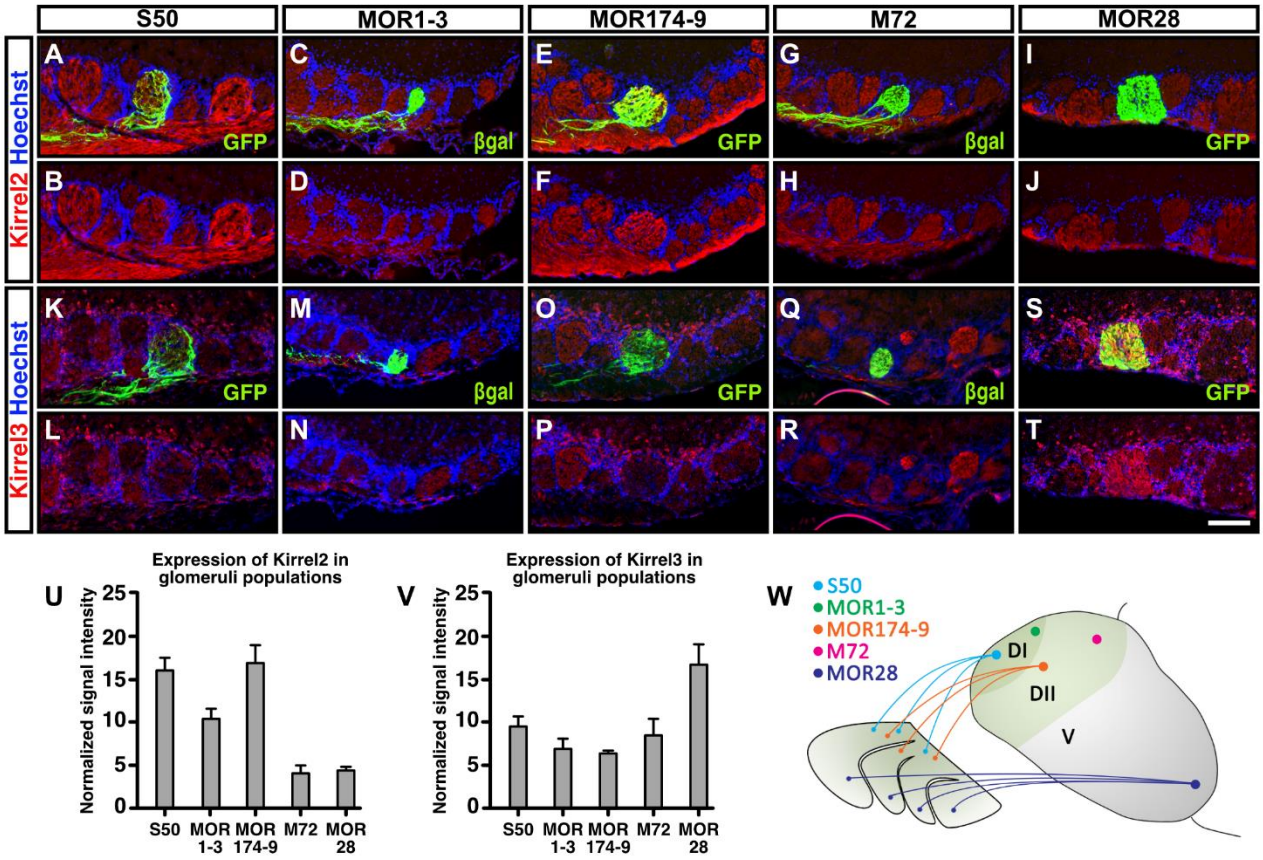

Figure 1. Differential expression of Kirrel2 and Kirrel3 in axons of specific OSN populations. (A-J) OB sections from adult wild-type mice expressing either GFP or the β-galactosidase (β-gal) enzyme in specific populations of OSNs were immunolabeled with Kirrel2 and GFP or β-gal antibodies to visualize the expression of Kirrel2 in *S50-GFP* (A,B), *MOR1-3-lacZ* (C,D), *MOR174-9-GFP* (E,F), *M72-lacZ* (G,H) and *MOR28-GFP* (I,J) glomeruli of the OB. Differential expression of Kirrel2 was observed in glomeruli surrounding the GFP- and β-gal-positive glomeruli. S50- and MOR174-9-positive axons appear to express higher levels of Kirrel2 (A,B,E,F), whereas MOR1-3-positive glomeruli express medium levels (C,D) and M72- and MOR28-positive glomeruli express low amounts of Kirrel2 (G-J). (K-T) Similar analyses were performed on OB sections immunolabeled with Kirrel3 and GFP or β-galactosidase (β-gal) antibodies. Although Kirrel3 expression levels are high in MOR28-positive glomeruli (S,T), lower levels of Kirrel3 were observed on S50- (K,L), MOR1-3- (M,N), MOR174-9- (O,P) and M72- (Q,R) expressing axons. (U,V) Relative signal intensities between glomeruli were measured as described in the Supplementary Materials and Methods and are quantified for Kirrel2 (U) and Kirrel3 (V) (*n*=3 for each population of glomeruli). Data are mean±s.e.m. (W) Diagram showing the approximate location of S50, MOR1-3, MOR174-9, M72 and MOR28 glomeruli in the OB along the dorsal-ventral axis. For characterization of the specificity of the Kirrel3 antibody, please refer to Fig. S1.

Kirrel2 is dispensable for the coalescence of S50, MOR1-3 and MOR28 axons in the OB

To determine whether Kirrel2 is required for the targeting of OSN axons, we first examined the targeting of DI-projecting S50- and MOR1-3-positive axons in control and *Kirrel2*$^{-/-}$ mice by whole- mount GFP epifluorescence and Xgal staining, respectively. Whole- mount assessment did not reveal a significant difference in the positioning of these glomeruli within the OB of *Kirrel2*$^{-/-}$ mice (Fig. 2A-L). Furthermore, there was no significant increase in the number of S50 and MOR1-3 glomeruli in the OB of these mice, demonstrating that Kirrel2 is dispensable for the targeting of these two populations of axons in the OB (Fig. 2O-S). Similarly, the position and number of MOR28 glomeruli in the OB was also unchanged in *Kirrel2*$^{-/-}$ mice (Fig. 2M-O,T,U).

Although ablation of Kirrel2 expression did not affect the coalescence of S50- and MOR1-3-positive axons, it remained possible that expression of Kirrel3 on these axons, or Kirrel3 upregulation in the absence of Kirrel2, might compensate for Kirrel2 loss in these OSNs. To test for potential compensation by Kirrel3, we crossed the *Kirrel2* mice with mice carrying a targeted insertion of a GFP cassette in the first exon of the *Kirrel3* gene, which lack Kirrel3 expression and show defects in the coalescence of vomeronasal sensory neuron axons [115]. Assessment of the targeting of MOR1-3-positive axons in *Kirrel2*$^{-/-}$; *Kirrel3*$^{-/-}$ mice revealed that both the location and number of MOR1-3 glomeruli were unchanged in these mice, demonstrating that both Kirrel2 and Kirrel3 are dispensable for the coalescence of these axons (Fig. 3A-D,I). Furthermore, ablation of both Kirrel2 and Kirrel3 did not affect the targeting of MOR28-positive axons (Fig. 3E-I).

In addition to axonal coalescence, Kirrel family members have been implicated in synapse formation in the hippocampus and accessory olfactory bulb [106, 181, 102, 114]. We therefore assessed the number of excitatory and inhibitory synapses in glomeruli of the OB in *Kirrel2*$^{-/-}$; *Kirrel3*$^{-/-}$ mice. In contrast to our previous findings in the accessory olfactory bulb of these mice, which showed reduced numbers of excitatory synapses, we could not detect a significant change in the number of synapses in the OB (Fig. 3J-Q). Taken together, these results demonstrate that Kirrel2 and Kirrel3 are dispensable for the targeting of specific populations of

OSNs that project to the most dorsal DI region of the OB and for the formation of synapses in the OB. Furthermore, unlike mosaic overexpression of Kirrel2 or Kirrel3, which leads to MOR28 glomeruli duplication [72], loss of these receptors does not affect the location and number of MOR28-positive glomeruli in the ventral region of the OB.

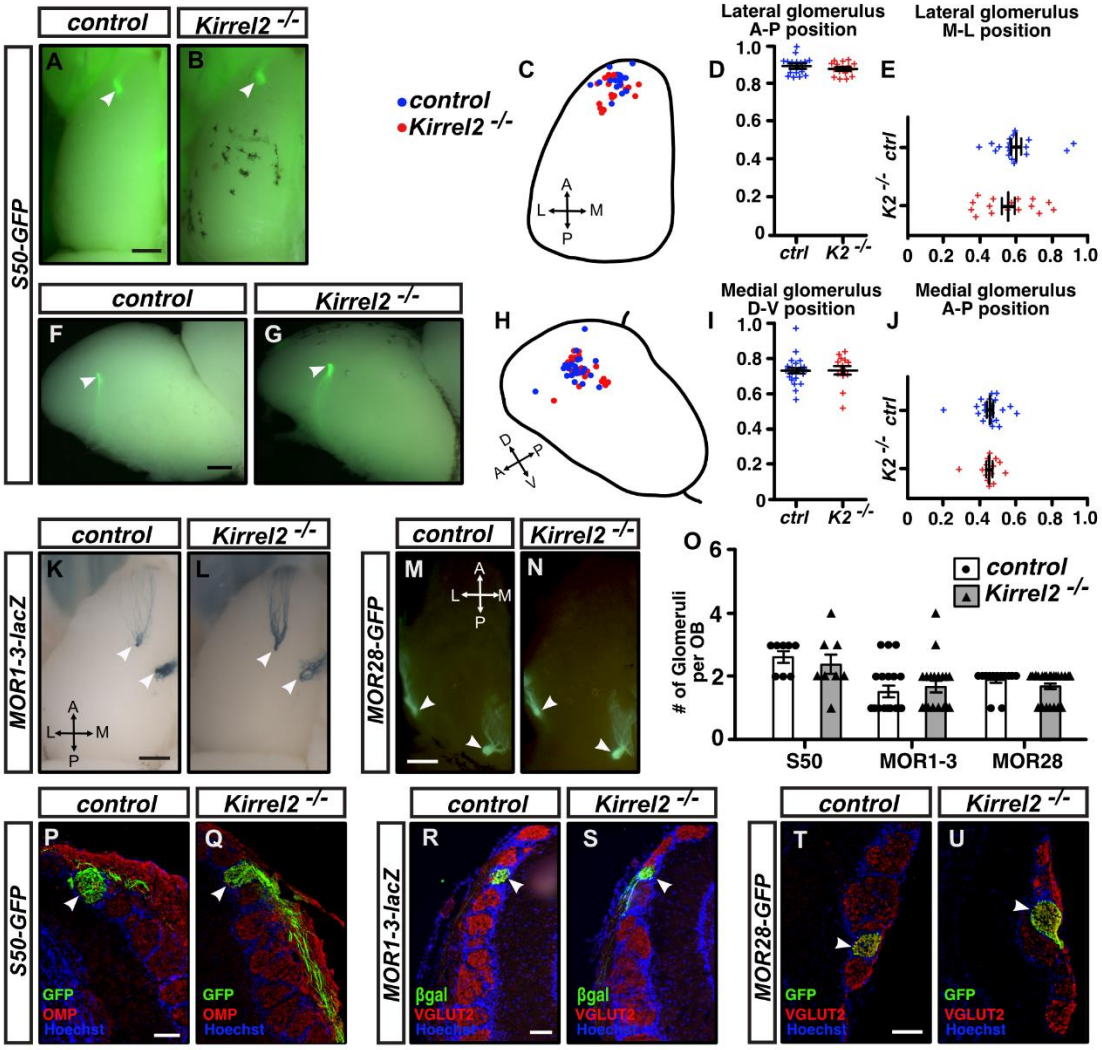

Figure 2. Kirrel2 is dispensable for the accurate formation of S50-, MOR1-3- and MOR28-positive glomeruli in the OB. (A-J) Whole-mount analysis of the location of *S50-GFP*-positive glomeruli in control and *Kirrel2*$^{-/-}$ mice. The lateral and medial S50 glomeruli are observed in dorsal (A,B) and medial (F,G) views of the OB in control and *Kirrel2*$^{-/-}$ mice. For all OBs analyzed, glomeruli locations were plotted on a diagram of the OB (C,H) and their positions along the anterior-posterior (A↔P), medial-lateral (M↔L) and dorsal-ventral (D↔V) axes were calculated and graphically represented (D,E,I,J). No significant difference in the position of S50 glomeruli was observed in *Kirrel2*$^{-/-}$ mice (control, *n*=17 OBs; *Kirrel2*$^{-/-}$, *n*=17 OBs). (K-N) Whole-mount analysis of the targeting of *MOR1-3-lacZ* (K,L; dorsal view of OB) and *MOR28-GFP* (M,N; ventral view of OB) glomeruli in control and *Kirrel2*$^{-/-}$ mice did not reveal a change in the positioning of these two sets of glomeruli in *Kirrel2*$^{-/-}$ mice (control, MOR1-3 *n*=10 and MOR28 *n*=10 OBs; *Kirrel2*$^{-/-}$, MOR1-3 *n*=10 and MOR28 *n*=10 OBs). (O-U) OB sections were immunolabeled with either OMP or VGLUT2 antibodies to delineate glomeruli and with either β-galactosidase (β-gal) or GFP antibodies to identify S50- (P,Q), MOR1-3- (R,S) or MOR28-positive (T,U) glomeruli. The number of

glomeruli per OB was counted and represented graphically in O. No significant change in the number of S50, MOR1-3 and MOR28 glomeruli was observed in *Kirrel2*$^{-/-}$ mice (control, S50 *n*=8, MOR1-3 *n*=17 and MOR28 *n*=13 OBs; *Kirrel2*$^{-/-}$, S50 *n*=8, MOR1-3 *n*=18 and MOR28 *n*=23 OBs). Data are mean±s.e.m. Student's *t*-test (unpaired) was performed. Arrowheads indicate individual GFP- or β-gal-positive glomeruli. Scale bars: 500 μm in A,B,F,G,K-N; 100 μm in P-U.

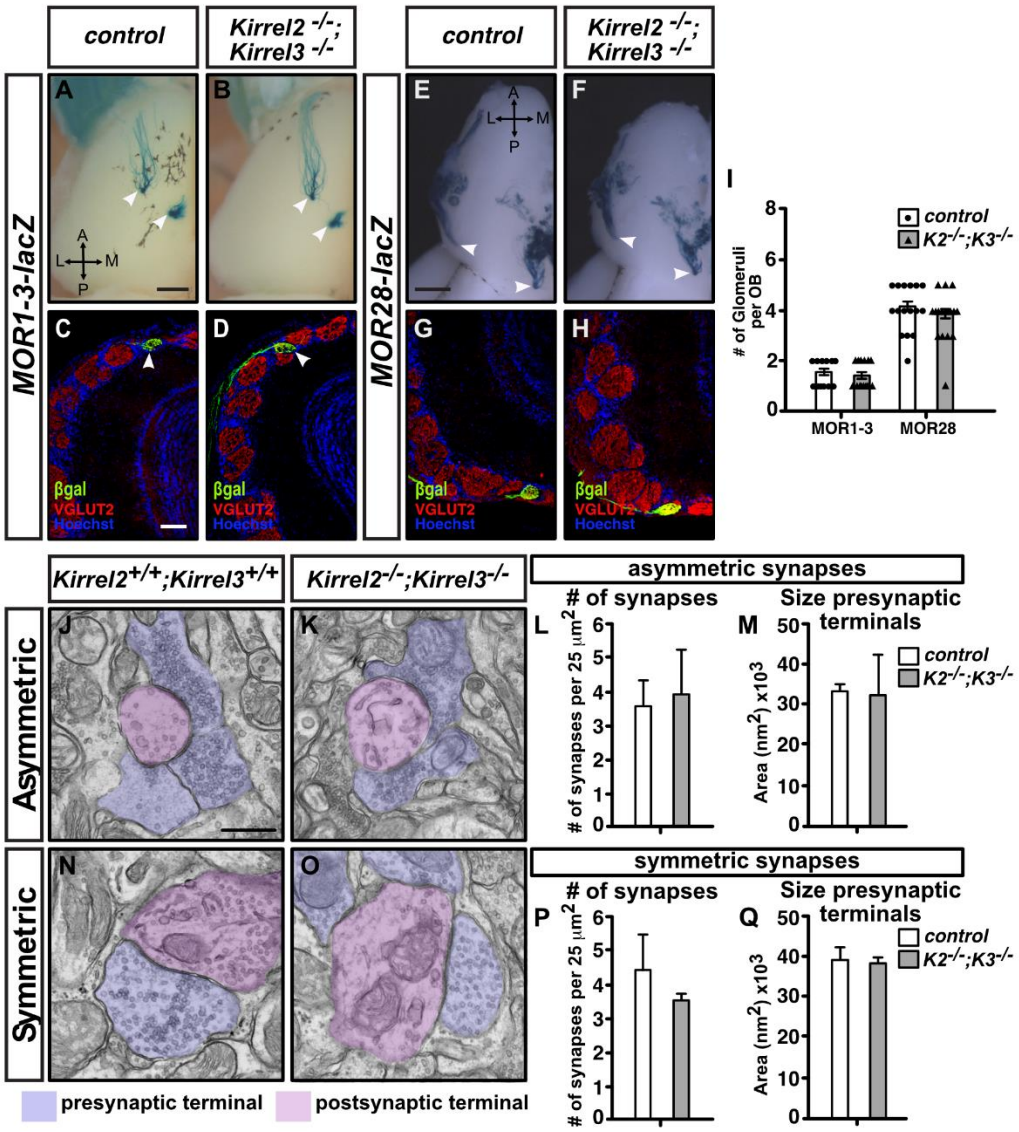

Figure 3. Kirrel3 does not compensate for loss of Kirrel2 in the targeting of MOR1-3- and MOR28-positive glomeruli in the OB. (A-I) Whole-mount examination of the location of *MOR1-3-lacZ*- (A,B; dorsal view of the OB) and *MOR28-lacZ*- (E,F; ventral view of the OB) positive glomeruli in control (A,E) and *Kirrel2*$^{-/-}$*; Kirrel3*$^{-/-}$ (B,F) mice (*MOR1-3-lacZ*: control, *n*=10 OBs, *Kirrel2*$^{-/-}$*; Kirrel3*$^{-/-}$, *n*=10 OBs; *MOR28-lacZ*: control, *n*=20 OBs, *Kirrel2*$^{-/-}$*; Kirrel3*$^{-/-}$, *n*=16 OBs). The number of MOR1-3 and MOR28 glomeruli was quantified on sections of the OBs from control and *Kirrel2*$^{-/-}$*; Kirrel3*$^{-/-}$ mice (C, D, G, H). OB sections were co-immunolabeled with VGLUT2 antibodies to delineate glomeruli and with β-galactosidase (β-gal) antibodies to identify MOR1-3- (C, D) or MOR28- (G, H) positive glomeruli. The number of glomeruli per OB was counted and represented graphically in I. The number of MOR1-3- and MOR28-positive glomeruli per OB is unchanged in *Kirrel2*$^{-/-}$*; Kirrel3*$^{-/-}$ mice when compared with controls (control, *MOR1-3-lacZ n*=14 and *MOR28-lacZ n*=18 OBs; *Kirrel2*$^{-/-}$*; Kirrel3*$^{-/-}$, MOR1-3 *n*=18 and MOR28 *n*=26 OBs). Arrowheads indicate individual GFP- or β-gal-positive glomeruli. (J-Q) Electron micrographs of the

glomerular layer of the OB in control (J, N) and *Kirrel2*$^{-/-}$*; Kirrel3*$^{-/-}$ (K, O) adult mice. Asymmetric (J,K) and symmetric (N,O) synapses were classified as excitatory and inhibitory synapses, respectively, according to criteria outlined in the Supplementary Materials and Methods. The number and size of the presynaptic terminals for both asymmetric (L, M) and symmetric (P, Q) synapses are unchanged in the OB of *Kirrel2*$^{-/-}$*; Kirrel3*$^{-/-}$mice. *n*=3 animals for control and *Kirrel2*$^{-/-}$*; Kirrel3*$^{-/-}$ mice. Data are mean±s.e.m. Student's *t*-test (unpaired) was performed. Scale bars: 500 μm in A, B, E, F; 100 μm in C, D,G,H; 500 nm in J,K,N,O.

Kirrel2 ablation leads to coalescence defects in OSN axons projecting to the DII region of the OB

We next considered the possibility that Kirrel2 may be involved in the coalescence of OSN axons that project to the DII region of the OB, which is located more ventrally than the DI region. Analysis of the projections of MOR174-9-positive OSNs revealed that, although the location of the main MOR174-9 glomerulus was unaltered in *Kirrel2*$^{-/-}$ mice (Fig. 4A-J), the number of MOR174-9- positive glomeruli was increased (Fig. 4M-O). To determine whether other populations of axons that innervate the DII region were also affected by loss of Kirrel2, we assessed the targeting of M72-positive axons in *Kirrel2*$^{-/-}$ mice. Whole-mount and immunohistochemical analyses of M72-positive projections revealed the formation of additional glomeruli in the OB of *Kirrel2*$^{-/}$ mice (Fig. 4K, L, M, P, Q). Furthermore, the additional

MOR174-9- and M72-positive glomeruli observed in the OB of *Kirrel2*$^{-/-}$ mice appeared to be heterogeneous and innervated by MOR174-9- and M72-negative populations of axons, indicating that their coalescence into glomeruli has been disturbed in the absence of Kirrel2 (Fig. 4N-Q; glomeruli marked by asterisks).

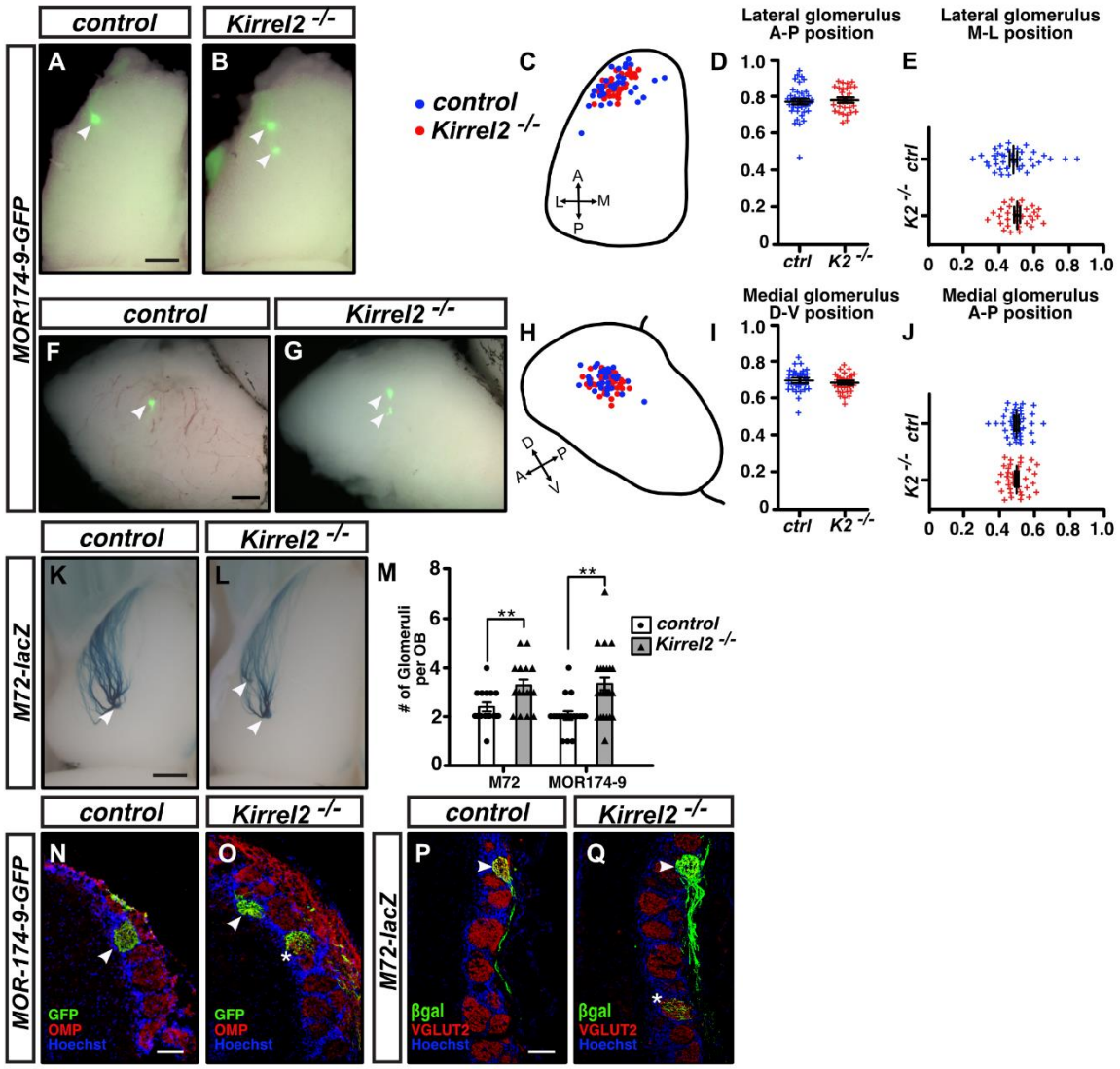

Figure 4. Defects in the targeting of MOR174-9- and M72-positive axons are observed in *Kirrel2*$^{-/-}$ mice. (A-J) Whole-mount analysis of the location of *MOR174-9-GFP*-positive glomeruli in control and *Kirrel2*$^{-/-}$ mice. A single MOR174-9 glomerulus is observed in both dorsal (A) and medial (F) views of the OB in most control mice, whereas additional glomeruli are observed in the OBs of *Kirrel2*$^{-/-}$ mice (B, G). For all OBs analyzed, glomerular locations were plotted on a diagram of the OB (C, H) and their positions along the anterior-posterior (A↔P), medial-lateral (M↔L) and dorsal-ventral (D↔V) axes were calculated and graphically represented (D, E, I, J). No significant difference in the position of MOR174-9 glomeruli was observed in *Kirrel2*$^{-/-}$ mice (control, *n*=37 OBs; *Kirrel2*$^{-/-}$, *n*=31 OBs). (K-L) Whole-mount analysis of the targeting of *M72-lacZ* axons (K, L) in the dorsal OB revealed additional M72-positive glomeruli in *Kirrel2*$^{-/-}$ mice (L, dorsal view of OB) (control, *n*=18 OBs; *Kirrel2*$^{-/-}$, *n*=12 OBs). (M-Q) To quantify the number of MOR174-9 and M72 glomeruli in the OBs of control and *Kirrel2*$^{-/-}$ mice, OB sections were immunolabeled with either OMP or VGLUT2 antibodies to delineate glomeruli and with GFP or β-galactosidase (β-gal) antibodies to identify MOR174-9 (N, O) and M72- (P, Q) positive glomeruli, respectively. The number of glomeruli per OB was counted and represented graphically in M. *Kirrel2*$^{-/-}$ OBs contained a significant increase in the number of MOR174-9 and M72 glomeruli when compared with control mice. Heterogenous innervation of some MOR174-9- and M72-positive glomeruli was observed in *Kirrel2*$^{-/-}$ mice (O, Q; glomeruli marked by an asterisk). (*MOR174-9-GFP*: control, *n*=19 OBs, *Kirrel2*$^{-/-}$, *n*=22 OBs; *M72-lacZ*: control, *n*=16 OBs, *Kirrel2*$^{-/-}$, *n*=16 OBs). Data are mean±s.e.m. Student's *t*-test (unpaired) was performed. ***P*<0.01. Arrowheads indicate individual GFP- or β-gal-positive glomeruli. Scale bars: 500 μm in A, B, F, G, K, L; 100 μm in N-Q

DISCUSSION

This study is the first loss-of-function demonstration of a requirement for a Kirrel family member in the formation of the olfactory glomerular map. Our results show that, although the differential expression of Kirrel2 and Kirrel3 provide axonal identity information in some populations of OSNs, Kirrel2/3-independent mechanisms also exist to ensure that accurate coalescence of populations of OSN axons in the DI region of the OB takes place. Taken together, these results indicate that different populations of OSN axons rely on different families of cell-surface receptors to regulate their coalescence during formation of the olfactory map.

Our results support the model that the differential expression of Kirrel2 between subsets of OSN axons is necessary for their precise coalescence into OB glomeruli. Although it remains possible, we think it is unlikely that expression of Kirrel2 in cells of the OB contributes to OSN axonal coalescence, as Kirrel2 is expressed at very low levels in the OB and its specific ablation in vomeronasal sensory neurons leads to axonal coalescence defects in the accessory olfactory bulb [114]. The previous demonstration that mosaic overexpression of Kirrel2 in subsets of MOR28-expressing axons leads to the splitting of these axons into two adjacent glomeruli, further supports an axonal role for Kirrel2 in this process [72]. Interestingly, loss of Kirrel3 [116] or the combined loss of Kirrel2 and Kirrel3 (Fig. 3) in MOR28- positive neurons does not affect glomerular targeting of their axons. It remains possible that ablating their expression in a mosaic fashion within MOR28-positive OSNs could recapitulate the phenotypes observed in the overexpression experiments.

The overall contribution of Kirrels to axonal identity in a specific type of OSN may be determined by the levels of expression of various other cell-surface adhesion molecules in these axons, such as BIG-2 (Contactin4) and Pcdh10, which have been implicated in OSN axonal targeting [159, 182]. OSN axons expressing higher levels, or a more diversified set of such proteins may be less reliant on the presence of Kirrel2 and Kirrel3 at their surface to coalesce accurately into glomeruli. Alternatively, the relative contribution of Kirrel2 to the coalescence of axons projecting to the DI and DII regions may be determined by the type of OR expressed by these axons. Class I ORs expressed in DI-projecting axons may be sufficient to impart axonal identity to these axons, whereas expression of class II ORs on axons innervating the DII region also requires Kirrel2/3

expression to impart axonal identity and promote coalescence [183, 184, 185,141,186, 187]. However, our observation that the coalescence of OSN axons expressing the Type II MOR28 OR is unaffected by the ablation of Kirrel2 and Kirrel3 suggests that the type of OR expressed does not represent the main difference between OSN populations that do or do not require Kirrel expression for their coalescence. Future identification of cell-surface receptors that are differentially expressed in DI- and DII- innervating axons should provide further insight into the mechanistic differences underlying the coalescence of axons from these two populations of OSNs.

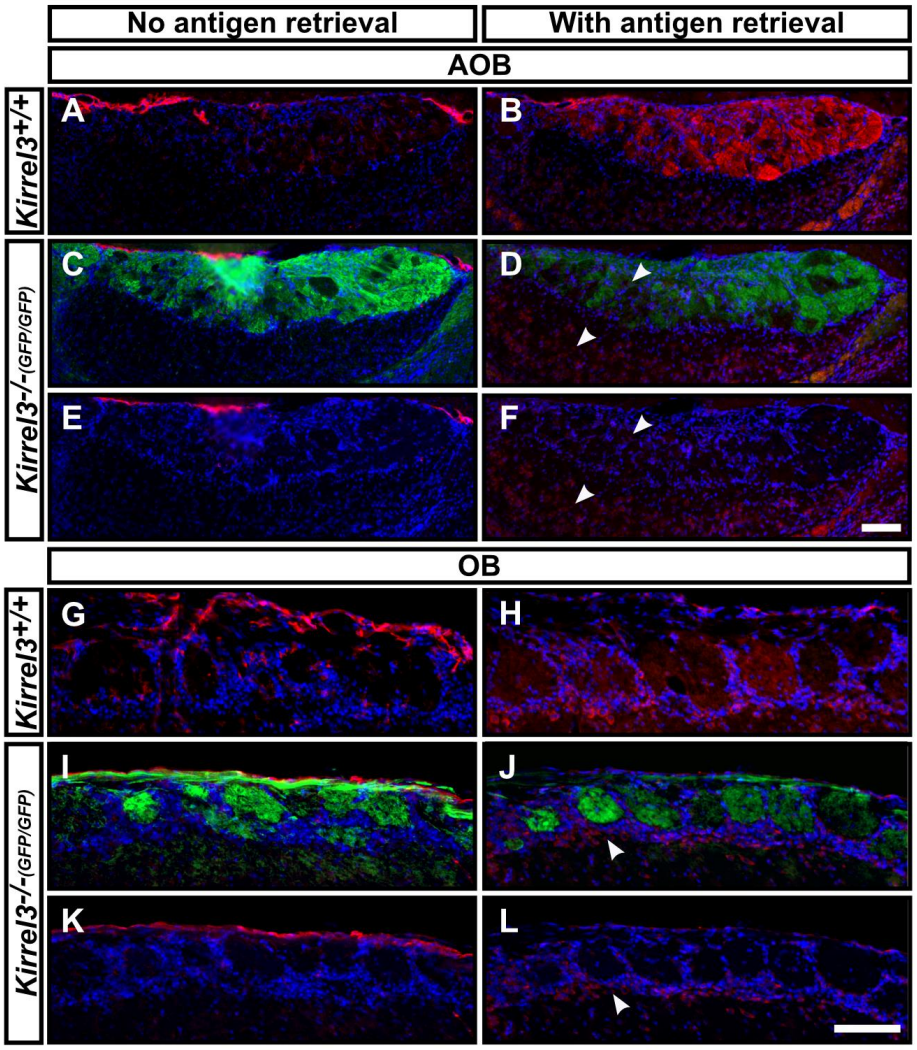

Figure S1. Characterization of the specificity of the Kirrel3 antibody by immunohistochemistry. To characterize the specificity of the Kirrel3 antibody used in our studies, alternating sagittal sections of OB from adult Kirrel3+/+ and Kirrel3-/- mice, expressing GFP in Kirrel3-positive cells, were immunostained with Kirrel3 (in red) and GFP antibodies (in green) using a protocol that involves an antigen retrieval procedure, and counterstained with Hoechst (in blue). When no antigen retrieval procedure is performed (A, C, E, G, I, K), weak Kirrel3 signal is observed in the AOB and OB of Kirrel3+/+ (A, G) but not in Kirrel3-/- mice (C,E,I,K). Performing an antigen retrieval step (B, D, F, H, J, L) enhanced the Kirrel3 signal observed in glomeruli of the AOB and OB (B, H) of Kirrel3+/+ but not in Kirrel3-/- mice (D, F, J, L), which allowed more precise characterization of Kirrel3 expression in OB glomeruli. The antigen retrieval protocol also resulted in the detection of a non-specific signal in the periglomerular and mitral/tufted cells of the bulbs (arrowheads), which varies in intensity between experiments and is observed in both control and Kirrel3-/- mice (B, D, F, H, J, L). Scale bars: 100 μm.

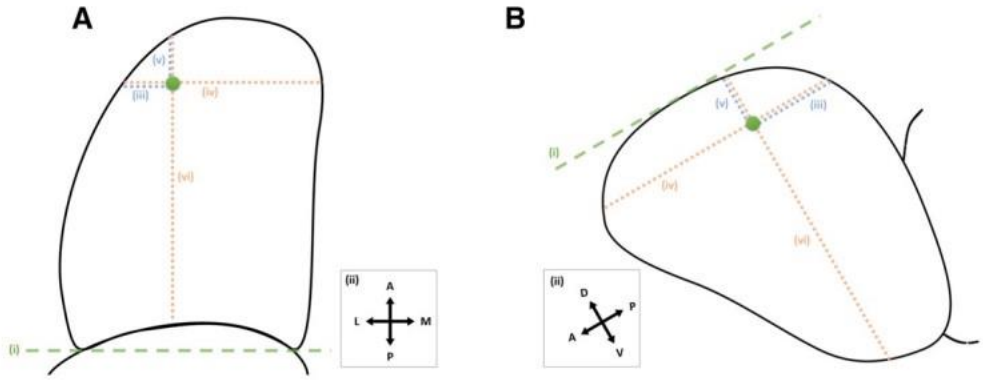

Figure S2. Diagrams representing the approach used to measure the location of lateral (A) and medial (B) glomeruli in pictures of whole-mount olfactory bulbs.

METHODS AND MATERIALS

Animals

Mice that have been previously described are as follows Kirrel3 [115] Kirrel2 [114], S50-ires-tau-GFP [183], M72-ires-tau-lacZ [188], MOR28-ires-tau-lacZ [189], MOR28-ires-tau-GFP [190], MOR174-9-ires-tau-GFP [172] and MOR1-3-ires-tau-lacZ [172]. These mice were maintained in a mixed background. All animal procedures have been approved by the Montreal Neurological Institute Animal Care Committee, in accordance with the guidelines of the Canadian Council on Animal Care. Most analyses included male and female mice.

Immunohistochemical procedures

Two to three-month old adult mice were anesthetized and perfused transcardially with ice-cold PBS containing 4% paraformaldehyde, dissected, and processed as previously described [146]. For Kirrel3 staining, an additional step of antigen retrieval was performed on a hot plate at 95°C, for 2min with ddH2O and then 10min with 0.01 M sodium citrate (pH 6.0). The sections were incubated overnight with primary antibody at 4°C using the following dilutions: anti-Kirrel2, 1:500 (R&D Systems, AF2930; characterized in Brignall et al. 2018), anti-Kirrel3, 1:100 (NeuroMab, clone N321C/49) , anti-GFP, 1:500 (Abcam, ab13970), anti-βgal. 1:500 (Abcam, ab9361), anti-OMP, 1:1000 (Wako Chemicals, 544-10001) and anti-vescicular transporter 2 (VGLUT2), 1:500

(Synaptic Systems, 135402). After rinsing in Tris-buffered saline. Primary antibody was detected with Alexa-488- or Alexa-546-conjugated secondary antibodies, 1:500 (Molecular Probes, A11056, A10036, A10040).

Analysis of glomerular numbers in the OB

Whole-mount OBs were stained with X-gal or processed for GFP fluorescence as previously described [172]. To count the number of GFP- or β-galactosidase (β-gal)-positive glomeruli in each OB, consecutive sections (20 μm) in the coronal plane through the whole OB of adult mice were immunostained with GFP, β-gal, VGLUT2 or OMP antibodies and counter-stained with Hoechst. The number of GFP- or β-gal positive glomeruli was counted on all sections of each OB from each mouse examined using ImageJ software. Student's t-tests (unpaired) were used to evaluate differences in glomerular location and numbers between control and mutant animals. Control animals included both wild -type and heterozygous littermates, and the number of OBs analyzed for each experiment is stated in the results section. Each OB was considered as an independent sample as the number of glomeruli between each OB varied in individual control and mutant mice.

Analysis of glomeruli positions in OBs

Whole mount OBs were processed for GFP fluorescence (S50-GFP or MOR174-9-GFP). To determine the location of a lateral glomerulus, a dorsal-view whole-mount image was taken (represented in figure S2.2 A). The medial-lateral axis was determined to be parallel to the border between the OB and the frontal cortex (i) while the perpendicular line to this border was labeled as the anterior-posterior axis (ii). For the medial-lateral position of a glomerulus, a line parallel to the medial-lateral axis was drawn through the glomerulus, and the ratio of the distance of the glomerulus to the most lateral edge of the OB along this line (iii) to the width of the OB at this plane of the bulb (iv) was calculated. For the anterior-posterior position of a glomerulus, a line parallel to the anterior -posterior axis was drawn through the glomerulus, and the ratio of the distance of the glomerulus to the most anterior edge of the OB along this line (v) to the length of the OB at this plane of the bulb (vi) was calculated. To determine the location of a medial glomerulus, a medial-view whole-mount image

was taken (represented in figure S2 B). The anterior-posterior axis was determined to be parallel to the dorsal edge of the OB (i), while the perpendicular line to this border was labeled as the dorsal-ventral axis (ii). For the anterior-posterior position of a glomerulus, a line parallel to the anterior-posterior axis was drawn through the glomerulus, and the ratio of the distance of the glomerulus to the most posterior edge of the OB along this line (iii) to the length of the OB at this plane of the bulb (iv) was calculated. For the dorsal-ventral position of a glomerulus, a line perpendicular to the anterior-posterior axis was drawn through the glomerulus, and the ratio of the distance of the glomerulus to the most dorsal edge of the OB along this line (v) to the height of the OB at this plane of the bulb (vi) was calculated.

Analysis of Kirrel2 and Kirrel3 expression levels between OSN populations

Serial coronal sections of the OB were collected onto alternating slides and stained for either Kirrel2 or Kirrel3 along with GFP or βgal to label the glomeruli of interest. Images of sections containing glomeruli were taken using Zen software by ZEISS, and all analysis was done using this program. Maximum values (MaxIntensity) on the display curve were set to ensure equal global staining levels across all sections between all experiments for each Kirrel. Minimum values (Background) to account for background levels of staining were measured by taking mean grey value of a sample portion of the external plexiform layer which is negative for Kirrels. Mean pixel intensity was measured for the glomerulus of interest (GlomIntensity) and the following formula was used to calculate the normalized glomerulus intensity: (Glom Intensity-Background)/Max Intensity. Normalized glomerulus intensity was averaged over all sections containing that glomerulus within one animal and mean normalized glomerulus intensity across al animals is graphically represented in the results section.

Electron microscopy and analysis of synapse numbers

OBs from perfused 3-month-old mice were sectioned and stained with uranyl acetate and Reynold'sead as described in detail in Brignall et al. 2018. Images were acquired using FEI Tecnai 12 120kV transmission electron microscope equipped with an AMT XR80C CCD camera system. At least ten micrographs from the glomerular layer of the OB from three mice of each genotype were analyzed as described below. Student's t-tests (unpaired) were used to evaluate differences between control and mutant animals.

Analysis of synapse number and axon terminal size in the glomerular layer of the OB

Electron micrographs of the glomerular layer of the OB were acquired at a magnification of 9,300x and analyzed in the Image J software to measure the number of synapses and the size of presynaptic terminals. The number of asymmetric and symmetric synapses were counted on each micrograph and represented as an average of synapses counted per 25μm^2 per mouse. The criteria used for synapse identification included an identifiable presynaptic area, an identifiable postsynaptic target cell, a clustering of synaptic vesicles in the presynaptic terminal near the presynaptic specialization, and a synaptic cleft between the pre and postsynaptic cell. Synapses that showed a postsynaptic density significantly thicker than the presynaptic density were defined as asymmetric excitatory synapses. Synapses with thin pre and post synaptic specializations and with pre and postsynaptic densities of similar thickness were defined as symmetric inhibitory synapses.

The size of the presynaptic terminals was analyzed by tracing the outline of the plasma membrane of the whole synaptic bouton visible on the micrograph and measuring the area using Image J software. The size of presynaptic terminals is represented as the average area of all presynaptic terminals measured in 25μm^2 of the OB per mouse.

Rationale for Chapter 3

In Chapter 2, we demonstrated a role for Kirrels in axon sorting in the main olfactory system. Since Kirrels have been proposed to regulate axonal targeting through their homophilic adhesion properties[113-115], we assess in Chapter 3 whether Kirrel3 homophilic adhesion contributes to the coalescence of axons in a glomerular field. We take advantage of the identification of key amino acid residues that are necessary for Kirrel3 homophilic adhesion to disrupt this adhesion[113] *in vivo*. Since Kirrel3 ablation leads to severe defects in the formation of the glomerular map in the accessory olfactory bulb[115] we examine the development of vomeronasal axonal projections in this system and demonstrate a requirement for Kirrel3 homophilic adhesion in the formation of the accessory olfactory bulb glomerular map.

Chapter 3: Understanding the role of homophilic cell adhesion property of Kirrel3 in axonal coalescence in the mouse accessory olfactory system

Neelima Vaddadi, Sabrina Quilez, Emilie Dumontier and Jean-François Cloutier

ABSTRACT

Vomeronasal sensory neurons project their axons from the vomeronasal organ to the accessory olfactory bulb to coalesce into spatially conserved glomeruli. Previous studies have shown that Kirrels 2 and 3 are required for axon sorting of vomeronasal sensory neuron axons in the accessory olfactory bulb. Ablation of Kirrel2 or Kirrel3 expression results in aberrant axon sorting of vomeronasal sensory neuron axons in the posterior region of the accessory olfactory bulb, resulting in formation of fewer and larger glomeruli. However, the molecular mechanism through which Kirrels promote axonal sorting remains unknown. Kirrel2 and Kirrel3 possess homophilic adhesion properties *in vitro*, suggesting that their differential expression and adhesion on vomeronasal sensory neuron axons may regulate axonal coalescence. We thus aim at understanding whether the homophilic cell adhesion property of Kirrel3 is important for its function in axonal coalescence of vomeronasal sensory neuron axons in this study. We demonstrate that selective disruption of Kirrel3 homophilic adhesion *in vivo* in mice leads to similar phenotypes observed in Kirrel3 knock-out mice, including altered glomerular structure and improper coalescence of vomeronasal sensory neuron axons. These results support a critical role Kirrel-dependent axonal adhesion in the sorting of vomeronasal sensory neuron axons in glomeruli of the accessory olfactory bulb.

INTRODUCTION

Olfactory sensory neurons in the vertebrate olfactory system expressing the same olfactory receptor project their axons into spatially conserved common target glomeruli in the olfactory bulb [191]. This allows the formation of a topographic odor map in the olfactory bulb [191]. In the mouse olfactory system, the expression of an olfactory receptor drives the expression of a set of cell surface receptors [72]. More specifically, expression of cell surface receptors Kirrel2 and Kirrel3 in OSN populations is correlated with OR expression and their expression level is dependent on odorant induced and spontaneous activity of olfactory receptors. Furthermore,

the expression pattern of Kirrel2 and Kirrel3 in the main mouse olfactory system is complementary. High Kirrel2 expressing OSNs and high Kirrel3 expressing OSNs segregate into separate glomeruli [192, 72].

The accessory olfactory system is primarily responsible for detecting chemosignals that are important for regulating social and sexual behaviours in most terrestrial vertebrates [130, 193]. This system constitutes vomeronasal sensory neurons whose axons project from the vomeronasal organ to the accessory olfactory bulb. VSNs expressing the same vomeronasal receptor coalesce into 6 to 30 spatially conserved glomeruli in the accessory olfactory bulb [162, 137, 163]. The coalescence of VSNs into their target glomeruli seems to be dependent on the level of expression of the Kirrel family of proteins [115]. VSN activity evoked by chemosignals guides the level of Kirrel protein expression whereby, loss of VSN activity for example, decreases Kirrel2 expression and increases Kirrel3 expression [115]. Different populations of VSNs express different amounts and combinations of Kirrel family proteins along their axons and all VSN axons expressing the same VR express similar levels of Kirrel2 and Kirrel3 proteins. Some VSN populations express complementary levels of Kirrel2 and Kirrel3 while some VSN populations express both Kirrel2 and Kirrel3 in varying levels [115]. Ablation of Kirrel3 results in improper axonal coalescence of VSN axons in the posterior region of the AOB resulting in fewer and larger glomeruli [115]. Similarly, Kirrel2 knockout mutants phenocopy the Kirrel3 knockout mutants, whereas a double knockout of both Kirrel2 and Kirrel3 results in the formation of glomeruli that are barely recognizable [115, 114].

The differential expression of Kirrels on olfactory sensory and vomeronasal sensory neuron axons has been proposed to regulate axonal coalescence into glomeruli through selective homophilic adhesion between Kirrel family members [115, 114, 72]. Homophilic adhesion of Kirrel proteins is mediated through their first Ig domain [113]. Crystal structure analyses revealed that the binding cores of Kirrel2 and Kirrel3 have different properties providing binding specificity [113]. While the Kirrel2 interacting interface is hydrophillic, that of Kirrel3 is hydrophobic [113]. This difference in the binding core allows selective homodimerization of Kirrel2 and Kirrel3 proteins and prevents them from cross reacting [113]. Furthermore, in vitro binding analyses of various Kirrel3 mutant proteins performed by our collaborators identified key amino acid residues, including glutamine 128, that are necessary for homophilic interactions [113]. Based on these observations, we used CRISPR-Cas9 genome

editing technologies to disrupt Kirrel3 homophilic binding *in vivo* and we show that this disruption leads to altered axonal coalescence and glomerular structure in the accessory olfactory bulb. These results confirm that the homophilic cell adhesion property of Kirrel3 is essential for its role in axonal coalescence in the mouse accessory olfactory system.

RESULTS

Generation and characterization of a knockin mouse with disrupted Kirrel3 homophilic cell adhesion in vivo.

The crystal structure and mutational analyses of Kirrel3 identified a glutamine (Q) amino acid located in the first Ig domain as essential for Kirrel3 homophilic binding. Substituting Q128 to an alanine (A) result in a loss of dimerization in size exclusion chromatography as well as loss of Kirrel3-mediated cellular aggregation in heterologous cells. In order to assess whether homophilic adhesion contributes to Kirrel3 function in wiring the olfactory systems, we examined the effect of abolishing Kirrel3 dimerization on vomeronasal sensory neuron axon targeting in the AOB. We engineered mice expressing a Kirrel3 protein harboring a Q128A amino acid substitution, which abolishes Kirrel3 dimerization, using CRISPR technology (Figure 1A-C). An analysis of Kirrel3 protein in lysates extracted from brain samples of wild-type and *Kirrel3*$^{Q128A/Q128A}$ mice revealed that Kirrel3 Q128A is expressed at comparable levels to the wild-type protein in the brain (Figure 1D, E). Additionally, cell surface biotinylation assays on brain slices from control and *Kirrel3*$^{Q128A/Q128A}$ mice, showed that the mutant protein is properly trafficked to the cell's surface (Figure 1F). We then investigated the expression patterns of Kirrel3 Q128A on VSN axons innervating the AOB. Kirrel3 is expressed on subsets of VSN axons innervating glomeruli throughout the AOB with a large proportion of glomeruli in the posterior region expressing Kirrel3[115]. Sagittal sections of the AOB stained for Kirrel3 demonstrated a clear localization of Kirrel3 in a majority of glomeruli in the posterior region of the AOB in both wild-type and *Kirrel3*$^{Q128A/Q128A}$ mice (Figure 1G).

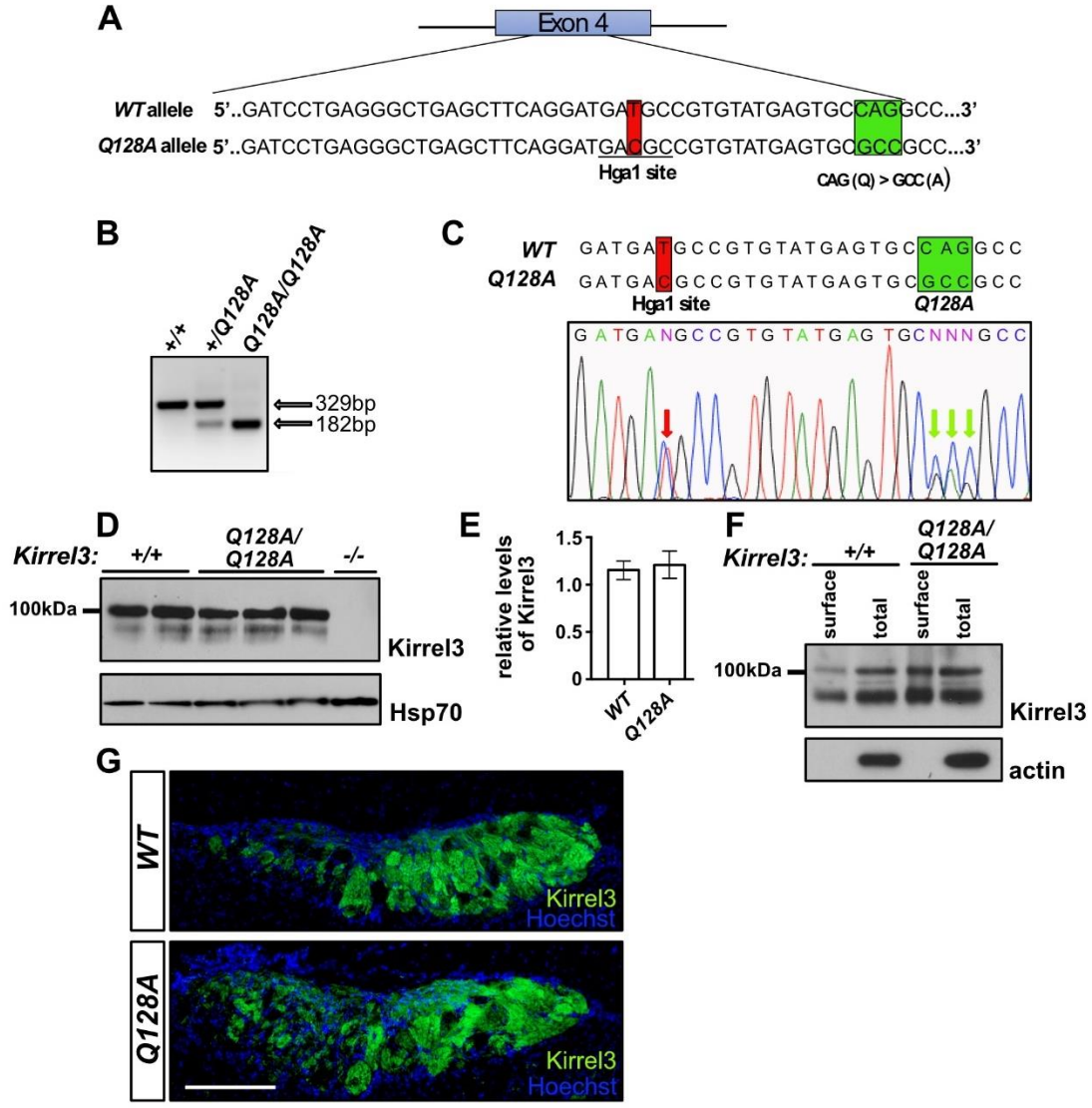

Figure 1. Characterization of the Kirrel3 Q128A mouse. (A) Diagram of the generation of the Kirrel3 Q128A mouse. Mice carrying a modified Kirrel3 allele containing mutations that modify amino acid 128 from a Q to an A, as well as a silent mutation introducing an HgaI restriction enzyme cutting site for genotyping purposes, were generated. Green square: Q to A mutations; red square: mutation creating an HgaI restriction site. (B and C) Identification of the Kirrel3 Q128A allele by restriction enzyme digest and DNA sequencing. Digestion with HgaI (B) and DNA sequencing (C) of a PCR fragment from exon 4 of the Kirrel3 allele demonstrate the presence of the newly introduced HgaI restriction site. DNA sequencing also reveals the presence of the three nucleotide substitutions resulting in the Q-to-A amino acid substitution in a Kirrel3$^{+/Q128A}$ mouse. The red arrows in the electropherogram in (C) indicate the overlapping peaks caused by the nucleotide substitutions in one of the Kirrel3 alleles. (D and E) Quantification of Kirrel3 protein by western blot of brain lysate collected from Kirrel3$^{+/+}$ and Kirrel3$^{Q128A/Q128A}$ mice shows that similar levels of Kirrel3 and Kirrel3 Q128A levels are expressed in the brain of these mice, respectively. Data were analyzed using unpaired t test; n = 3 for Kirrel3$^{+/+}$ and n = 4 for Kirrel3$^{Q128A/Q128A}$ mice. (F) Surface membrane distribution of Kirrel3 Q128A in acute brain slices. Western blots of acute brain slice lysate collected from Kirrel3$^{+/+}$ and Kirrel3$^{Q128A/Q128A}$ mice following incubation with biotin and isolation of surface proteins by batch streptavidin chromatography. Both Kirrel3 and Kirrel3 Q128A are distributed to the cell surface. (G) Immunohistochemistry on sagittal sections of the AOB from Kirrel3$^{+/+}$ and Kirrel3$^{Q128A/Q128A}$ adult mice labeled with antibodies against Kirrel3 and Hoechst. The Kirrel3 and Kirrel3 Q128 proteins can be detected in subsets of glomeruli in both the anterior and posterior regions of the AOB in Kirrel3$^{+/+}$ and Kirrel3$^{Q128A/Q128A}$ mice, respectively. The scale bar represents 200 mm.

Kirrel3 Q128A mice show altered glomerular structure and axonal coalescence defects.

Since *Kirrel3*$^{-/-}$ mice show altered glomeruli structure in the posterior region of the AOB [115], we next performed a detailed analysis of the glomerular layer in *Kirrel3*$^{Q128A/Q128A}$ mice. To visualize and delineate glomeruli, sagittal sections of the AOB of control and *Kirrel3*$^{Q128A/Q128A}$ mice were stained with anti-VGLUT2, which marks excitatory pre-synaptic terminals in the AOB. As previously observed in *Kirrel3*$^{-/-}$ mice [115], the size and number of glomeruli in the anterior region of the AOB appears unaffected in *Kirrel3*$^{Q128A/Q128A}$ mice when compared to control animals (Figures 2 A, B, G, H). In contrast, and as observed in *Kirrel3*$^{-/-}$ mice, the posterior region of the AOB in *Kirrel3*$^{Q128A/Q128A}$ mice contains significantly fewer glomeruli and the average size of each glomerulus in increased by ~43% (Figures 2 A-D, J, L), indicating that axonal coalescence is likely affected.

To ensure that the disruption of glomerular targeting observed in the Kirrel3 Q128A mutant mice is not a secondary cause of possible off target effects of CRISPR cutting elsewhere in the genome during the generation of this mutant mouse, we have taken two approaches. First three independent founder lines were analyzed in parallel and individually crossed with c57Bl6 mice for three generations to ensure segregation of any off-target mutations. Furthermore, the accessory olfactory bulb of mice descending from all three founder lines were analyzed (Figure 2). Qualitative assessment of the accessory olfactory bulb glomerular structure in mice derived from all three founder lines revealed altered organization of the glomeruli in the posterior region of the accessory olfactory bulb, demonstrating the specificity of the genome editing approach.

To examine the targeting and coalescence of VSN axons, we crossed the *Kirrel3*$^{Q128A/Q128A}$ mice with mice expressing *tau-lacZ* in a specific population of VSNs that expresses the vomeronasal receptor EC2 and innervates specifically the posterior region of the AOB [148]. EC2-positive VSNs also express Kirrel3 [115]. As expected, the segregation of EC2-positive axons to the posterior region of the AOB was unaffected in *Kirrel3*$^{Q128A/Q128A}$ mice since this process does not require Kirrel3 expression (Figure 2 G, H) [115]. In control animals, coalescing EC2-positive axons form small well-defined glomeruli that are innervated by a single population of VSN axons (Figure 2 I, J). In contrast, EC2-positive axons coalesce into larger heterogenous

glomeruli innervated by additional populations of VSN axons in *Kirrel3*$^{Q128A/Q128A}$ mice, as previously observed in Kirrel3$^{-/-}$ mice (Figure 2 K, L) [115]. Thus, the Kirrel3 homophilic binding is necessary for proper coalescence of VSN axons into glomeruli of the AOB.

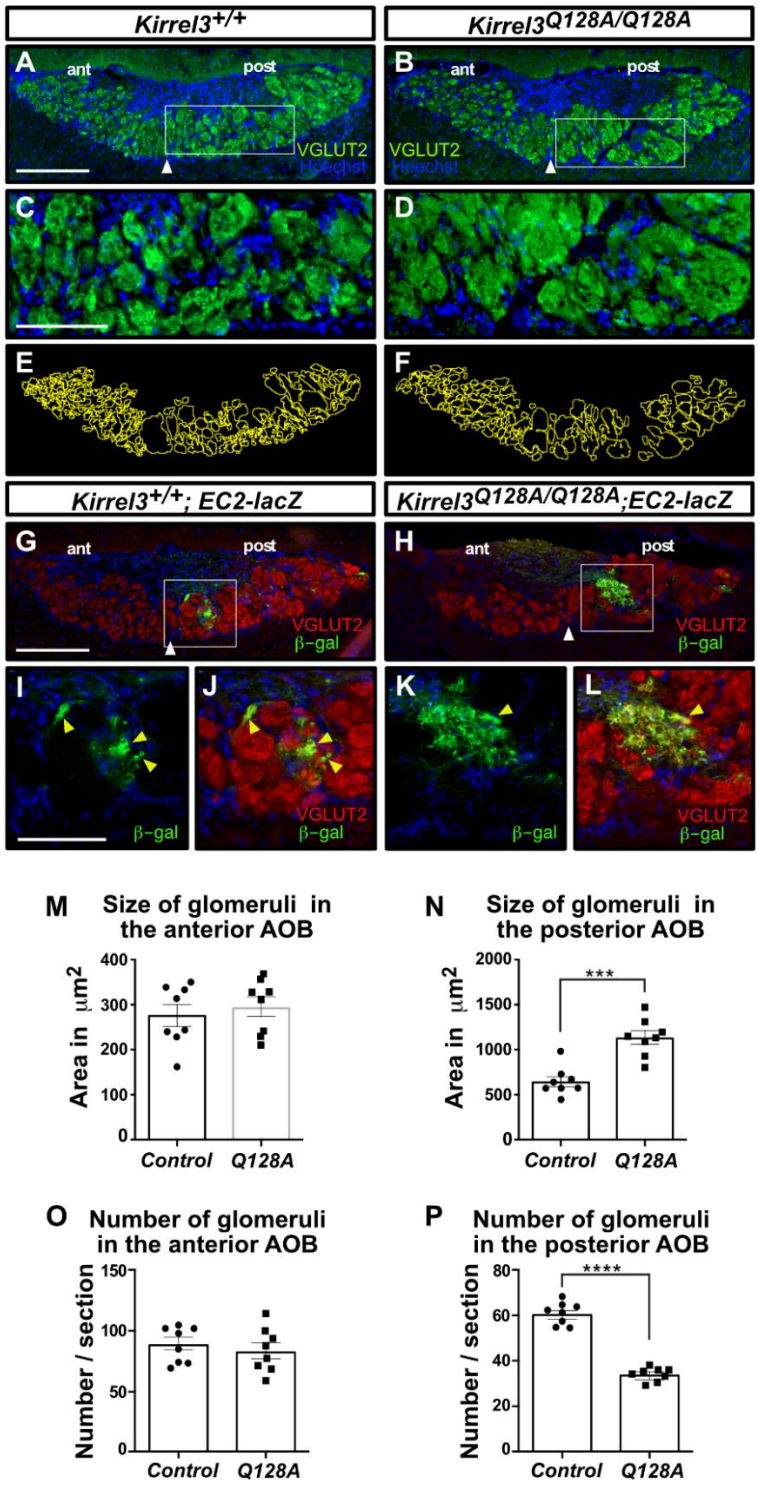

Figure 2. Glomerulus structure is altered in the AOB of Kirrel3$^{Q128A/Q128A}$ mice. (A–F) Parasagittal sections of the AOB from adult Kirrel3$^{+/+}$ (A and C) and Kirrel3$^{Q128A/Q128A}$ (B and D) mice labeled with a VGLUT2 antibody and Hoechst (A–D). Higher magnification of outlined regions in (A) and (B) are shown in (C) and (D), respectively. Glomeruli in the posterior region of the AOB in Kirrel3$^{Q128A/Q128A}$ mice appear significantly larger and less numerous than those in Kirrel3$^{+/+}$ mice (E and F).White arrowheads denote the boundary between the anterior (ant)

and posterior (post) regions of the AOB; n > 8 mice for each genotype.(G–L) Parasagittal sections of the AOB from adult Kirrel3$^{+/+}$; EC2-lacZ (G) and Kirrel3$^{Q128A/Q128A}$; EC2-lacZ (H) mice labeled with a VGLUT2 (red) and β-galactosidase (green) antibodies and Hoechst (G–L). Higher magnification of outlined regions in (G) and (H) are shown in (I) and (J) and (D) and (L), respectively. EC2-positive axons coalesce into small and well-defined glomeruli in Kirrel3$^{+/+}$; EC2-lacZ mice (yellow arrowheads; I and J) but innervate larger heterogenous glomeruli in Kirrel3$^{Q128A/Q128A}$ mice (yellow arrowheads in K and L); n = 2 mice for each genotype. (M–P) Quantification of the size and number of glomeruli in the anterior (G and I) and posterior regions (H and J) of the AOB in adult control and Kirrel3$^{Q128A/Q128A}$ mice. A representation of the glomerulus outlining approach used for quantification using sections in (A) and (B) as examples are shown in (E) and (F), respectively. A significant increase in the size of glomeruli in the posterior (control: 644.0 ± 56.2 mm2; Kirrel3$^{Q128A/Q128A}$: 1,134.1 ± 74.5 mm2), but not anterior (control: 284.0 ± 19.6 mm2; Kirrel3$^{Q128A/Q128A}$: 295.6 ± 22.1 mm2), region of the AOB is observed in the Kirrel3$^{Q128A/Q128A}$ mice (G and H). There is also a decrease in glomerulus numbers in the posterior (control: 61.15 ± 1.75; Kirrel3$^{Q128A/Q128A}$: 34.27 ± 1.02), but not anterior (control: 87.21 ± 4.92; Kirrel3$^{Q128A/Q128A}$: 84.22 ± 6.33), region of the AOB in Kirrel3$^{Q128A/Q128A}$ mice (J). Data were analyzed using unpaired t test; n = 8 mice for each genotype. ****p value < 0.0001 (glomerular counts); ***p value < 0.001 (glomerular size); error bars: ±standard error of the mean (SEM); scale bars, 250 mm in (A) and (B) and 100 mm in (C) and (D).

DISCUSSION

The wiring of the nervous system is guided by a combination of intercellular interactions mediated by cell surface receptors [194]. The interactions can be heterotypic, usually allowing for establishing connectivity between different neuronal types, guiding growth of axons in a gradient field established by cues or by contacts between processes resulting in attraction or repulsion. Homotypic interactions can also be used to establish synaptic connections (as Kirrel3 is proposed to mediate in the hippocampus), lead to contact-mediated repulsion or to fasciculation and coalescence of axons. Kirrel2 and Kirrel3 are differentially expressed in sets of sensory neurons whose axons are segregated into separate glomeruli in the accessory and main olfactory bulbs. This differential expression of Kirrel2 and Kirrel3 likely generates a molecular code of recognition that

contributes to the coalescence of axons expressing the same sensory receptor into glomeruli. However, the molecular mechanism through which differential expression of Kirrel family members in populations of sensory axons modulates their segregation into glomeruli remained to be addressed.

We showed that the dimerization Kirrel3 through its first Ig domain directly contributes to axonal coalescence and glomerulus formation. Analysis of axonal targeting and glomerular morphology in the AOB of *Kirrel3*$^{Q128A/Q128A}$ mice closely resembled those of the *Kirrel3* knockout, where glomeruli increase in size and are heterogeneously innervated in the posterior AOB. We have confirmed that the Q128A mutant displays correctly to the cell surface, which implies that the observed AOB phenotype is not due to misfolding or trafficking errors. Though we did not test Kirrel2 loss-of-function mutations *in vivo*, Kirrel2 shares a closely related structure and evolutionary history with Kirrel3, and it is reasonable to assume that the dimerization interface on Kirrel2 may also control glomerulus formation in a similar manner.

While Kirrel homodimerization is necessary for proper axonal coalescence and glomerulus formation, additional factors also contribute to this process, including vomeronasal and olfactory receptor expression, and neuronal activity [162, 177,178, 179, 192, 163, 180]. Furthermore, the combinatorial expression of additional families of cell surface molecules likely adds to the axonal molecular diversity necessary to segregate large populations of axons into glomerular target fields by modulating the adhesion of similar axons or repulsion of dissimilar axons [175,159, 176,72]. Kirrel3 is expressed in a majority of VSN axons innervating the posterior region of the AOB as well as in subsets of axons innervating the anterior part of the AOB. While glomerular formation is affected in the posterior region of the AOB in both Kirrel3$^{Q128A/Q128A}$ and *Kirrel3*$^{-/-}$ mice, we could not detect statistically significant changes in glomeruli formation in the anterior AOB in these mice (Figure 2, [115]). This observation suggests that additional families of CAMs may be expressed specifically in VSN neurons innervating the anterior AOB and compensate for the loss of Kirrel3 function in the targeting of these axons to the anterior AOB.

Whether Kirrels' function as axonal sorting molecules relies strictly on its adhesive properties to promote coalescence of like axons or also necessitates intracellular signaling that impinges on this process

remains to be determined. Nonetheless, multiple lines of evidence support the idea that Kirrels and its homologs act as more than just "molecular Velcro" in nervous system development. In hippocampal neuron cultures, Kirrel3 homophilic adhesion is required, but not sufficient for synapse formation, and mutations that occur outside of the D1 binding domains and even in the intracellular domains prevent synapse formation, despite being able to form homodimeric complexes [112]. The *C. elegans* homologs SYG-1 and SYG-2 were shown to be signaling receptors, whose functions depend on the exact geometry of ectodomain dimerization also mediated by D1 [195]. Finally, Kirrels carry conserved and functional signaling motifs in their cytoplasmic domain, including phosphorylation sites, PDZ motifs, and actin cytoskeleton recruitment sequences [196, 197,198, 199, 200, 201,202] . These findings suggest that Kirrel3 undergoes active signaling once the homodimeric complexes have formed. Future studies assessing a requirement for the Kirrel intracellular domain in selective axonal segregation and synapse specification in the nervous system should help address the contribution of Kirrel signaling to these processes.

METHODS AND MATERIALS

Animals

The *Kirrel3 Q128A* mouse line was generated as follows: sgRNAs were designed using the open access software Breaking-Cas (https://bioinfogp.cnb.csic.es/tools/breakingcas) [203] and tested for cutting efficiency using a T7 assay as previously described [204]. One-cell stage C57Bl6 mouse zygotes were microinjected with the sgRNA, Cas9 protein, and a donor DNA template to introduce the required DNA mutations in the *Kirrel3* allele (see Figure 1A) and were implanted in surrogate female mice. Offsprings were screened for the presence of the target mutations by PCR, restriction enzyme analysis, and DNA sequencing. Three *Kirrel3 Q128A* founder lines were chosen for further analyses and backcrossed for three generations in the C57Bl6 background to segregate any potential off-target mutations. Analyses of the glomerular structure of the AOB presented in Figure 2 was performed on *Kirrel3 Q128A* mice derived from a single founder line. Similar analyses were also performed on *Kirrel3 Q128A* mice derived from two other founder lines and revealed similar phenotypes (data

not shown). The *EC2-tau-lacZ* (Tg(Vmn2r43-lacZ*)#Ddg) mouse line has previously been described [148]. All animal procedures have been approved by The Neuro Animal Care Committee and McGill University, in accordance with guidelines of Canadian Council of Animal Care.

Immunohistochemistry

Two to three-month-old adult mice were anesthetized and perfused transcardially with 10 ml ice-cold 1x PBS followed by 10 ml 4% paraformaldehyde solution in 1x PBS. Brains were dissected and post-fixed in 4% paraformaldehyde solution for 30 min followed by 24 h cryoprotection in 30% sucrose. 20 µm-thick sagittal AOB sections were collected on microscope slides and incubated overnight at 4°C with the following primary antibodies: Anti-VGLUT2, 1:500 (Synaptic Systems) or anti-Kirrel3, 1:100 (Neuromab). After rinsing in Tris-Buffered Saline, the appropriate secondary antibody-Alexa 488 conjugate (Molecular Laboratories) was applied at 1:500 dilution to detect the primary antibody and BS lectin at 1:1500 (Vector Laboratories) was applied along with the secondary antibody. Sections were counter-stained with Hoechst at 1:20,000 dilution (ThermoFisher Scientific).

Analysis of Glomeruli in the AOB

Analysis of the size and number of glomeruli in AOB sections were performed as previously described [114, 115]. 20 µm-thick sagittal sections of the AOB were obtained from *Kirrel3*$^{+/+}$, *Kirrel3* $^{+/Q128A}$, and *Kirrel3* $^{Q128A/Q128A}$ mouse brains. A blinded analysis measuring glomerular size and number using Fiji software [205] was performed on 8 to 10 consecutive sections from both AOBs that contained anterior and posterior regions of similar sizes at comparable medial-lateral level. Each VGLUT2 positive unit surrounded by a region of non-innervated neuropil was defined as a glomerulus and was manually traced on Fiji by an expert. The number of glomeruli and their sizes was measured from each section examined and the average values for each mouse brain was calculated. Since no difference was observed between *Kirrel3*$^{+/+}$ and *Kirrel3* $^{+/Q128A}$ mice, they were grouped together and designated as Controls. The anterior-posterior AOB border was identified by staining sections with BS lectin (data not shown). Littermates were used for analyses.

Analysis of Kirrel3 protein expression

Whole brain lysates were harvested using 20 mM HEPES, 320 mM sucrose with protease inhibitors (0.1 µg/µl Leupeptin/Aprotinin and 1 mM PMSF). Protein concentration of lysate was determined using the Bio-Rad protein concentration assay and equal amounts of protein were loaded and subjected to SDS-PAGE gel electrophoresis followed by transfer to PVDF membranes (Immobilon-P). Membranes were probed with mouse anti-Kirrel3 1:100 (Neuromab Clone N321C/49; catalog no. 75-333) that detects the long and short isoforms of Kirrel3, rat anti-HSC70/HSP73 1:10,000 (Enzo Life Sciences), or rabbit anti-β-actin 1:1,000 (Cell Signalling Technology), followed with appropriate HRP-conjugated secondary antibodies. Blots were developed using SuperSignal West Femto Kit (Thermo Fisher Scientific). Quantification of relative protein levels was performed on scanned immunoblots using Fiji software.

Cell surface biotinylation in acute brain slices

Cell surface biotinylation assay was performed as described in [206]. Acute mouse brain slices were prepared from *Kirrel3*$^{Q128A/Q128A}$ and *Kirrel3*$^{+/+}$ mice, placed in ACSF and allowed to recover in a recovery chamber for 1 hour at room temperature. Two slices were incubated in in chilled ACSF containing 1 mg/ml EZ-link Sulfo-NHS-SS-Biotin (Thermo Fisher Scientific) for 45 minutes. The biotin was then quenched with two washes of 10 mM Glycine in ACSF at 4°C followed by three washes in ice cold ACSF for 5 min. Slices were then harvested in RIPA buffer (10 mM Tris pH 7.45, 150 mM NaCl, 1 mM EDTA, 1% Triton X-100, 0.1% SDS and 1% sodium deoxycholate) supplemented with protease and phosphatase inhibitors (100 mM PMSF and PhosSTOP tablet (Roche)). Biotinylated proteins were precipitated with streptavidin-agarose beads (Thermo Fisher Scientific) at 4°C overnight, washed, and eluted from beads using SDS-PAGE reducing sample buffer. Equal amounts of protein were then subjected to a Western Blot analysis as described above

Rationale for Chapter 4

In Chapter 2 and Chapter 3, we discuss the role and mechanism behind the role of Kirrel family of proteins in axon sorting in the mouse main and accessory olfactory systems respectively. More specifically in Chapter 3, we focus on understanding the role of homophilic cell adhesion property of Kirrel3 in VSN axon sorting in the mouse accessory olfactory system. In Chapter 4, we focus on the role of Kirrel family member Kirrel3 in the regulation of dendritic complexity of the post-synaptic component of the olfactory circuit, viz 2nd order projection neurons called mitral cells. In comparison to the accessory olfactory system, dendritic complexity regulation of mitral cells in the main olfactory system is relatively simple and easier to study[120,136-138]. We thus focus on the role of Kirrel3 in the regulation dendritic complexity of mitral cells in the main olfactory system.

It is known from previous studies that neuronal activity in OSNs regulates the expression of Kirrels in these cells[72]. It is also known that neuronal activity in mitral cells is involved in the regulation of their dendritic complexity[170]. It is therefore possible that neuronal activity in mitral cells could control the levels of Kirrel3 in mitral cells, and this in turn could regulate dendritic complexity of mitral cells. Thus, in Chapter 4, we investigate whether Kirrel3 is expressed in mitral cells and whether it's ablation or lack of homophilic adhesion *in vivo* affects mitral cell dendritic complexity.

Chapter 4: Understanding the role of Kirrel3 in the regulation of mitral cell dendritic complexity in the mouse main olfactory system

Neelima Vaddadi, Barbara Morquette, Reesha Raja, Emilie Dumontier and Jean-François Cloutier

ABSTRACT

The binding of odorant molecules to olfactory receptors on olfactory sensory neurons leads to activation of second order neurons, termed mitral cells, in the olfactory bulb, which project to higher brain centres. During development, dendritic projections of mitral cells mature during the postnatal period, with each mitral cell ultimately sending an apical dendrite to a single glomerulus. This maturation is dependent on mitral cell activity, as overexpression of inward rectifying potassium channels Kir2.1 or blocking of NMDARs in mitral cells also results in perturbed pruning of mitral cell dendrites. The expression of cell adhesion molecules in mitral cells may contribute to the targeting and pruning of mitral cell apical dendrite by stabilizing synaptic contacts in glomeruli between olfactory sensory neuron axons and mitral cell dendrites expressing similar levels of cell adhesion molecules. Interestingly, Kirrel2 and Kirrel3 expression in olfactory sensory neurons is regulated by neuronal activity, suggesting that activity in mitral cells could potentially regulate dendritic complexity and pruning by modulating expression of Kirrel family members. In this study we show that Kirrel3 is expressed in mitral cells of the olfactory bulb and that it is required for regulating mitral cell dendritic complexity. We also show that the homophilic cell adhesion property of Kirrel3 is dispensable for its role in regulation of mitral cell dendritic complexity, thereby suggesting that Kirrel3 may have its effect on dendritic development by binding to an unknown ligand.

INTRODUCTION

Processing of olfactory information in the mouse olfactory bulb relies on the formation of stereotypic connections between olfactory sensory neurons (OSNs) and second order neurons in neuropil structures, termed glomeruli [121]. Most OSNs, whose cell bodies reside in the olfactory epithelium, express a single type

of olfactory receptor [121]. These OSNs project their axons to the mouse main olfactory bulb (MOB) in such a way that all axons of OSNs expressing the same olfactory receptor coalesce together into a few glomeruli where they synapse onto the dendrites of mitral cells [124]. These mitral cell project their axons to higher brain centers, such as the piriform cortex, the amygdala, the olfactory cortex, the olfactory tubercle, the anterior olfactory nucleus, and the entorhinal cortex, to relay olfactory sensory information [123,124].

Mitral cells are born in the ventricular zone between E11.5 to E13 and they migrate to the olfactory bulb where they settle into the intermediate zone [125]. From the intermediate zone they extend their axons to the cortex via the lateral olfactory tract [125]. The cell bodies of the mitral cells reorient themselves from a tangential position to a radial position and extend primary dendrites into the glomerular layer [125]. The mitral cell bodies are positioned radially in the mitral cell layer as the name suggests. Mitral cell primary dendrites meet OSN axons in the developing glomerular layer of the OB to form a protoglomerulus around E15-E16 [125]. Early on in development, a single mitral cell extends multiple primary dendrites into multiple glomeruli [126]. However, during postnatal stages, dendrites undergo pruning, leading to the adult pattern of innervation whereby the vast majority of mitral cells possess a single dendrite that populates a single glomerulus [126]. Our understanding of the processes that regulate mitral cell complexity and pruning remains limited. Studies suggest that Notch, Nectin and TrkB are examples of molecules involved in regulating mitral cell dendritic branching while TARSH and BMPR2 are involved in regulating mitral cell dendritic pruning[85,127,167–169]. Neuronal activity also contributes to the pruning of mitral cell dendrites [170]. Changes in spontaneous activity in mitral cells induced through overexpression of the inward rectifying potassium channels Kir2.1 results in reduced pruning of mitral cell dendrites[170]. Blocking NMDA-mediated activity in mitral cells also disrupts mitral cell dendrite pruning. has been shown to play an important role in mitral cell pruning[170]. In contrast, manipulating OSN spontaneous and odorant-mediated activity by knocking out the CNGA2 channel had minimal effect on adult mitral cell dendrite complexity, although dendritic pruning was slightly delayed[126].

Since spontaneous and NMDA mediated activity seem to play an important role in mitral cell dendritic pruning, we hypothesized that the cell adhesion molecule Kirrel3, whose expression is regulated by neuronal activity in

olfactory sensory neurons, might contribute to the regulation of mitral cell dendritic development. We showed that Kirrel3 is expressed in mitral cells of the olfactory bulb during postnatal development and in the adult. Using retrograde DiI labelling to visualize mitral cell dendrites in wild-type and and *Kirrel3* mutant mice, we show that loss of Kirrel3 leads to the higher numbers of immature dendritic projections in the adult olfactory bulb. In contrast, loss of Kirrel3 cell adhesion in *Kirrel3*$^{Q128A/Q128A}$ mice did not affect mitral cell dendritic complexity, demonstrating that Kirrel3 contribution to this process is independent of its cell adhesion properties.

RESULTS

Characterization of *Kirrel3* expression in the mitral cell circuit

To begin to assess whether Kirrel3 contributes to the regulation of mitral cell dendritic complexity, we first examined its expression in cells of the olfactory bulb by *in situ* hybridization at a postnatal stage when dendritic pruning takes place (P7) and in adults when mitral cell dendrites are fully developed. *Kirrel3* mRNA was observed in cell bodies of mitral cells located in the mitral cell layer and in periglomerular cells that surround the glomeruli in the glomerular layer at both ages. *Kirrel3* was also detected in some cell bodies in the external plexiform layer that are likely tufted cells. Interestingly the levels of *Kirrel3* expression appeared to vary between different mitral cells. Similar differential expression of Kirrel3 has also been reported in axons of OSN innervating glomeruli.

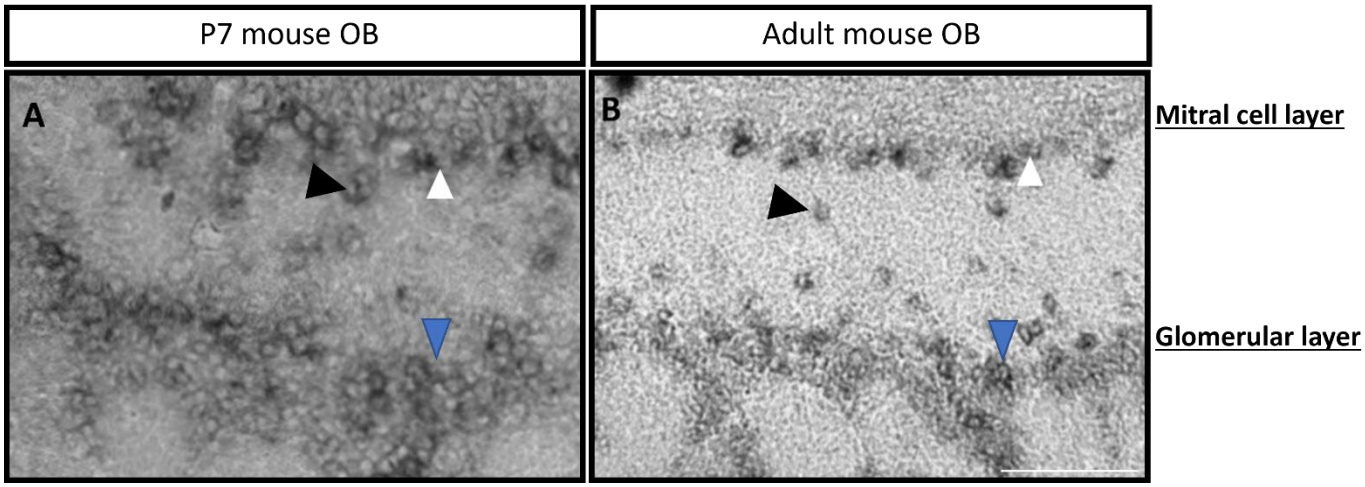

Figure 1. Characterization of expression pattern of *Kirrel3* in the olfactory bulb. (A) *In situ* hybridization of olfactory bulb sections from P0 and adult mouse brains with an antisense cRNA probe for *Kirrel3* that has been previously characterized for specificity [114,115]. White arrows indicate mitral cells, black arrows indicate tufted cells, and blue arrows indicate periglomerular cells in the glomerular layer. Scale bar: 100µm

Visualizing mitral cells in the mouse brain using diI labelling

To examine the function of Kirrel3 in mitral cell dendritic complexity, we first established a method to visualize mitral cell dendrites at a single neuron level. We used a retrograde labelling technique by placing a crystal of DiI (1,1′-dioctadecyl-3,3,3′,3′-tetramethylindocarbocyanine) in the lateral olfactory tract, which contains mitral cell axons exiting the olfactory bulb and projecting to higher brain centres. The dye was allowed to diffuse into the olfactory bulb for 3 to 4 weeks leading to sparse labeling of random cells in olfactory bulb. By looking at the morphology and location of these sparsely labelled cells, we were able to identify mitral cells and examine the complexity of their dendrites. An adult mitral cell has a single apical dendrite projecting to a single glomerulus with lateral dendrites extending sideways making dendrodendritic synapses with adjacent mitral cells.

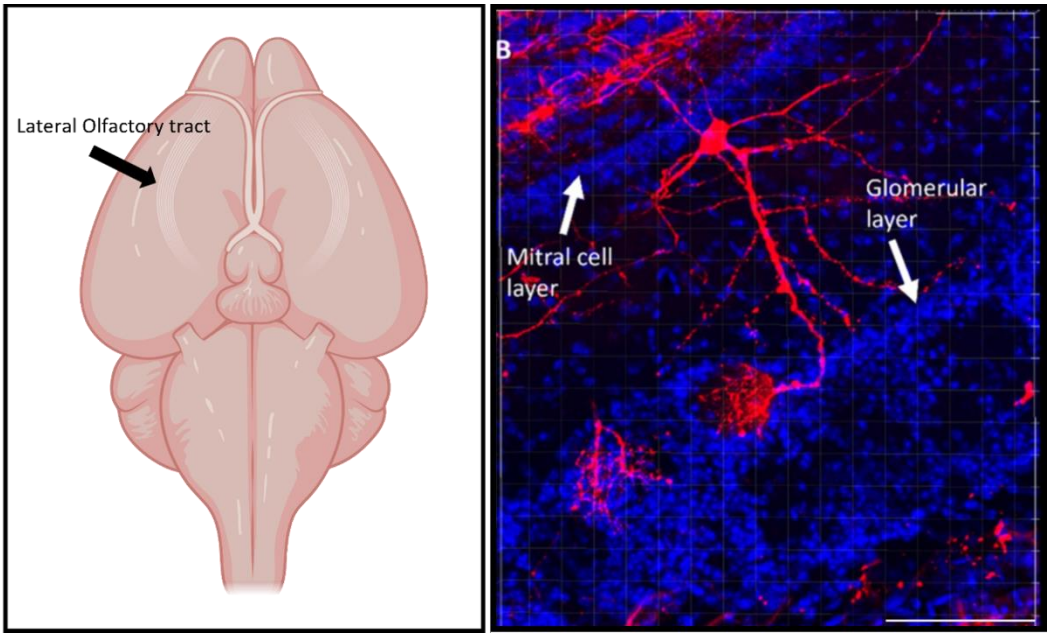

Figure 2. Visualizing mitral cells in the adult mouse brain using DiI labelling. (A) Schematic showing the ventral face of the mouse brain. Mitral cell axons exiting the mouse olfactory bulb form the lateral olfactory tract (black arrow). A crystal of lipophilic DiI is placed in the lateral olfactory tract and allowed to diffuse for 3 to 4 weeks leading to the labeling of individual mitral cells in the olfactory bulb. (B) Based on morphology and cell body location, labeled mitral cells projecting dendrites to glomeruli can be identified. In the adult brain, a mitral cell projects its primary dendrite to a single glomerulus in the glomerular layer (white arrow). Scale bar: 100µm

Loss of Kirrel3 leads to altered mitral cell dendritic complexity in the adult olfactory bulb. During embryonic development, immature mitral cells of the olfactory bulb extend multiple primary dendrites into multiple glomeruli. As a mitral cell matures during early postnatal stages, the supernumerary dendritic branches are pruned off such that a single mature mitral cell extends an apical dendrite to a single glomerulus. Early on in development the proportion of immature mitral cells is higher than mature mitral cells but by adulthood nearly 85-87% of the mitral cells project to a single glomerulus [126,127]. In order to determine whether Kirrel3 plays a role in the regulation of mitral cell dendritic complexity, we assessed the projections of mitral cell dendrites in the brain of *Kirrel3* null adult mice. While in wild-type animals approximately 10% of the mitral cells analyzed projected their apical dendrite to more than one glomerulus, more than 30% of mitral cells analyzed in *Kirrel3*$^{-/-}$ mice had apical dendrites that projected to multiple glomeruli. These results indicate that Kirrel3 contributes to regulating mitral cell dendritic complexity.

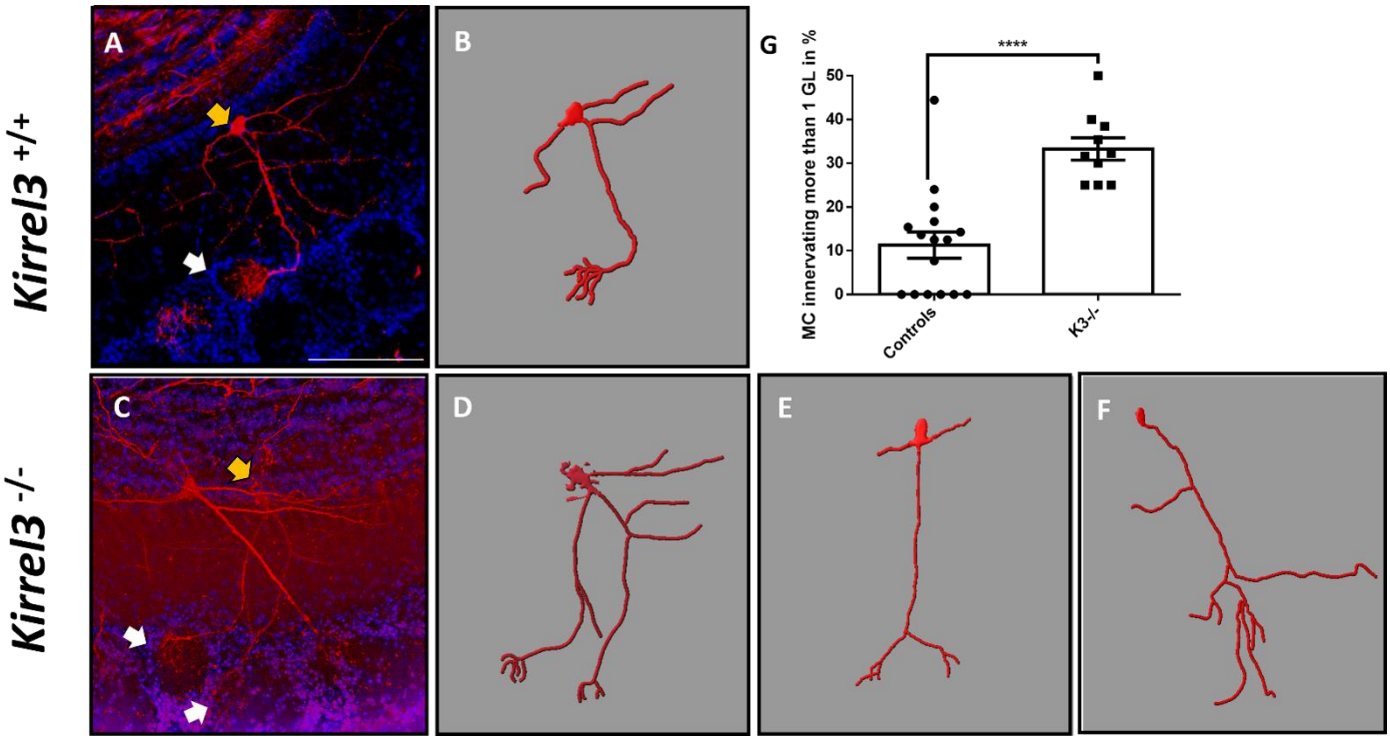

Figure 3. Loss of Kirrel3 leads to increased number of mitral cells with extranumerary dendritic branches in the adult olfactory bulb. (A and C) Confocal images of DiI-labeled mitral cells in adult olfactory bulb from control (A) and *Kirrel3*$^{-/-}$ (C) mice. Mitral cells located in the mitral cell layer project their main dendrite to glomeruli in the glomerular layer. Cell layers are identified by Hoechst staining (blue). (B, D-F) Imaris 3D reconstructions of mitral cells from control and *Kirrel3*$^{-/-}$ mice. B and D are traces of cells shown in A and C, while E and F show additional examples of mitral cells in *Kirrel3*$^{-/-}$ mice projecting dendrites to multiple glomeruli. Arrowheads in (A) and (C) indicate the mitral cell bodies (yellow) and glomeruli (white) innervated by the mitral cells dendrites. (G) Quantification of the proportion of mitral cells innervating more than one glomerulus for each mouse brain analyzed in controls and *Kirrel3*$^{-/-}$ mice (GL-Glomerulus). (Controls n=16 mice, 187 cells and Kirrel3-/- n=10 mice, 191 cells.). Scale bar: 100µm

The homophilic cell adhesion property of Kirrel3 is dispensable for its role in regulating mitral cell dendritic complexity: We have shown that ablating Kirrel3 expression led to an increase in the proportion of mitral cells innervating multiple glomeruli in the adult mouse brain. It remains to be determined whether Kirrel3 prevents excessive branching of mitral cells dendrites in early development or is necessary to promote pruning of these dendrites at later stages of development. Either way, it is possible that Kirrel3-Kirrel3 interactions between mitral cell dendrites and OSN axons in glomeruli, or periglomerular cells, could regulate dendritic complexity. To test the contribution of Kirrel3 homophilic interaction in mitral cell dendritic complexity, we assessed mitral cell dendritic projections into glomeruli in *Kirrel3* $^{Q128A/Q128A}$ mutant mice.

Upon comparing glomerular innervation by mitral cell primary dendrites in wild-type and *Kirrel3* $^{Q128A/Q128A}$ mice, we found no significant difference in the proportion of mitral cells innervating more than one glomerulus. Thus, we show that the homophilic cell adhesion property of Kirrel3 is dispensable for its role in regulating mitral cell dendritic complexity.

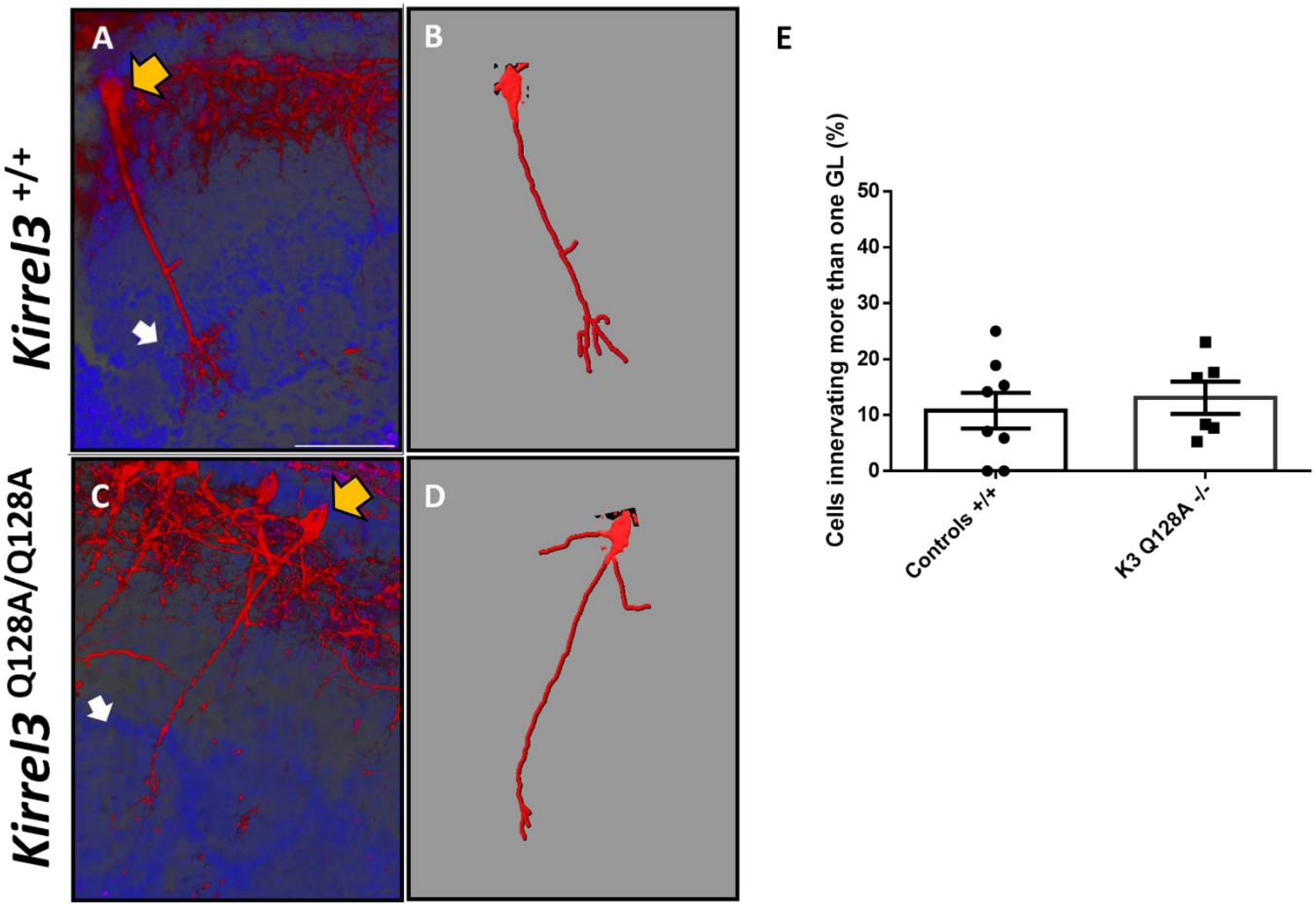

Figure 4. Kirrel3 Homophilic cell adhesion property is dispensable for its role in the regulation of mitral cell dendritic complexity. (A-D) Confocal images of DiI-labeled mitral cells and their Imaris 3D reconstructions in adult olfactory bulb from control (A, B) and *Kirrel3* $^{Q128/Q128A}$ (C, D) mice. In both control and *Kirrel3* $^{Q128/Q128A}$ mice, mitral cells located in the mitral cell layer project their main dendrite to glomeruli to a single glomerulus in the glomerular layer. Cell layers are identified by Hoechst staining (blue). Arrowheads in (A) and (C) indicate the mitral cell bodies (yellow) and glomeruli (white) innervated by the mitral cells dendrites. (E) Quantification of the proportion of mitral cells innervating more than one glomerulus for each mouse brain analyzed in controls and Kirrel3 $^{Q128/Q128A}$ mice (GL-Glomerulus). (Controls n=8 mice, 134 cells and Kirrel3$^{Q128A/Q128A}$ n=6 mice, 149 cells.) Scale bar: 100µm

DISCUSSION

Our understanding of the molecular mechanisms underlying the developmental regulation of mitral cell dendrites remains limited. Our study shows that Kirrel3 is expressed in mitral cells and that it contributes to dendritic development in these cells. Loss of Kirrel3 leads to increased numbers of mitral cells projecting dendrites to multiple glomeruli in the adult olfactory bulb. Early on in development, immature mitral cells extend multiple primary dendrites into multiple glomeruli [126,127]. As a mitral cell matures, a single mitral cell innervates a single glomerulus in adult mice [126,127]. Kirrel3 may therefore regulate mitral cell dendritic complexity by controlling branching of mitral cell dendrites, as they project to glomeruli, or by promoting pruning of excess dendrites during postnatal stages of development. A future examination of mitral cell dendrite complexity at early postnatal stages of development in *Kirrel3* null mice should reveal whether loss of Kirrel3 leads to excess branching, resulting in greater numbers of mitral cells projecting dendrites to multiple glomeruli in the adult. Should mitral cell dendrite complexity be similar in control and *Kirrel3* null mice at early postnatal stages, this would suggest that Kirrel3 influences the pruning of these dendrites rather than their branching.

Kirrel3 may control the development and/or pruning of mitral cell dendrites by regulating/stabilizing interactions between mitral cell dendrites and OSN axons in glomeruli of the OB through Kirrel3-mediated homophilic adhesion. However, we did not observe a significant difference in the proportion of mitral cells innervating more than one glomerulus between Control and *Kirrel3Q128A* mice, demonstrating that the homophilic cell adhesion property of Kirrel3 is dispensable for its role in the regulation of mitral cell dendritic complexity. It remains possible that interactions between Kirrel3 expressed on mitral cell dendrites and unidentified Kirrel3 binding proteins on OSN axons may contribute to regulating the stability and pruning of mitral cell dendrites. For example, expression of the known Kirrel3 ligand Nephrin on OSNs could contribute to this process [207].

Kirrel3 may also have an effect on dendritic complexity by regulating other receptors that have been implicated in dendrite branching and pruning. NMDA receptor activity promotes dendritic pruning and Kirrel3 may

enhance its recruitment to the surface through interactions of its intracellular PDZ motif with protein complexes that stabilize NMDA receptor surface expression [170,208]. Kirrel3 could impinge on BMP receptor signalling, which stabilizes synapses and promote pruning of unstable dendritic branches [127]. The potential molecular mechanisms of action of Kirrel3 in mitral cell dendrite complexity are further developed in the general discussion presented in Chapter 5.

In summary, we show a role for Kirrel3 in the regulation of mitral cell dendritic complexity and demonstrate that this activity does not depend on Kirrel3 homophilic adhesion.

METHODS AND MATERIALS

Animals

Mice that were previously described i.e. Kirrel3 -/- [115] and Kirrel3 Q128A/Q128A [113] were used for analysis. All animal procedures have been approved by Montreal Neurological Institute Animal Care Committee, in accordance with guidelines of Canadian Council of Animal Care. All analysis included male and female mice.

In situ hybridization

Dioxygenin or fluorescein-labeled cRNA probes were synthesized by in vitro transcription using DIG or Flu labeling mix (Roche, Mannheim, Germany) according to the manufacturer's recommendations. Probes were synthesized from cDNA clones encoding Kirrel3 (kind gifts of Dr David Ginty, Johns Hopkins School of Medicine, Baltimore, USA). Fresh frozen brains were cryosectioned at 20 μm, fixed, and processed as previously described [144].

DiI labelling

Adult mice (3 months or older) were perfused using 10ml of 1x PBS and 20ml of 4% Paraformaldehyde (PFA) in 0.1M PB. Following perfusion, the full brains with intact OB and lateral olfactory tract (LOT) were dissected

out, an incision was made on the left and right lateral olfactory tracts and a crystal of DiI was added in each incision. The brains were then incubated in 4% PFA in 0.1M PB for 3 to 4 weeks to allow the crystal to diffuse to the OB. Following the incubation period, the brains were solidified in an agar block (2% agarose in 1x PBS). 280 µm thick sections were then obtained using a vibratome. The sections were collected in a 24 well plate in a 1:3000 Hoechst solution prepared in 1x PBS. Sections were mounted in 70% glycerol and imaged at 20X using Confocal microscopy.

Analysis

Mitral cell confocal images were visualized and analyzed on IMARIS software. The periglomerular cells in the glomerular layer were identified using Hoechst stain and the mitral cells labelled with DiI were in red. Only those dendrites reaching the glomerular layer reaching a discernable glomerulus were counted in the analysis. Mitral cells were analyzed and scored for number of cells sending a single primary dendrite into a single glomerulus and mitral cells sending multiple dendrites into multiple glomeruli. An unpaired t test was performed comparing the proportion of mitral cells out of total cells counted per animal innervating more than one glomerulus in WTs and K3 knockouts; and WTs and K3 Q128A animals. 5 to 50 cells per mouse were traced and analyzed.

Chapter 5: Discussion and Conclusion

5.1. Kirrel function in the coalescence of sensory neuron axons in the olfactory systems.

The coalescence of axons projecting from sensory neuron into glomeruli of the olfactory and accessory olfactory bulbs is likely dependent on attractive and repulsive forces between axons that express similar or different ORs or VRs [72,87,114,115]. Attractive forces between like axons have been proposed to be regulated through the differential expression of cell adhesion molecules that form molecular codes of identity for these axons [87,114,115]. Through loss-of-function approaches, we have tested the requirement for a specific family of CAMs, the Kirrels, for the targeting of OSN axons in the OB. We examined the impact of loss of Kirrel2 on the targeting of five populations of OSN axons expressing varying levels of this receptors and projecting to different dorso-ventral regions of the OB. We observed that Kirrel2 is required in populations of OSNs targeting to the DII region of the OB, but dispensable in OSNs targeting their axons to the DI and most ventral parts of the OB, indicating a region-specific role for Kirrel2 in OSN axonal targeting. Furthermore, ablating both Kirrel2 and Kirrel3 in DI and ventral OSNs did not affect axonal targeting, suggesting that compensation by other Kirrel family members is unlikely the cause of a lack of phenotype observed in these populations of OSNs.

It is interesting that mosaic overexpression of Kirrel2 or Kirrel3 in OSNs expressing the OR MOR28 show defects in axon sorting but ablating expression of Kirrel2 and Kirrel3 in all OSNs has no impact on the sorting of this axonal sub-population. It is possible that ablating expression of Kirrel2 and Kirrel3 in all populations of axons does not significantly change the cell adhesive molecular code of this population of axons compared to axons targeting to adjacent glomeruli but that ablating their expression specifically in MOR28-positive axons could affect their axonal sorting.

The wiring of OSN axons in the DII region of the OB is critical for the processing of specific odors, such as TMT, that induce innate freezing behaviours in mice. The ablation of DII targeting axons or their mistargeting to more ventral regions of the OB in OSN-specific *Robo2* mutant mice leads to a reduced response to TMT

and reduced avoidance. It would be interesting to assess whether improper coalescence of axons within this region in Kirrel2 mutant mice also results in altered avoidance responses to TMT, which would suggest that the fine targeting of these axons to specific glomeruli is essential for odor response.

We also observed that ablating expression of Kirrel2 and Kirrel3 did not noticeably affect the structure and order of glomeruli in the OB. The glomeruli that are formed when ablating Kirrel2, or both Kirrel2 and Kirrel3 have similar shape and remain very distinct. This is in sharp contrast to our previous observations in the accessory olfactory where ablating expression of either Kirrel2 or Kirrel3, or both, disrupts glomerular architecture and leads to fused larger glomeruli [114,115]. This observation suggests that Kirrels likely have a greater contribution to the coalescence of axons in the accessory olfactory system, when compared to the main olfactory system. Considering that a larger number of OSNs expressing different ORs exist compared to the number of different VSNs expressing specific VRs, it is likely that additional families of cell adhesion molecules also contribute to the formation of the complex glomerular map in the OB. It is possible that other molecules, such as Big-2, Pcdh10, and Ephrins also contribute to the molecular identity code of OSN axons[72,159,176,182]. Single cell RNAseq approaches at developmental time points when axons are projecting could reveal the molecular diversity of OSN axons and allow the identification of new candidate receptors that permit differential coalescence of axons in the various regions of the OB.

5.2. Essential role of cell adhesive properties in Kirrel function in the coalescence of sensory neuron axons in the olfactory systems.

Studies of Kirrel overexpression and our own loss-of-function analyses have revealed a critical role for Kirrels as receptors that promote the coalescence of OSN and VSN axons into glomeruli [72,114,115]. Based on their pattern of expression in these populations of neurons, and on their ability to modulate homophilic cell adhesion *in vitro*, it was proposed that Kirrels influence axonal colescence through their adhesive properties [102,112,113]. To examine the contribution of homophilic adhesion to Kirrel function in axonal coalescence, we used genetic engineering to introduce mutations in the *Kirrel3* gene that lead to a substitution of glutamine 128 to an alanine residue and disrupts Kirrel3 homophilic adhesion. We showed that blocking Kirrel3 adhesion in vivo leads to similar defects in VSN axonal coalescence as completely ablating its expression, indicating that the homophilic property is essential for Kirrel3 function in VSN axonal

coalescence. Although it is likely that Kirrel3 adhesion also regulates coalescence of OSN axons, testing this possibility will require the future identification of specific subsets of OSN neurons that require Kirrel3 for their axonal coalescence. An examination of axonal targeting of three different populations of OSNs in *Kirrel3*$^{-/-}$ mice did not show any defects in coalescence in these populations of neurons, suggesting that as for Kirrel2, it is likely required in subsets of OSN populations (unpublished results). Hence, additional experiments will be necessary to fully assess the role of Kirrel3 cell adhesion in OSN axonal coalescence.

While we have demonstrated that the introduction of the Q128A substitution disrupts Kirrel3 homophilic, it remains possible that this substitution could also affect Kirrel3 interaction with other proteins that have been shown to bind to Kirrel family proteins. For example, Nephrin-Kirrel interactions modulate slit-diaphragm formation in the kidney [103]. While the expression and function of Nephrin has not been carefully examined in the olfactory systems, it may contribute to Kirrel3 function in axonal coalescence. Another possible protein interactor for Kirrel3 is Robo. A study in *C.elegans* has shown that the Kirrel homolog SYG-1 interacts with cleaved extracellular domain of Robo and serves as an attractive cue for glial migration [111]. Robo2 plays a critical role in the targeting of VSN axons in the AOB but is mainly necessary for the anterior-posterior segregation of axons within this structure and does not influence axonal coalescence into glomeruli [160].

Furthermore, loss of Kirrel3 does not affect VSN axonal segregation into the anterior and posterior regions of the AOB [115], making it unlikely that Robo2 contributes to Kirrel3 function in this system.

It remains to be determined whether Kirrel3 homophilic interactions are also necessary for its function in other processes. For example, Kirrel3 homophilic interactions have been proposed to underlie synapse formation in the hippocampus [102]. Furthermore, the double ablation of Kirrel2 and Kirrel3 leads to reduced numbers of excitatory synapses in the AOB, although it is unclear whether loss of Kirrel3 alone would be sufficient to affect the number of synapses in the AOB [114]. An examination of synapses in the AOB of Kirrel3 Q128A mice using electron microscopy may reveal a function for Kirrel3 homophilic adhesion in synapse formation or maintenance.

Although our findings indicate that Kirrel homophilic interactions act as "velcro" for like axons to promote their coalescence into specific glomeruli, it remains possible that active signaling through the Kirrel3 intracellular domain contributes to its function in axonal coalescence. A recent study looking at 6 commonly observed missense variants of Kirrel3 showed that two of these missense variants have intact transcellular binding but impaired synaptogenic function [112]. 3 out of 6 missense variants had both impaired transcellular binding and synaptogenic function, thereby showing that homophilic property of Kirrel3 is necessary but not sufficient for its synaptogenic function [112]. Future rescue experiments by expressing wild-type or an intracellular domain deletion of Kirrel3 in vomeronasal sensory neurons of *Kirrel3*$^{-/-}$ could address whether the Kirrel3 intracellular domain is necessary for its function in axonal coalescence.

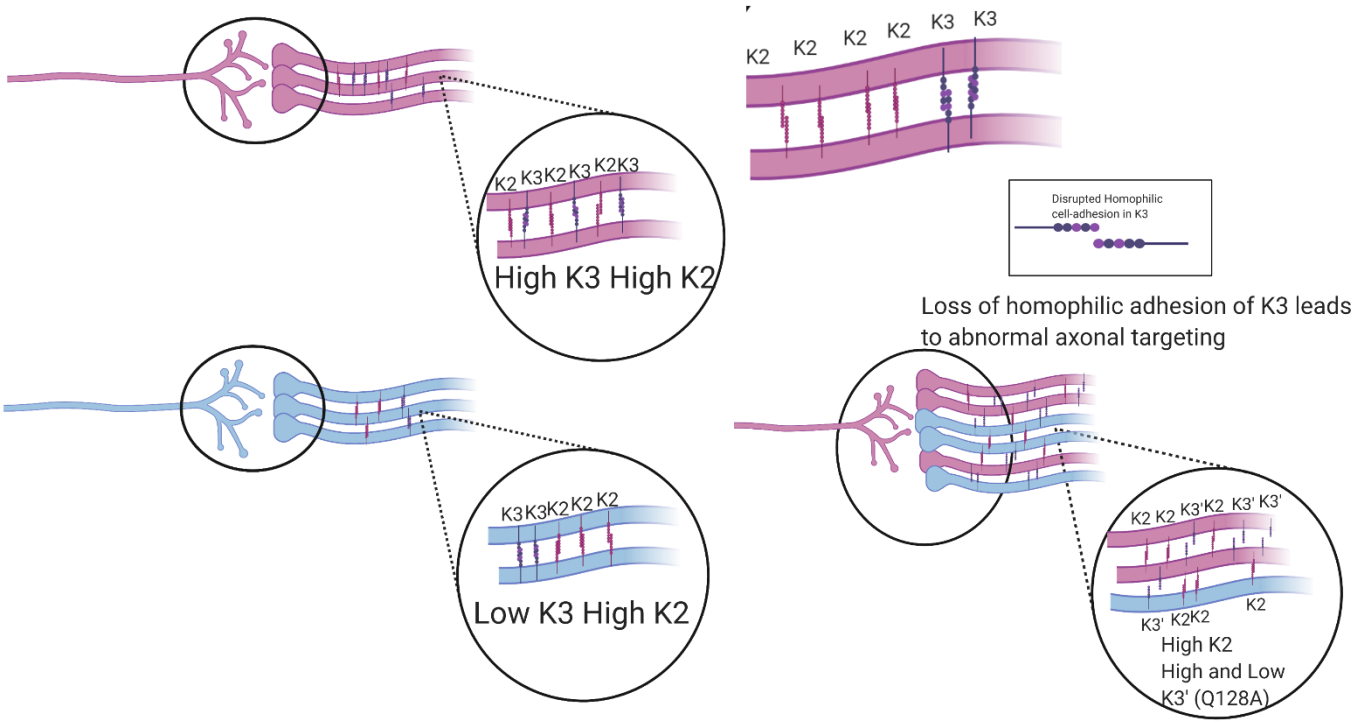

Figure 1. Proposed effect of loss of Kirrel cell adhesion on axonal sorting. VSN axons expressing different vomeronasal receptors (pink or blue) innervate different glomeruli. All axons expressing the same vomeronasal receptor express similar levels/combinations of Kirrel2 and Kirrel3, which provides molecular diversity to allow like axons to sort with each other. Disrupting homophilic cell adhesion property of Kirrel3 results in the loss of contribution of Kirrel3 to this molecular identity code and leads to coalescence of axons that were otherwise different into the same glomerulus, resulting in formation of fewer and larger heterogenous glomeruli innervated by different axon populations each expressing a specific vomeronasal receptor.

5.3. Understanding the role of Kirrel3 in the regulation of mitral cell dendritic complexity in the mouse main olfactory system

The main olfactory system comprises of olfactory sensory neurons that project their axons from the olfactory epithelium to the main olfactory bulb where they synapse onto the dendrites of second order projection neurons, the mitral cells, in neuropil structures called glomeruli [124]. These glomeruli are lined by inhibitory interneurons called periglomerular cells [124]. The mitral cells have their cell bodies located in the mitral cell layer in the olfactory bulb from where they project their dendrites into the glomerular layer and innervate glomeruli [124]. Early on in development, a single mitral cell innervates multiple glomeruli [126,127]. However, over the course of development, these excess dendritic branches are pruned off such that in the adult mouse brain the vast majority of mitral cells innervate a single glomerulus [126,127]. To date, few mechanisms have been identified that modulate mitral cell dendrite complexity and pruning. Our studies identify Kirrel3 as a novel regulator of mitral cell dendrite complexity and brings forth several key questions about potential mechanisms through which Kirrel3 may have its effect.

Modulation of neuronal activity has been implicated in the regulation of mitral cell pruning during postnatal development. It is known from literature that blocking NMDA receptor activity results in impaired pruning of mitral cell dendrites [170]. NMDA receptor activity promotes actin depolymerization, leading to pruning of excessive branches [170]. It has also been shown that blocking spontaneous activity in mitral cells results in impaired mitral cell dendritic pruning [170]. Interestingly, neuronal activity is known to regulate the expression level of Kirrel3 in olfactory sensory neurons, suggesting it may have a similar effect in other neuronal types, such as mitral cells [72]. It is therefore possible that Kirrel3 expression in mitral cell dendrite promotes the recruitment of NMDAR at the cell surface leading to pruning of mitral cell dendrites (Figure 3). This could be achieved through a direct interaction with the NMDAR or through interactions of the Kirrel3 intracellular domain, which contains a PDZ binding motif, with protein complexes that modulate NMDAR recruitment. Proteomics analyses of Kirrel3 interactors in neurons could further reveal an involvement of Kirrel3 in NMDAR recruitment and signalling.

Another potential way through which Kirrel3 may be modulating the stabilization of dendrites is through interactions with proteins on OSNs axons that innervate mitral cell dendrites. Mitral cell dendrite Kirrel3 could interact with Kirrel3 on OSN axons, leading to the stabilization of specific branches of mitral cells. However, our observation that loss of Kirrel3 adhesive properties does not lead to defects in mitral cell dendrite complexity does not support this model. It remains possible that Kirrel3 could interact with other Kirrel3 ligands expressed on OSN axons, such as Nephrin, to regulate mitral cell dendrite stabilization. Alternatively, Kirrel3 may regulate BMPR signalling, which has been implicated in regulating the stabilization of dendrites [127]. In its unbound form, the BMPR promotes actin depolymerization and destabilization of mitral cell dendrites leading to pruning of dendrites [127]. Kirrel3 may modulate the binding affinity of BMP to its receptor or impinge on this pathway through intracellular signalling.

It remains unknown whether the defect in glomerular innervation by mitral cells observed in adult *Kirrel3* $^{-/-}$ mice is due to a pruning defect early on in development or an over branching defect (shown in figure 5.3.2). An examination of mitral cell branching at early postnatal time points should help address this question. Assessing mitral cell glomerular dendritic projections at P0 and P4 would provide insight into this question. If there is overbranching in the absence of Kirrel3, we would expect to see mitral cells with more branches innervating greater numbers of glomeruli in *Kirrel3* $^{-/-}$ mice at P0. If it is the case, this would lead to incomplete pruning of mitral cells by adulthood, as observed in *Kirrel3* $^{-/-}$ mice, despite a normal pruning process. If similar numbers of dendrites are observed at P0 in control and mutant mice, an examination of dendritic projections at P4 would help establish that early pruning mechanisms are affected as by P4, 50% of mitral cells only innervate a single glomerulus. If we observe a significantly higher proportion of mitral cells innervating more than one glomerulus in *Kirrel3*$^{-/-}$ mice as compared to controls at P4, it would indicate that the pruning defects arise earlier than P4.

Although Kirrel3 is expressed in mitral cells and likely regulate their complexity through a cell autonomous process, its expression in OSN axons and in periglomerular cells that make contact with mitral cell dendrites raises the possibility that Kirrel3 expression in these two types of cells also contribute to mitral cell dendritic

development. Furthermore, microglia have been shown to play an important role in pruning of dendrites in other brain regions. It is possible that microglia in the olfactory bulb also play a role in pruning of mitral cell dendrites, although it remains to be assessed whether Kirrel3 is expressed in this type of cell. To specifically examine the function of Kirrel3 in these various cell types, the use of a conditional floxed *Kirrel3* allele will be necessary. Kirrel3 expression will be ablated using cell-specific Cre mouse lines, such as Tbx21-Cre for mitral cells and OMP-Cre for OSNs, and its effect on mitral cell dendrite development examined as described in Chapter 4.

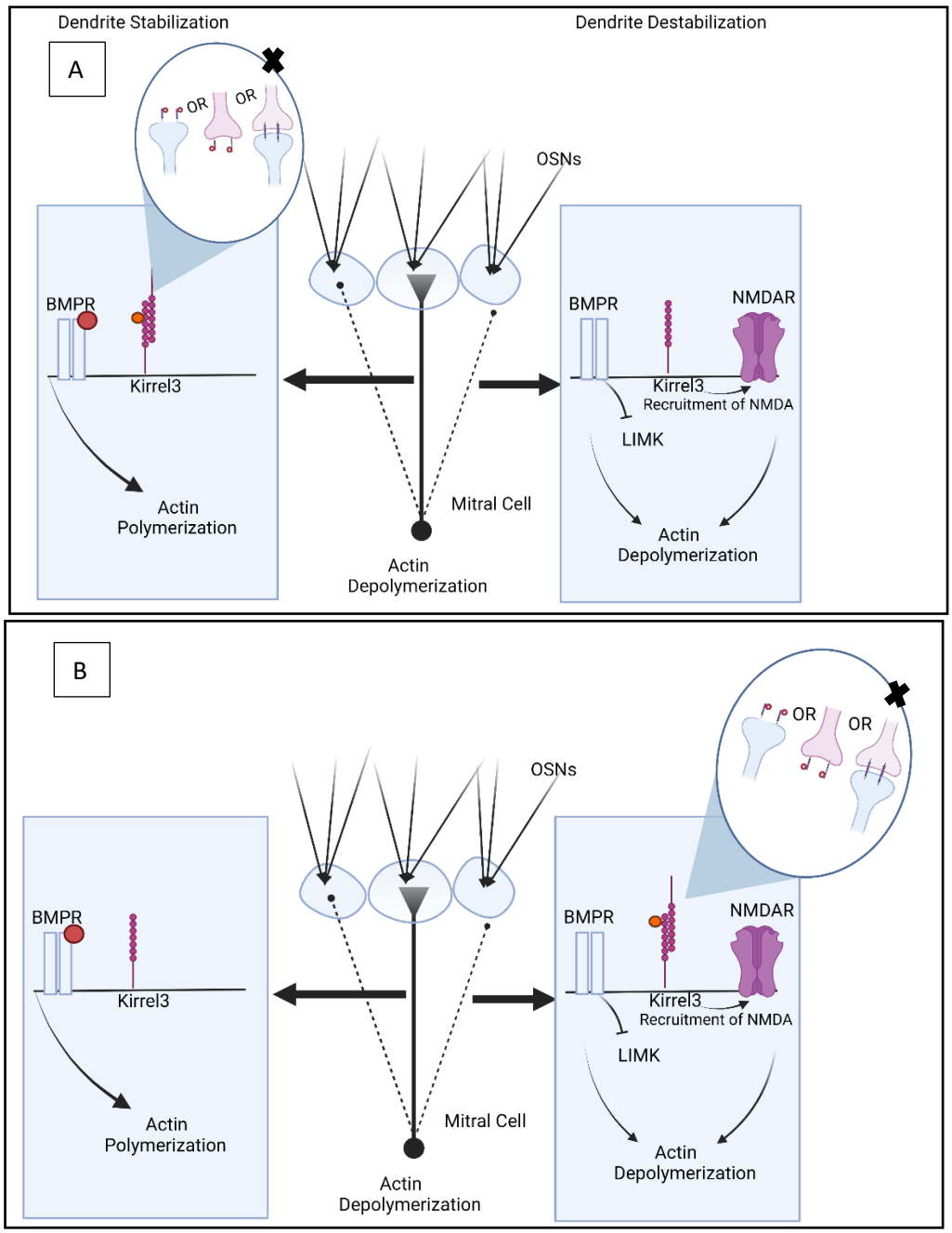

Figure 2. Potential mechanisms of Kirrel3 action in mitral cell dendrite development. This figure presents possible ways that Kirrel3 could regulate mitral cell dendritic complexity. (A) Kirrel3 could be involved in mitral cell dendritic pruning through the recruitment of NMDA receptors to the cell surface via their PDZ binding motifs leading to dendrite destabilization. It is possible that Kirrel3 bound to a ligand, just like BMPRs, stabilizes synapses. (B) Alternatively, vice versa is also a possibility. Kirrel3 in the unbound state could be important for synapse stabilization and Kirrel3 bound to Kirrel3, or to an unknown ligand, could be important for destabilizing mitral cell synapses.

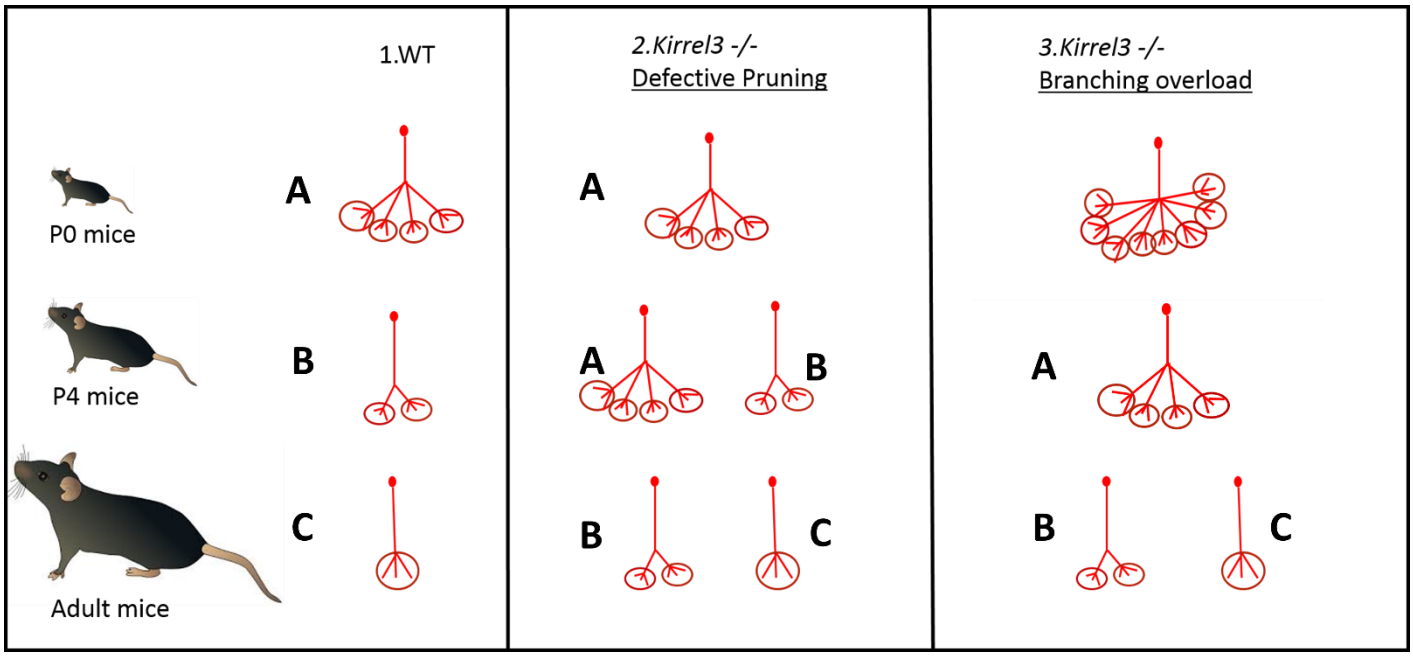

Figure 3. Proposed approaches to assess a function of Kirrel3 in branching versus pruning of mitral cell dendrites. In control animals, mitral cell dendritic complexity is regulated over the course of development leading to a mitral cell projecting a single apical dendrite to a glomerulus in the adult (scenario 1). If loss of Kirrel3 leads to increased branching of mitral cells, we would expect to observe more branches projecting to more glomeruli at P0, which would lead to increased numbers of mitral cells projecting to multiple glomeruli at P4 and in adulthood, despite normal pruning (scenario 3). In contrast if there is an early pruning defect in *Kirrel3*$^{-/-}$ mice, we would expect to observe similar branching at P0 but a higher proportion of mitral cells projecting dendrites to multiple glomeruli at P4 and in the adult (scenario 2).

5.4 Summary and Conclusion

In this thesis, we examined the function of Kirrel family members in the wiring of the olfactory systems. We demonstrate that Kirrels play critical roles in the sorting and targeting of chemosensory neuron axons through their ability to homophilically interact. We also reveal a new function for Kirrel3 in modulating mitral cell dendrite complexity in the olfactory bulb.

These studies add an important contribution to the field taking us a step closer to better understanding how a healthy brain wires itself. Kirrels seem to have a conserved function in circuit formation across different species; from worms to flies to mice [87,108,181]. It is thus very likely that conceptually, the roles we demonstrate for Kirrels in mice apply to humans as well. Furthermore, Kirrel3 is highly expressed in various other brain regions, making it likely that it contributes to regulating wiring and dendritic complexity in these regions, such as the cortex [104]. Mutations in Kirrel3 in humans has been linked to neurodevelopmental disorders, such as autism and intellectual disability [117]. Thus, understanding how Kirrels are important in the wiring of a healthy brain will provide us with valuable insight for the development of approaches to mitigate various neurodevelopmental disorders.

Bibliography

1. Tau, G. Z. & Peterson, B. S. Normal development of brain circuits. *Neuropsychopharmacology* **35**, 147–168 (2010).

2. Faguet, J., Maranhao, B., Smith, S. L. & Trachtenberg, J. T. Ipsilateral eye cortical maps are uniquely sensitive to binocular plasticity. *J. Neurophysiol.* **101**, 855–861 (2009).

3. Huang, Z. J. & Zeng, H. Genetic approaches to neural circuits in the mouse. *Annu. Rev. Neurosci.* **36**, 183–215 (2013).

4. Dalva, M. B., McClelland, A. C. & Kayser, M. S. Cell adhesion molecules: signalling functions at the synapse. *Nat. Rev. Neurosci.* **8**, 206–220 (2007).

5. Schroeder, A. & de Wit, J. Leucine-rich repeat-containing synaptic adhesion molecules as organizers of synaptic specificity and diversity. *Exp. Mol. Med.* **50**, 1–9 (2018).

6. Tai, C.-Y., Kim, S. A. & Schuman, E. M. Cadherins and synaptic plasticity. *Curr. Opin. Cell Biol.* **20**, 567–575 (2008).

7. Park, Y. K. & Goda, Y. Integrins in synapse regulation. *Nat. Rev. Neurosci.* **17**, 745–756 (2016).

8. Cutforth, T. *et al.* Axonal ephrin-As and odorant receptors: coordinate determination of the olfactory sensory map. *Cell* **114**, 311–322 (2003).

9. Hisaoka, T., Komori, T., Kitamura, T. & Morikawa, Y. Abnormal behaviours relevant to neurodevelopmental disorders in Kirrel3-knockout mice. *Sci. Rep.* **8**, 1408 (2018).

10. Baig, D. N., Yanagawa, T. & Tabuchi, K. Distortion of the normal function of synaptic cell adhesion molecules by genetic variants as a risk for autism spectrum disorders. *Brain Res. Bull.* **129**, 82–90 (2017).

11. Kim, C., Ye, F. & Ginsberg, M. H. Regulation of integrin activation. *Annu. Rev. Cell Dev. Biol.* **27**, 321–345 (2011).

12. Luo, B.-H., Carman, C. V. & Springer, T. A. Structural basis of integrin regulation and signaling. *Annu. Rev. Immunol.* **25**, 619–647 (2007).

13. Cingolani, L. A. *et al.* Activity-dependent regulation of synaptic AMPA receptor composition and abundance by beta3 integrins. *Neuron* **58**, 749–762 (2008).

14. Cingolani, L. A. & Goda, Y. Differential involvement of beta3 integrin in pre- and postsynaptic forms of adaptation to chronic activity deprivation. *Neuron Glia Biol.* **4**, 179–187 (2008).

15. Kramár, E. A., Bernard, J. A., Gall, C. M. & Lynch, G. Alpha3 integrin receptors contribute to the consolidation of long-term potentiation. *Neuroscience* **110**, 29–39 (2002).

16. Chavis, P. & Westbrook, G. Integrins mediate functional pre- and postsynaptic maturation at a hippocampal synapse. *Nature* **411**, 317–321 (2001).

17. Pasterkamp, R. J., Peschon, J. J., Spriggs, M. K. & Kolodkin, A. L. Semaphorin 7A promotes axon outgrowth through integrins and MAPKs. *Nature* **424**, 398–405 (2003).

18. Hama, H., Hara, C., Yamaguchi, K. & Miyawaki, A. PKC signaling mediates global enhancement of excitatory synaptogenesis in neurons triggered by local contact with astrocytes. *Neuron* **41**, 405–415 (2004).

19. Kramár, E. A., Lin, B., Rex, C. S., Gall, C. M. & Lynch, G. Integrin-driven actin polymerization consolidates long-term potentiation. *Proc Natl Acad Sci USA* **103**, 5579–5584 (2006).

20. Shi, Y. & Ethell, I. M. Integrins control dendritic spine plasticity in hippocampal neurons through NMDA receptor and Ca2+/calmodulin-dependent protein kinase II-mediated actin reorganization. *J. Neurosci.* **26**, 1813–1822 (2006).

21. Warren, M. S. *et al.* Integrin β1 signals through Arg to regulate postnatal dendritic arborization, synapse density, and behavior. *J. Neurosci.* **32**, 2824–2834 (2012).

22. McGeachie, A. B. *et al.* β3 integrin is dispensable for conditioned fear and hebbian forms of plasticity in the hippocampus. *Eur. J. Neurosci.* **36**, 2461–2469 (2012).

23. Carter, M. D. *et al.* Absence of preference for social novelty and increased grooming in integrin β3 knockout mice: initial studies and future directions. *Autism Res.* **4**, 57–67 (2011).

24. Chan, C.-S. *et al.* Beta 1-integrins are required for hippocampal AMPA receptor-dependent synaptic transmission, synaptic plasticity, and working memory. *J. Neurosci.* **26**, 223–232 (2006).

25. Ushkaryov, Y., Er, P., Geppert, M. & Sudhof, T. Neurexins: Synaptic Cell Surface Proteins Related to the α-Latroxin Receptor and Laminin.*Science*. Vol 257, 50-55 (1992).

26. Dean, C. & Dresbach, T. Neuroligins and neurexins: linking cell adhesion, synapse formation and cognitive function. *Trends Neurosci.* **29**, 21–29 (2006).

27. Nam, C. I. & Chen, L. Postsynaptic assembly induced by neurexin-neuroligin interaction and neurotransmitter. *Proc Natl Acad Sci USA* **102**, 6137–6142 (2005).

28. Graf, E. R., Zhang, X., Jin, S.-X., Linhoff, M. W. & Craig, A. M. Neurexins induce differentiation of GABA and glutamate postsynaptic specializations via neuroligins. *Cell* **119**, 1013–1026 (2004).

29. Scheiffele, P., Fan, J., Choih, J., Fetter, R. & Serafini, T. Neuroligin expressed in nonneuronal cells triggers presynaptic development in contacting axons. *Cell* **101**, 657–669 (2000).

30. Song, J. Y., Ichtchenko, K., Südhof, T. C. & Brose, N. Neuroligin 1 is a postsynaptic cell-adhesion molecule of excitatory synapses. *Proc Natl Acad Sci USA* **96**, 1100–1105 (1999).

31. Missler, M. *et al.* a-Neurexins couple Ca21 channels to synaptic vesicle exocytosis. *Nature* **423**,939-948 (2003).

32. Anderson, G. R. *et al.* β-Neurexins Control Neural Circuits by Regulating Synaptic Endocannabinoid Signaling. *Cell* **162**, 593–606 (2015).

33. Chih, B., Engelman, H. & Scheiffele, P. Control of excitatory and inhibitory synapse formation by neuroligins. *Science* **307**, 1324–1328 (2005).

34. Levinson, J. N. *et al.* Neuroligins mediate excitatory and inhibitory synapse formation: involvement of PSD-95 and neurexin-1beta in neuroligin-induced synaptic specificity. *J. Biol. Chem.* **280**, 17312–17319 (2005).

35. Varoqueaux, F., Jamain, S. & Brose, N. Neuroligin 2 is exclusively localized to inhibitory synapses. *Eur. J. Cell Biol.* **83**, 449–456 (2004).

36. Levinson, J. N. & El-Husseini, A. New players tip the scales in the balance between excitatory and inhibitory synapses. *Mol. Pain* **1**, 12 (2005).

37. Prange, O., Wong, T. P., Gerrow, K., Wang, Y. T. & El-Husseini, A. A balance between excitatory and inhibitory synapses is controlled by PSD-95 and neuroligin. *Proc Natl Acad Sci USA* **101**, 13915–13920 (2004).

38. Cline, H. Synaptogenesis: a balancing act between excitation and inhibition. *Curr. Biol.* **15**, R203-5 (2005).

39. Hussain, N. K. & Sheng, M. Neuroscience. Making synapses: a balancing act. *Science* **307**, 1207–1208 (2005).

40. Rubenstein, J. L. R. & Merzenich, M. M. Model of autism: increased ratio of excitation/inhibition in key neural systems. *Genes Brain Behav.* **2**, 255–267 (2003).

41. Philibert, R. A., Winfield, S. L., Sandhu, H. K., Martin, B. M. & Ginns, E. I. The structure and expression of the human neuroligin-3 gene. *Gene* **246**, 303–310 (2000).

42. Arikkath, J. & Reichardt, L. F. Cadherins and catenins at synapses: roles in synaptogenesis and synaptic plasticity. *Trends Neurosci.* **31**, 487–494 (2008).

43. Brigidi, G. S. & Bamji, S. X. Cadherin-catenin adhesion complexes at the synapse. *Curr. Opin. Neurobiol.* **21**, 208–214 (2011).

44. Paradis, S. *et al.* An RNAi-based approach identifies molecules required for glutamatergic and GABAergic synapse development. *Neuron* **53**, 217–232 (2007).

45. Silverman, J. B. *et al.* Synaptic anchorage of AMPA receptors by cadherins through neural plakophilin-related arm protein AMPA receptor-binding protein complexes. *J. Neurosci.* **27**, 8505–8516 (2007).

46. Tang, L., Hung, C. P. & Schuman, E. M. A role for the cadherin family of cell adhesion molecules in hippocampal long-term potentiation. *Neuron* **20**, 1165–1175 (1998).

47. Murase, S. & Schuman, E. M. The role of cell adhesion molecules in synaptic plasticity and memory. *Curr. Opin. Cell Biol.* **11**, 549–553 (1999).

48. de Wit, J. & Ghosh, A. Control of neural circuit formation by leucine-rich repeat proteins. *Trends Neurosci.* **37**, 539–550 (2014).

49. O'Sullivan, M. L. *et al.* FLRT proteins are endogenous latrophilin ligands and regulate excitatory synapse development. *Neuron* **73**, 903–910 (2012).

50. Woo, J., Kwon, S.-K. & Kim, E. The NGL family of leucine-rich repeat-containing synaptic adhesion molecules. *Mol. Cell. Neurosci.* **42**, 1–10 (2009).

51. Kim, S. *et al.* NGL family PSD-95-interacting adhesion molecules regulate excitatory synapse formation. *Nat. Neurosci.* **9**, 1294–1301 (2006).

52. Soto, F., Watkins, K. L., Johnson, R. E., Schottler, F. & Kerschensteiner, D. NGL-2 regulates pathway-specific neurite growth and lamination, synapse formation, and signal transmission in the retina. *J. Neurosci.* **33**, 11949–11959 (2013).

53. Ko, J., Fuccillo, M. V., Malenka, R. C. & Südhof, T. C. LRRTM2 functions as a neurexin ligand in promoting excitatory synapse formation. *Neuron* **64**, 791–798 (2009).

54. de Wit, J. *et al.* LRRTM2 interacts with Neurexin1 and regulates excitatory synapse formation. *Neuron* **64**, 799–806 (2009).

55. Um, J. W. *et al.* LRRTM3 Regulates Excitatory Synapse Development through Alternative Splicing and Neurexin Binding. *Cell Rep.* **14**, 808–822 (2016).

56. Ko, J. S. *et al.* PTPσ functions as a presynaptic receptor for the glypican-4/LRRTM4 complex and is essential for excitatory synaptic transmission. *Proc Natl Acad Sci USA* **112**, 1874–1879 (2015).

57. Takashima, N. *et al.* Impaired cognitive function and altered hippocampal synapse morphology in mice lacking Lrrtm1, a gene associated with schizophrenia. *PLoS ONE* **6**, e22716 (2011).

58. de Wit, J. *et al.* Unbiased discovery of glypican as a receptor for LRRTM4 in regulating excitatory synapse development. *Neuron* **79**, 696–711 (2013).

59. Siddiqui, T. J. *et al.* An LRRTM4-HSPG complex mediates excitatory synapse development on dentate gyrus granule cells. *Neuron* **79**, 680–695 (2013).

60. Aruga, J. & Mikoshiba, K. Identification and characterization of Slitrk, a novel neuronal transmembrane protein family controlling neurite outgrowth. *Mol. Cell. Neurosci.* **24**, 117–129 (2003).

61. Yim, Y. S. *et al.* Slitrks control excitatory and inhibitory synapse formation with LAR receptor protein tyrosine phosphatases. *Proc Natl Acad Sci USA* **110**, 4057–4062 (2013).

62. Um, J. W. *et al.* Structural basis for LAR-RPTP/Slitrk complex-mediated synaptic adhesion. *Nat. Commun.* **5**, 5423 (2014).

63. Takahashi, H. *et al.* Selective control of inhibitory synapse development by Slitrk3-PTPδ trans-synaptic interaction. *Nat. Neurosci.* **15**, 389–98, S1 (2012).

64. Shmelkov, S. V. *et al.* Slitrk5 deficiency impairs corticostriatal circuitry and leads to obsessive-compulsive-like behaviors in mice. *Nat. Med.* **16**, 598–602, 1p following 602 (2010).

65. Lie, E. *et al.* SALM4 suppresses excitatory synapse development by cis-inhibiting trans-synaptic SALM3-LAR adhesion. *Nat. Commun.* **7**, 12328 (2016).

66. Li, Y. *et al.* Splicing-Dependent Trans-synaptic SALM3-LAR-RPTP Interactions Regulate Excitatory Synapse Development and Locomotion. *Cell Rep.* **12**, 1618–1630 (2015).

67. Choi, Y. *et al.* SALM5 trans-synaptically interacts with LAR-RPTPs in a splicing-dependent manner to regulate synapse development. *Sci. Rep.* **6**, 26676 (2016).

68. Lacy, S. E., Bönnemann, C. G., Buzney, E. A. & Kunkel, L. M. Identification of FLRT1, FLRT2, and FLRT3: a novel family of transmembrane leucine-rich repeat proteins. *Genomics* **62**, 417–426 (1999).

69. Silva, J.-P. *et al.* Latrophilin 1 and its endogenous ligand Lasso/teneurin-2 form a high-affinity transsynaptic receptor pair with signaling capabilities. *Proc Natl Acad Sci USA* **108**, 12113–12118 (2011).

70. Yamagishi, S. *et al.* FLRT2 and FLRT3 act as repulsive guidance cues for Unc5-positive neurons. *EMBO J.* **30**, 2920–2933 (2011).

71. Rodger, J., Salvatore, L. & Migani, P. Should I stay or should I go? Ephs and ephrins in neuronal migration. *Neurosignals* **20**, 190–201 (2012).

72. Serizawa, S. *et al.* A neuronal identity code for the odorant receptor-specific and activity-dependent axon sorting. *Cell* **127**, 1057–1069 (2006).

73. Dalva, M. B. *et al.* EphB receptors interact with NMDA receptors and regulate excitatory synapse formation. *Cell* **103**, 945–956 (2000).

74. Henkemeyer, M., Itkis, O. S., Ngo, M., Hickmott, P. W. & Ethell, I. M. Multiple EphB receptor tyrosine kinases shape dendritic spines in the hippocampus. *J. Cell Biol.* **163**, 1313–1326 (2003).

75. Penzes, P. *et al.* Rapid induction of dendritic spine morphogenesis by trans-synaptic ephrinB-EphB receptor activation of the Rho-GEF kalirin. *Neuron* **37**, 263–274 (2003).

76. Kayser, M. S., McClelland, A. C., Hughes, E. G. & Dalva, M. B. Intracellular and trans-synaptic regulation of glutamatergic synaptogenesis by EphB receptors. *J. Neurosci.* **26**, 12152–12164 (2006).

77. Knöll, B., Zarbalis, K., Wurst, W. & Drescher, U. A role for the EphA family in the topographic targeting of vomeronasal axons. *Development* **128**, 895–906 (2001).

78. Cho, J. H., Prince, J. E. A. & Cloutier, J.-F. Axon guidance events in the wiring of the mammalian olfactory system. *Mol. Neurobiol.* **39**, 1–9 (2009).

79. Takeuchi, H. & Sakano, H. Neural map formation in the mouse olfactory system. *Cell. Mol. Life Sci.* **71**, 3049–3057 (2014).

80. Yoshihara, Y., Oka, S., Ikeda, J. & Mori, K. Immunoglobulin superfamily molecules in the nervous system. *Neurosci. Res.* **10**, 83–105 (1991).

81. Fearnley, S., Raja, R. & Cloutier, J.-F. Spatiotemporal expression of IgLON family members in the developing mouse nervous system. *Sci. Rep.* **11**, 19536 (2021).

82. Oguro-Ando, A. *et al.* Cntn4, a risk gene for neuropsychiatric disorders, modulates hippocampal synaptic plasticity and behavior. *Transl. Psychiatry* **11**, 106 (2021).

83. Rønn, L. C., Berezin, V. & Bock, E. The neural cell adhesion molecule in synaptic plasticity and ageing. *Int. J. Dev. Neurosci.* **18**, 193–199 (2000).

84. Biederer, T. *et al.* SynCAM, a synaptic adhesion molecule that drives synapse assembly. *Science* **297**, 1525–1531 (2002).

85. Fujiwara, T. *et al.* Nectin-1 spots regulate the branching of olfactory mitral cell dendrites. *Mol. Cell. Neurosci.* **68**, 143–150 (2015).

86. Millard, S. S. & Zipursky, S. L. Dscam-mediated repulsion controls tiling and self-avoidance. *Curr. Opin. Neurobiol.* **18**, 84–89 (2008).

87. Vaddadi, N. *et al.* Kirrel2 is differentially required in populations of olfactory sensory neurons for the targeting of axons in the olfactory bulb. *Development* **146**, (2019).

88. Hashimoto, T., Yamada, M., Maekawa, S., Nakashima, T. & Miyata, S. IgLON cell adhesion molecule Kilon is a crucial modulator for synapse number in hippocampal neurons. *Brain Res.* **1224**, 1–11 (2008).

89. Struyk, A. F. *et al.* Cloning of neurotrimin defines a new subfamily of differentially expressed neural cell adhesion molecules. *J. Neurosci.* **15**, 2141–2156 (1995).

90. Rosen, C., Lisanti, M. & Salzer, J. Expression of Unique Sets of GPI-linked Proteins by Different Primary Neurons In Vitro. *The Journal of Cell Biology* **117**,618-627 (1992).

91. Sabater, L. *et al.* A novel non-rapid-eye movement and rapid-eye-movement parasomnia with sleep breathing disorder associated with antibodies to IgLON5: a case series, characterisation of the antigen, and post-mortem study. *Lancet Neurol.* **13**, 575–586 (2014).

92. Schofield, P. R. *et al.* Molecular characterization of a new immunoglobulin superfamily protein with potential roles in opioid binding and cell contact. *EMBO J.* **8**, 489–495 (1989).

93. Cheng, S. *et al.* Family of neural wiring receptors in bilaterians defined by phylogenetic, biochemical, and structural evidence. *Proc Natl Acad Sci USA* **116**, 9837–9842 (2019).

94. Gascon, E., Vutskits, L. & Kiss, J. Z. Polysialic acid-neural cell adhesion molecule in brain plasticity: from synapses to integration of new neurons. *Brain Res. Rev.* **56**, 101–118 (2007).

95. Aonurm-Helm, A., Zharkovsky, T., Jürgenson, M., Kalda, A. & Zharkovsky, A. Dysregulated CREB signaling pathway in the brain of neural cell adhesion molecule (NCAM)-deficient mice. *Brain Res.* **1243**, 104–112 (2008).

96. Gnanapavan, S. & Giovannoni, G. Neural cell adhesion molecules in brain plasticity and disease. *Mult. Scler. Relat. Disord.* **2**, 13–20 (2013).

97. Leshchyns'ka, I. & Sytnyk, V. Synaptic cell adhesion molecules in alzheimer's disease. *Neural Plast.* **2016**, 6427537 (2016).

98. Inoue, T. *et al.* Nectin-1 spots as a novel adhesion apparatus that tethers mitral cell lateral dendrites in a dendritic meshwork structure of the developing mouse olfactory bulb. *J. Comp. Neurol.* **523**, 1824–1839 (2015).

99. Samanta, D. & Almo, S. C. Nectin family of cell-adhesion molecules: structural and molecular aspects of function and specificity. *Cell. Mol. Life Sci.* **72**, 645–658 (2015).

100. Matthews, B. J. *et al.* Dendrite self-avoidance is controlled by Dscam. *Cell* **129**, 593–604 (2007).

101. Fuerst, P. G., Koizumi, A., Masland, R. H. & Burgess, R. W. Neurite arborization and mosaic spacing in the mouse retina require DSCAM. *Nature* **451**, 470–474 (2008).

102. Martin, E. A. *et al.* The intellectual disability gene Kirrel3 regulates target-specific mossy fiber synapse development in the hippocampus. *eLife* **4**, e09395 (2015).

103. Donoviel, D. B. *et al.* Proteinuria and perinatal lethality in mice lacking NEPH1, a novel protein with homology to NEPHRIN. *Mol. Cell. Biol.* **21**, 4829–4836 (2001).

104. Tissue expression of KIRREL1 - Summary - The Human Protein Atlas. https://www.proteinatlas.org/ENSG00000183853-KIRREL1/tissue.

105. Chao, D. L. & Shen, K. Functional dissection of SYG-1 and SYG-2, cell adhesion molecules required for selective synaptogenesis in C. elegans. *Mol. Cell. Neurosci.* **39**, 248–257 (2008).

106. Shen, K. & Bargmann, C. I. The immunoglobulin superfamily protein SYG-1 determines the location of specific synapses in C. elegans. *Cell* **112**, 619–630 (2003).

107. Schneider, T. *et al.* Restricted expression of the irreC-rst protein is required for normal axonal projections of columnar visual neurons. *Neuron* **15**, 259–271 (1995).

108. Fischbach, K.-F. *et al.* The irre cell recognition module (IRM) proteins. *J. Neurogenet.* **23**, 48–67 (2009).

109. Helmstädter, M., Höhne, M. & Huber, T. B. A brief overview on IRM function across evolution. *J. Neurogenet.* **28**, 264–269 (2014).

110. Ramos, R. G. *et al.* The irregular chiasm C-roughest locus of Drosophila, which affects axonal projections and programmed cell death, encodes a novel immunoglobulin-like protein. *Genes Dev.* **7**, 2533–2547 (1993).

111. Qu, Z., Zhang, A. & Yan, D. Robo functions as an attractive cue for glial migration through SYG-1/Neph. *eLife* **9**, (2020).

112. Taylor, M. R. *et al.* Kirrel3-Mediated Synapse Formation Is Attenuated by Disease-Associated Missense Variants. *J. Neurosci.* **40**, 5376–5388 (2020).

113. Wang, J. *et al.* Molecular and structural basis of olfactory sensory neuron axon coalescence by Kirrel receptors. *Cell Rep.* **37**, 109940 (2021).

114. Brignall, A. C. *et al.* Loss of Kirrel family members alters glomerular structure and synapse numbers in the accessory olfactory bulb. *Brain Struct. Funct.* **223**, 307–319 (2018).

115. Prince, J. E. A., Brignall, A. C., Cutforth, T., Shen, K. & Cloutier, J.-F. Kirrel3 is required for the coalescence of vomeronasal sensory neuron axons into glomeruli and for male-male aggression. *Development* **140**, 2398–2408 (2013).

116. Völker, L. A. *et al.* Neph2/Kirrel3 regulates sensory input, motor coordination, and home-cage activity in rodents. *Genes Brain Behav.* **17**, e12516 (2018).

117. Bhalla, K. *et al.* Alterations in CDH15 and KIRREL3 in patients with mild to severe intellectual disability. *Am. J. Hum. Genet.* **83**, 703–713 (2008).

118. Guerin, A. *et al.* Interstitial deletion of 11q-implicating the KIRREL3 gene in the neurocognitive delay associated with Jacobsen syndrome. *Am. J. Med. Genet. A* **158A**, 2551–2556 (2012).

119. Firestein, S. How the olfactory system makes sense of scents. *Nature* **413**, 211–218 (2001).

120. Principles of Animal Communication, Second Edition. http://sites.sinauer.com/animalcommunication2e/.

121. Sakano, H. Neural map formation in the mouse olfactory system. *Neuron* **67**, 530–542 (2010).

122. Imai, T. & Sakano, H. Roles of odorant receptors in projecting axons in the mouse olfactory system. *Curr. Opin. Neurobiol.* **17**, 507–515 (2007).

123. Inokuchi, K. *et al.* Nrp2 is sufficient to instruct circuit formation of mitral-cells to mediate odour-induced attractive social responses. *Nat. Commun.* **8**, 15977 (2017).

124. Nagayama, S., Homma, R. & Imamura, F. Neuronal organization of olfactory bulb circuits. *Front. Neural Circuits* **8**, 98 (2014).

125. Blanchart, A., De Carlos, J. A. & López-Mascaraque, L. Time frame of mitral cell development in the mice olfactory bulb. *J. Comp. Neurol.* **496**, 529–543 (2006).

126. Lin, D. M. *et al.* Formation of precise connections in the olfactory bulb occurs in the absence of odorant-evoked neuronal activity. *Neuron* **26**, 69–80 (2000).

127. Aihara, S., Fujimoto, S., Sakaguchi, R. & Imai, T. BMPR-2 gates activity-dependent stabilization of dendrites during mitral cell remodeling. *BioRxiv* (2020) doi:10.1101/2020.10.30.358861.

128. Parrish-Aungst, S., Shipley, M. T., Erdelyi, F., Szabo, G. & Puche, A. C. Quantitative analysis of neuronal diversity in the mouse olfactory bulb. *J. Comp. Neurol.* **501**, 825–836 (2007).

129. Pinching, A. J. & Powell, T. P. The neuron types of the glomerular layer of the olfactory bulb. *J. Cell Sci.* **9**, 305–345 (1971).

130. Brignall, A. C. & Cloutier, J.-F. Neural map formation and sensory coding in the vomeronasal system. *Cell. Mol. Life Sci.* **72**, 4697–4709 (2015).

131. Berghard, A. & Buck, L. Sensory Transduction in Vomeronasal Neurons: Evidence for Gao, Gai2, and Adenylyl Cyclase II as Major Components of a Pheromone Signaling Cascade. *J Neuroscience*.**16(3)**,909-918 (1996).

132. Dulac, C. & Axel, R. A novel family of genes encoding putative pheromone receptors in mammals. *Cell* **83**, 195–206 (1995).

133. Loconto, J. *et al.* Functional expression of murine V2R pheromone receptors involves selective association with the M10 and M1 families of MHC class Ib molecules. *Cell* **112**, 607–618 (2003).

134. Ishii, T. & Mombaerts, P. Expression of nonclassical class I major histocompatibility genes defines a tripartite organization of the mouse vomeronasal system. *J. Neurosci.* **28**, 2332–2341 (2008).

135. Ishii, T., Hirota, J. & Mombaerts, P. Combinatorial coexpression of neural and immune multigene families in mouse vomeronasal sensory neurons. *Curr. Biol.* **13**, 394–400 (2003).

136. Takami, S. & Graziadei, P. P. Light microscopic Golgi study of mitral/tufted cells in the accessory olfactory bulb of the adult rat. *J. Comp. Neurol.* **311**, 65–83 (1991).

137. Del Punta, K., Puche, A., Adams, N. C., Rodriguez, I. & Mombaerts, P. A divergent pattern of sensory axonal projections is rendered convergent by second-order neurons in the accessory olfactory bulb. *Neuron* **35**, 1057–1066 (2002).

138. Meeks, J. P., Arnson, H. A. & Holy, T. E. Representation and transformation of sensory information in the mouse accessory olfactory system. *Nat. Neurosci.* **13**, 723–730 (2010).

139. Astic, L. & Saucier, D. Anatomical mapping of the neuroepithelial projection to the olfactory bulb in the rat. *Brain Res. Bull.* **16**, 445–454 (1986).

140. Saucier, D. & Astic, L. Analysis of the topographical organization of olfactory epithelium projections in the rat. *Brain Res. Bull.* **16**, 455–462 (1986).

141. Miyamichi, K., Serizawa, S., Kimura, H. M. & Sakano, H. Continuous and overlapping expression domains of odorant receptor genes in the olfactory epithelium determine the dorsal/ventral positioning of glomeruli in the olfactory bulb. *J. Neurosci.* **25**, 3586–3592 (2005).

142. Ressler, K. J., Sullivan, S. L. & Buck, L. B. A zonal organization of odorant receptor gene expression in the olfactory epithelium. *Cell* **73**, 597–609 (1993).

143. Vassar, R., Ngai, J. & Axel, R. Spatial segregation of odorant receptor expression in the mammalian olfactory epithelium. *Cell* **74**, 309–318 (1993).

144. Cho, J. H., Lépine, M., Andrews, W., Parnavelas, J. & Cloutier, J.-F. Requirement for Slit-1 and Robo-2 in zonal segregation of olfactory sensory neuron axons in the main olfactory bulb. *J. Neurosci.* **27**, 9094–9104 (2007).

145. Nguyen-Ba-Charvet, K. T., Di Meglio, T., Fouquet, C. & Chédotal, A. Robos and slits control the pathfinding and targeting of mouse olfactory sensory axons. *J. Neurosci.* **28**, 4244–4249 (2008).

146. Cho, J. H., Kam, J. W. K. & Cloutier, J.-F. Slits and Robo-2 regulate the coalescence of subsets of olfactory sensory neuron axons within the ventral region of the olfactory bulb. *Dev. Biol.* **371**, 269–279 (2012).

147. Walz, A., Rodriguez, I. & Mombaerts, P. Aberrant sensory innervation of the olfactory bulb in neuropilin-2 mutant mice. *J. Neurosci.* **22**, 4025–4035 (2002).

148. Cloutier, J.-F. *et al.* Differential requirements for semaphorin 3F and Slit-1 in axonal targeting, fasciculation, and segregation of olfactory sensory neuron projections. *J. Neurosci.* **24**, 9087–9096 (2004).

149. Schwarting, G. A. *et al.* Semaphorin 3A is required for guidance of olfactory axons in mice. *J. Neurosci.* **20**, 7691–7697 (2000).

150. Schwarting *et al* Semaphorin 3A-mediated axon guidance regulates convergence and targeting of P2 odorant receptor axons *European Journal of Neuroscience.* **19**, 1800-1810 (2004).

151. Taniguchi, M. *et al.* Distorted odor maps in the olfactory bulb of semaphorin 3A-deficient mice. *J. Neurosci.* **23**, 1390–1397 (2003).

152. Scolnick, J. A. *et al.* Role of IGF signaling in olfactory sensory map formation and axon guidance. *Neuron* **57**, 847–857 (2008).

153. Imai, T., Suzuki, M. & Sakano, H. Odorant receptor-derived cAMP signals direct axonal targeting. *Science* **314**, 657–661 (2006).

154. Col, J. A. D., Matsuo, T., Storm, D. R. & Rodriguez, I. Adenylyl cyclase-dependent axonal targeting in the olfactory system. *Development* **134**, 2481–2489 (2007).

155. Chesler, A. T. *et al.* A G protein/cAMP signal cascade is required for axonal convergence into olfactory glomeruli. *Proc Natl Acad Sci USA* **104**, 1039–1044 (2007).

156. Zapiec, B., Bressel, O. C., Khan, M., Walz, A. & Mombaerts, P. Neuropilin-1 and the Positions of Glomeruli in the Mouse Olfactory Bulb. *eNeuro* **3**, (2016).

157. Imai, T. *et al.* Pre-target axon sorting establishes the neural map topography. *Science* **325**, 585–590 (2009).

158. Assens, A. *et al.* Alteration of Nrp1 signaling at different stages of olfactory neuron maturation promotes glomerular shifts along distinct axes in the olfactory bulb. *Development* **143**, 3817–3825 (2016).

159. Kaneko-Goto, T., Yoshihara, S.-I., Miyazaki, H. & Yoshihara, Y. BIG-2 mediates olfactory axon convergence to target glomeruli. *Neuron* **57**, 834–846 (2008).

160. Prince, J. E. A. *et al.* Robo-2 controls the segregation of a portion of basal vomeronasal sensory neuron axons to the posterior region of the accessory olfactory bulb. *J. Neurosci.* **29**, 14211–14222 (2009).

161. Cloutier, J. F. *et al.* Neuropilin-2 mediates axonal fasciculation, zonal segregation, but not axonal convergence, of primary accessory olfactory neurons. *Neuron* **33**, 877–892 (2002).

162. Belluscio, L., Koentges, G., Axel, R. & Dulac, C. A map of pheromone receptor activation in the mammalian brain. *Cell* **97**, 209–220 (1999).

163. Rodriguez, I., Feinstein, P. & Mombaerts, P. Variable patterns of axonal projections of sensory neurons in the mouse vomeronasal system. *Cell* **97**, 199–208 (1999).

164. Harrison, S. J., Nishinakamura, R. & Monaghan, A. P. Sall1 regulates mitral cell development and olfactory nerve extension in the developing olfactory bulb. *Cereb. Cortex* **18**, 1604–1617 (2008).

165. Imamura, F. & Greer, C. A. Pax6 regulates Tbr1 and Tbr2 expressions in olfactory bulb mitral cells. *Mol. Cell. Neurosci.* **54**, 58–70 (2013).

166. Bastakis, G. G., Savvaki, M., Stamatakis, A., Vidaki, M. & Karagogeos, D. Tag1 deficiency results in olfactory dysfunction through impaired migration of mitral cells. *Development* **142**, 4318–4328 (2015).

167. Cheng, T.-W. & Gong, Q. Secreted TARSH regulates olfactory mitral cell dendritic complexity. *Eur. J. Neurosci.* **29**, 1083–1095 (2009).

168. Imamura, F. & Greer, C. A. Dendritic branching of olfactory bulb mitral and tufted cells: regulation by TrkB. *PLoS ONE* **4**, e6729 (2009).

169. Muroyama, Y., Baba, A., Kitagawa, M. & Saito, T. Olfactory sensory neurons control dendritic complexity of mitral cells via notch signaling. *PLoS Genet.* **12**, e1006514 (2016).

170. Fujimoto, S. *et al.* Spontaneous activity generated within the olfactory bulb establishes the discrete wiring of mitral cell dendrites. *BioRxiv* (2019) doi:10.1101/625616.

171. Lorenzon, P. *et al.* Circuit formation and function in the olfactory bulb of mice with reduced spontaneous afferent activity. *J. Neurosci.* **35**, 146–160 (2015).

172. Cho, J. H., Prince, J. E. A., Cutforth, T. & Cloutier, J.-F. The pattern of glomerular map formation defines responsiveness to aversive odorants in mice. *J. Neurosci.* **31**, 7920–7926 (2011).

173. Nakashima, A. *et al.* Agonist-independent GPCR activity regulates anterior-posterior targeting of olfactory sensory neurons. *Cell* **154**, 1314–1325 (2013).

174. Takeuchi, H. *et al.* Sequential arrival and graded secretion of Sema3F by olfactory neuron axons specify map topography at the bulb. *Cell* **141**, 1056–1067 (2010).

175. Ihara, N., Nakashima, A., Hoshina, N., Ikegaya, Y. & Takeuchi, H. Differential expression of axon-sorting molecules in mouse olfactory sensory neurons. *Eur. J. Neurosci.* **44**, 1998–2003 (2016).

176. Mountoufaris, G. *et al.* Multicluster Pcdh diversity is required for mouse olfactory neural circuit assembly. *Science* **356**, 411–414 (2017).

177. Feinstein, P. & Mombaerts, P. A contextual model for axonal sorting into glomeruli in the mouse olfactory system. *Cell* **117**, 817–831 (2004).

178. Feinstein, P., Bozza, T., Rodriguez, I., Vassalli, A. & Mombaerts, P. Axon guidance of mouse olfactory sensory neurons by odorant receptors and the beta2 adrenergic receptor. *Cell* **117**, 833–846 (2004).

179. Movahedi, K., Grosmaitre, X. & Feinstein, P. Odorant receptors can mediate axonal identity and gene choice via cAMP-independent mechanisms. *Open Biol.* **6**, (2016).

180. Rodriguez-Gil, D. J. *et al.* Odorant receptors regulate the final glomerular coalescence of olfactory sensory neuron axons. *Proc Natl Acad Sci USA* **112**, 5821–5826 (2015).

181. Shen, K., Fetter, R. D. & Bargmann, C. I. Synaptic specificity is generated by the synaptic guidepost protein SYG-2 and its receptor, SYG-1. *Cell* **116**, 869–881 (2004).

182. Williams, E. O. *et al.* Delta protocadherin 10 is regulated by activity in the mouse main olfactory system. *Front. Neural Circuits* **5**, 9 (2011).

183. Bozza, T. *et al.* Mapping of class I and class II odorant receptors to glomerular domains by two distinct types of olfactory sensory neurons in the mouse. *Neuron* **61**, 220–233 (2009).

184. Dewan, A. *et al.* Single olfactory receptors set odor detection thresholds. *Nat. Commun.* **9**, 2887 (2018).

185. Kobayakawa, K. *et al.* Innate versus learned odour processing in the mouse olfactory bulb. *Nature* **450**, 503–508 (2007).

186. Tsuboi, A., Miyazaki, T., Imai, T. & Sakano, H. Olfactory sensory neurons expressing class I odorant receptors converge their axons on an antero-dorsal domain of the olfactory bulb in the mouse. *Eur. J. Neurosci.* **23**, 1436–1444 (2006).

187. Zhang, X. *et al.* High-throughput microarray detection of olfactory receptor gene expression in the mouse. *Proc Natl Acad Sci USA* **101**, 14168–14173 (2004).

188. Zheng, C., Feinstein, P., Bozza, T., Rodriguez, I. & Mombaerts, P. Peripheral olfactory projections are differentially affected in mice deficient in a cyclic nucleotide-gated channel subunit. *Neuron* **26**, 81–91 (2000).

189. Barnea, G. *et al.* Odorant receptors on axon termini in the brain. *Science* **304**, 1468 (2004).

190. Shykind, B. M. *et al.* Gene switching and the stability of odorant receptor gene choice. *Cell* **117**, 801–815 (2004).

191. Mombaerts, P. *et al.* Visualizing an olfactory sensory map. *Cell* **87**, 675–686 (1996).

192. Nakashima, A. *et al.* Structured spike series specify gene expression patterns for olfactory circuit formation. *Science* **365**, (2019).

193. Dulac, C. & Torello, A. T. Molecular detection of pheromone signals in mammals: from genes to behaviour. *Nat. Rev. Neurosci.* **4**, 551–562 (2003).

194. Sanes, J. R. & Zipursky, S. L. Synaptic specificity, recognition molecules, and assembly of neural circuits. *Cell* **181**, 536–556 (2020).

195. Özkan, E. *et al.* Extracellular architecture of the SYG-1/SYG-2 adhesion complex instructs synaptogenesis. *Cell* **156**, 482–494 (2014).

196. Bulchand, S., Menon, S. D., George, S. E. & Chia, W. The intracellular domain of Dumbfounded affects myoblast fusion efficiency and interacts with Rolling pebbles and Loner. *PLoS ONE* **5**, e9374 (2010).

197. Chia, P. H., Chen, B., Li, P., Rosen, M. K. & Shen, K. Local F-actin network links synapse formation and axon branching. *Cell* **156**, 208–220 (2014).

198. Gerke, P. *et al.* Neuronal expression and interaction with the synaptic protein CASK suggest a role for Neph1 and Neph2 in synaptogenesis. *J. Comp. Neurol.* **498**, 466–475 (2006).

199. Harita, Y. *et al.* Neph1, a component of the kidney slit diaphragm, is tyrosine-phosphorylated by the Src family tyrosine kinase and modulates intracellular signaling by binding to Grb2. *J. Biol. Chem.* **283**, 9177–9186 (2008).

200. Huber, T. B. *et al.* The carboxyl terminus of Neph family members binds to the PDZ domain protein zonula occludens-1. *J. Biol. Chem.* **278**, 13417–13421 (2003).

201. Sellin, L. *et al.* NEPH1 defines a novel family of podocin interacting proteins. *FASEB J.* **17**, 115–117 (2003).

202. Yesildag, B., Bock, T., Herrmanns, K., Wollscheid, B. & Stoffel, M. Kin of IRRE-like Protein 2 Is a Phosphorylated Glycoprotein That Regulates Basal Insulin Secretion. *J. Biol. Chem.* **290**, 25891–25906 (2015).

203. Oliveros, J. C. *et al.* Breaking-Cas-interactive design of guide RNAs for CRISPR-Cas experiments for ENSEMBL genomes. *Nucleic Acids Res.* **44**, W267-71 (2016).

204. Sakurai, T., Watanabe, S., Kamiyoshi, A., Sato, M. & Shindo, T. A single blastocyst assay optimized for detecting CRISPR/Cas9 system-induced indel mutations in mice. *BMC Biotechnol.* **14**, 69 (2014).

205. Schindelin, J. *et al.* Fiji: an open-source platform for biological-image analysis. *Nat. Methods* **9**, 676–682 (2012).

206. Gabriel, L. R., Wu, S. & Melikian, H. E. Brain slice biotinylation: an ex vivo approach to measure region-specific plasma membrane protein trafficking in adult neurons. *J. Vis. Exp.* (2014) doi:10.3791/51240.

207. Gene Detail :: Allen Brain Atlas: Mouse Brain. http://mouse.brain-map.org/gene/show/33922.

208. Liu, Y. F. *et al.* Autism and Intellectual Disability-Associated KIRREL3 Interacts with Neuronal Proteins MAP1B and MYO16 with Potential Roles in Neurodevelopment. *PLoS ONE* **10**, e0123106 (2015).

sciwheel/placeholder/bibliographysciwheel/placeholder/bibliographysciwheel/placeholder/bibliography